DISSERTATION

Funktionelle Konnektivitätsdynamik bei Anti-NMDA Rezeptor Enzephalitis

Functional connectivity dynamics in anti-NMDA receptor encephalitis

zur Erlangung des akademischen Grades
Doctor rerum medicinalium (Dr. rer. medic.)

vorgelegt der Medizinischen Fakultät
Charité – Universitätsmedizin Berlin

von

Nina Claudia von Schwanenflug

Erstbetreuung: Prof. Dr. med. Carsten Finke

Datum der Promotion: 28.02.2025

Table of contents

List of tables

List of figures

List of abbreviations

AG	-	Angular gyrus
BOLD	-	blood oxygen level dependent
CB	-	cerebellar network
DAMS	-	distance across meta-states
DMN	-	default-mode network
dATT	-	dorsal attention network
FC	-	functional connectivity
FDR	-	false discovery rate
fMRI	-	functional magnetic resonance imaging
FPN	-	fronto-parietal network
HPC	-	hippocampus
IFG	-	inferior frontal gyrus
IQR	-	interquartile range
MRI	-	magnetic resonance imaging
mPFC	-	medial prefrontal cortex
mRS	-	modified Rankin Scale
NMDARE	-	anti-NMDA receptor encephalitis
POS	-	parieto-occipital gyrus
SFG	-	superior frontal gyrus
SM	-	sensori-motor network
TE	-	echo time
TPOJ	-	temporo-parieto-occipital junction
TR	-	repetition time
VIS	-	visual network

Abstract

Anti-NMDA receptor encephalitis (NMDARE) is an autoimmune disorder marked by the production of antibodies against the NMDA receptor, an ionotropic glutamate receptor in the central nervous system. NMDA receptors play a crucial role in synaptic plasticity and neurotransmission. The presence of these auto-antibodies results in decreased NMDA receptor levels, leading to diverse neurological and psychiatric manifestations including psychosis, seizures, and movement disorders.

Routine clinical structural magnetic resonance imaging (MRI) often fails to detect abnormalities despite severe disease manifestation. Conversely, advanced imaging methods like resting-state functional MRI consistently reveal disrupted functional connectivity (FC) associated with disease symptoms. In general, resting-state FC refers to the temporal coherence of intrinsic, spontaneous brain signals across different regions. Traditional FC analysis are limited to a static view of brain activity as they average FC over the entire scan. In contrast, new *dynamic* time-resolved analysis methods capture temporal fluctuations in FC, providing valuable insights into the dynamic nature of brain activity with increased temporal resolution.

This thesis work applied these novel methodological advancements to study functional dynamics and its clinical relevance in NMDARE patients from two perspectives: In *Study I*, spatial and temporal patterns of four major FC states were identified and compared between patients and healthy controls. In *Study II*, a novel, graph-based method was used to investigate alterations in the sequence of state exploration, which refers to transitions between different patterns of spontaneous brain activity over time.

In *Study I*, NMDARE patients exhibited alterations in FC in three out of four states, along with a shift in the amount of time spent in different states. Patients also showed increased volatility in state transitions, correlating with disease severity. Using machine learning, dynamic FC models outperformed static models in discriminating patients from controls. These findings highlight state-dependent changes and distinct dynamic profile of state dynamics in NMDARE. *Study II* complemented these findings and further investigated alterations in the dynamics of state exploration and transition trajectories, revealing reduced resilience of state transitions and compromised transition networks associated with disease severity.

Overall, our analyses demonstrate that NMDARE is linked to a clinically significant destabilization of brain state transitions, providing new insights into the functional reorganization of brain dynamics in this disease. Moreover, our results highlight the potential of time-resolved FC analyses as a means of identifying novel biomarkers in NMDARE and other neuropsychiatric disorders.

Keywords: neuroinflammatory disease • autoimmune encephalitis • anti-NMDA recptor encephalitis • brain imaging • functional magnetic resonance imaging • resting-state fMRI • spontaneous brain activity • functional connectivity dynamics • graph theory • brain states • transition trajectories

Zusammenfassung

Anti-NMDA-Rezeptor-Enzephalitis (NMDARE) ist eine Autoimmunerkrankung, die durch die Bildung von Auto-Antikörpern gegen den NMDA-Rezeptor gekennzeichnet ist. NMDA-Rezeptoren gehören zu den ionotropen Glutamatrezeptoren des zentralen Nervensystems und spielen eine entscheidende Rolle in der synaptischen Plastizität und Neurotransmission. Die Bildung dieser Antikörper führt zu einer Verringerung der Anzahl von NMDA-Rezeptoren, was sich in schwerwiegenden neurologischen und psychiatrischen Symptomen wie Psychosen, Krampfanfällen und Bewegungsstörungen manifestiert.

Klinische Routineuntersuchungen mittels struktureller Magnetresonanztomographie (MRT) zeigen trotz dieser Erkrankungsschwere typischerweise keine Auffälligkeiten. Dagegen zeigen Verfahren wie funktionelles MRT (fMRT) konsistente Veränderungen der funktionellen Konnektivität (FC), die mit Krankheitssymptomen korrelieren. Im Allgemeinen beschreibt FC die zeitliche Kohärenz zwischen den Signalen verschiedener Hirnregionen. Hierbei mitteln herkömmliche Analysen die FC über den gesamten Scan, was einer *statischen* Beschreibung von Hirnaktivität entspricht. Im Gegensatz dazu erfassen neue, *zeitaufgelöste* Methoden Fluktuationen der FC und liefern so wertvolle Einblicke in die Dynamik von Hirnaktivität.

Die vorliegende Arbeit untersucht Veränderungen in der dynamischen FC bei NMDARE-Patienten aus zwei Perspektiven: In *Studie I* wurden räumliche und zeitliche Muster der vier Hauptkonnektivitätszustände identifiziert und zwischen Gesunden und Patienten verglichen. In *Studie II* wurde eine neuartige, graphenbasierte Methode verwendet, um Veränderungen in der Explorationsabfolge funktioneller Hirnzustände zu untersuchen.

In *Studie I* zeigten NMDARE-Patienten Veränderungen in drei von vier Zuständen sowie Unterschiede in der Verweildauer in den verschiedenen Hirnzuständen. Die Patienten zeigten auch eine erhöhte Volatilität in den Zustandsübergängen, die mit der Schwere der Erkrankung korrelierte. Beim Einsatz von maschinellem Lernen schnitten dynamische FC-Modelle bei der Unterscheidung zwischen Patienten und Kontrollen besser ab als statische Modelle. Diese Ergebnisse verdeutlichen zustandsabhängige Veränderungen und das spezifische dynamische FC-Profil bei NMDARE. *Studie II* baut auf diesen Erkenntnissen auf und untersuchte speziell Veränderungen in der Dynamik der Exploration von Konnektivitätszuständen sowie deren Übergangsmuster. Hier

zeigten Patienten eine verringerte Stabilität der Zustandsübergänge, die ebenfalls mit der Erkrankungsschwere korrelierte.

Insgesamt zeigen unsere Analysen, dass NMDARE mit einer klinisch signifikanten Destabilisierung funktioneller Hirnzustände verbunden ist. Damit liefern sie wichtige Erkenntnisse über die funktionelle Reorganisation von Hirnaktivität bei der Erkrankung. Darüber hinaus unterstreichen unsere Ergebnisse auch das Potenzial von zeitabhängigen FC-Analysen zur Identifizierung neuer Biomarker bei NMDARE und anderen neuropsychiatrischen Störungen.

Stichwörter: Neuroinflammatorische Erkrankung • Autoimmunenzephalitis • Anti-NMDA-Rezeptorenzephalitis • Bildgebung • funktionelle Magnetresonanztomographie • MRT im Ruhezustand • spontane Hirnaktivität • funktionelle Konnektivitätsdynamiken • Graphentheorie • Konnektivitätszustände • Transitionsverhalten

1. Clinical background & Introduction to functional connectivity

1.1. Anti-NMDA receptor encephalitis (NMDARE)

Anti-N-methyl-D-aspartate receptor encephalitis (NMDARE) is a severe autoantibody-mediated inflammatory disease that was first described in 2007 [1]. NMDARE is the most common form of autoimmune encephalitis with an estimated incidence of approximately 0.15 per 100.000 population per year and a prevalence of 0.6 out of 100.000 [2,3]. The disease is characterized by the presence of Immunoglobulin G antibodies in the cerebro-spinal fluid and a gradual progression of symptomatology that includes distinct psychopathology and multistage neuropsychiatric features (Fig 1A) [4,5]. Approximately 70% of patients experience a prodromal stage with nonspecific inflammatory symptoms, followed by very prominent psychiatric symptoms in 90% of case. These symproms, often including disorganized, agitated or violent behavior, hallucinations, and mood instabilities, can be difficult to differentiate from primary psychiatric disorders. At a later stage, patients show severe neurological symptoms such as dyskinesia, autonomic dysfunction, and seizures, which often require intensive care [4–6]. Although the disease is potentially fatal, around 80% of patients show a favorable clinical outcome after 24 months, with early immunotherapy and no emergency care being the main predictors of positive outcome [7]. Nonetheless, a prolonged phase of recovery including memory deficits and executive dysfunctions often persists several years after disease onset [8–10]. Within the first 24 months, patients experience a 12% risk of generally milder relapses, with some having multiple episodes. Hence, regular cerebrospinal fluid analysis is recommended for early detection of recurrence [7]. First-line treatments include high-dose corticosteroids, intravenous immunoglobulin, and/or plasmapheresis. If necessary, second-line options like rituximab or cyclophosphamide can be administered [5].

The disease typically affects young females at a median age of 21 years, with a ratio of 8:2 compared to males. However, disease onset can vary considerably, ranging from <1 to 85 years, while the set of symptoms may differ between children and adults at disease onset [5,11]. Although the exact cause is still unclear, the main confirmed etiologies of NMDARE are paraneoplastic manifestations associated with an underlying ovarian teratoma in around one-third of the cases as well as preceding herpes simplex virus encephalitis [1,12].

In NMDARE, the NR1 subunit of the NMDA receptor is targeted by auto-antibodies, leading to an reduction of the receptors on the synaptic surface (Fig 1B) [13,14]. NMDA receptors belong to the class of ionotropic glutamate receptors that are expressed ubiquitously throughout the human brain – with the highest density in the medial prefrontal cortex (mPFC) and the CA1 region of the hippocampus (Fig 1C) [15,16]. Excitatory synaptic transmission of a neural signal is dependent on the presynaptic release of glutamate that diffuses across the synaptic cleft and binds to postsynaptic NMDA receptors [17]. Through the activation of calcium-dependent signaling cascades, NMDA receptors enhance signal transduction and influence both the functional and structural plasticity of synapses, dendrites, and neurons [17]. As such, NMDA receptor dysfunction can cause a wide range of symptoms and is thought to play a key role in several neuropsychiatric diseases, such as schizophrenia and mood disorders [18–20]. Therefore, insights from NMDARE have potential transdiagnostic implications and could advance our understanding of shared psychiatric symptoms.

Although a causal relationship between the depletion of receptors and the clinical presentation of NMDARE is assumed, a decrease in antibody titer does not correlate with symptom regression [21]. Brain imaging techniques have been explored in the quest of assessment tools that adequately describe disease progression and potentially serve as prognostic markers. However, standard structural magnetic resonance imaging (MRI) shows little to no abnormalities in 50-80% of patients [22,23], creating a “clinico-radiological paradox”, where a severe disease course is observed in the absence of visible morphological abnormalities. To address this paradox, advanced MRI techniques, such as functional MRI (fMRI) have been investigated to enhance our understanding of the link between clinical impairment and brain reorganization.

Below, we first turn to central concepts of measuring spontaneous brain activity with fMRI (section 1.2), recent methodological advancements that enable a time-resolved account of brain activity (section 1.3) as well as the application of these advancements in clinical populations (section 1.3.1).

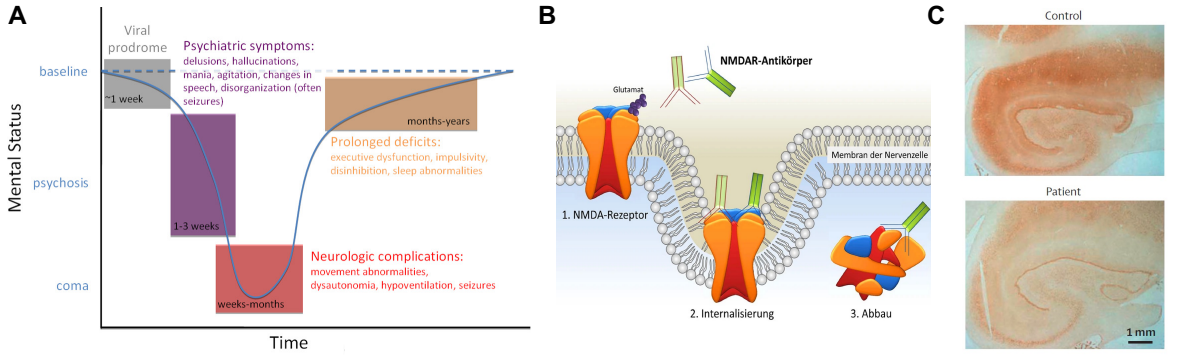

Figure 1: Clinical manifestation of NMDARE and disease mechanism. A The disease typically presents with a distinct neuropsychiatric syndrome characterized by a viral prodromal phase, as well as prominent neurological and psychiatric symptoms. From Kayser & Dalmau 2016 *[6]*. **B** NMDARE is caused by antibodies targeting the NR1 subunit of the NMDA receptor. This results in internalization and degradation of the receptor, leading to a significant reduction in receptor density on the synaptic surface. From Lang & Prüß 2016 *[14]*. **C** Illustration of a hippocampal section from a healthy individual (top) and a patient with NMDARE (bottom), immunostained with NR1 antibody. Note the visibly lower receptor density in the patient. From Dalmau *et al.* 2011 *[13]*.

1.2. Imaging spontaneous brain activity: a window into functional organization

As a non-invasive tool, fMRI detects changes in brain activity by indirectly measuring localized macroscopic activity through blood flow and oxygenation[1] [24–26]. This allows for the study of the diverse spontaneous neural activity that occurs in the human brain, which fluctuates in structured patterns across different temporal and spatial scales [27,28]. In the early stages, fMRI studies were mainly based on *task-induced* modulation (i.e., exposure to a motor, sensory, or cognitive demand/ 'task') of the blood oxygen level dependent (BOLD) signal, which considerably advanced the understanding of brain function and spatial organization. In contrast, spontaneous, or *resting-state* BOLD fluctuations were considered noise (i.e., physiological, movement, or scanner artifacts) that were usually minimized through averaging of the BOLD time series [27,29]. In the following years, however, accumulating evidence to the contrary showed that resting-state brain activity is not random but provides insights into the fundamental organization of infra-slow (< 0.1Hz) neural activity (Fig 2A) [27,30–34]. In

[1] Functional MRI utilizes localized fluctuations in blood oxygenation measuring ferromagnetic properties of hemoglobin [24]. While oxygenated hemoglobin is diamagnetic (i.e., only paired electron pairs), deoxygenated hemoglobin contains unpaired electrons and is magnetizable. As neural activity metabolizes oxygen, the blood oxygen level dependent (BOLD) signal is used as a proxy to localize brain activation via blood flow and temporarily increased local oxygenation levels – a process termed neurovascular coupling [25]. Importantly, in contrast to other vascular territories in the body, vasodilation in the brain is much less determined by systemic factors (e.g., catecholamines and instead shows a high degree of autoregulation by local factors that help meet the brain's need for constant blood supply and water homeostasis [26].

their seminal work, Biswal *et al*. demonstrated strong coupling of these low-frequency fluctuations across homologous motor areas in the human cortex [30]. This temporal dependency led to the pivotal idea that brain regions which show a strong temporal correlation in their activity are functionally connected [30] – a concept that is commonly referred to as functional connectivity (FC) (Fig 2B).

This discovery initiated a new era in neuroimaging research that has provided fundamental insights into the intrinsic functional architecture of the human brain. Estimated from whole-brain correlations of BOLD time series, human brain activity can be decomposed into networks of functionally connected brain regions (Fig 2C) [31,33,35]. These resting-state networks are robust, exhibit distinct spatiotemporal features, and are highly reproducible [33]. This network architecture is commonly summarized as the *functional connectome* and is typically subdivided into a visual, a sensori-motor, an attentional, a fronto-parietal, and a default-mode network, each of which possesses distinct functional characteristics [36–38]. While the sensori-motor network has been implicated in the planning and performing of motor actions, the default-mode network is typically attributed with internal processes including autobiographical memory and mind-wandering [30,39]. Furthermore, functional networks can be broadly divided into primary sensory and association networks that are organized along a hierarchy from lower-order unimodal to higher-order transmodal functional systems [33,40].

These findings have been extended to individualized descriptions of brain organization: functional connectome “fingerprinting” can reliably identify individual participants from large study populations with up to ~95% accuracy based on their unique patterns of FC [41]. It has been posited that these inter-individual differences of connectomics can even predict inter-individual differences in cognition (attention, intelligence, or working memory) [41–43]. However, to what extent a direct mapping of inter-individual differences in behavior onto individual differences in functional organization is attainable, is still under debate [44].

To understand brain function in both healthy and diseased states, researchers have investigated the relationship between clinical symptoms and alterations in functional connectomics, using both correlational approaches and mechanistic models of brain function [45–47]. These studies demonstrated that focal lesions in different locations can lead to identical or similar clinical symptoms [48], thus supporting the concept of spatially distributed but functionally integrated processing systems. From this

standpoint, it is important to investigate disease-related alterations in the brain not only in terms of local activity changes but also at the level of large-scale resting-state functional networks [45].

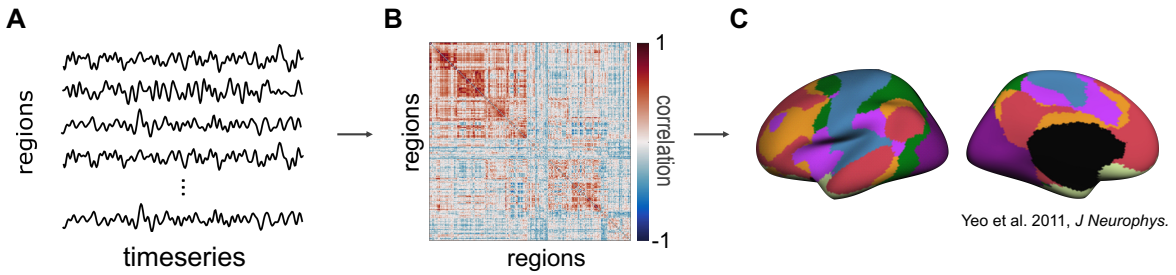

Figure 2: Functional organization of the brain as measured with resting-state fMRI. A Region-wise time series of spontaneous, intrinsic brain activity captured by resting-state fMRI. **B** Correlated activity among functionally related brain regions over time, known as functional connectivity (FC), is evident in the activity patterns. The correlation matrix visualizes the temporal coherence between any two regions in the brain. Red indicates highly correlated activity, blue highly anti-correlated activity. **C** FC is organized into large-scale functional resting-state networks, typically including a visual network, a sensori-motor network, an attentional network, a fronto-parietal network, and a default-mode network. The network architecture depicted here is based on the commonly used estimation by Yeo et al. *[33]*.

1.2.1. Prior evidence of functional reorganization in patients with NMDARE

Patients with NMDARE have been reported to exhibit distributed impairments in FC, affecting most of the large-scale networks, and specifically sensori-motor, fronto-parietal, lateral-temporal, and visual networks [49]. Furthermore, impairment in the connectivity of the default-mode network was consistently observed between hippocampal and medial prefrontal regions [49,50]. Importantly, decreases in FC correlated with individual memory performance [49,50] and psychiatric symptom presentation [49], underlining the clinical relevance of functional disruptions in the manifestation of NMDARE.

Despite their usefulness, conventional resting-state analyses have a significant limitation in that they rely on the averaged correlation of BOLD time series over a multi-minute scan, producing a "static" view of brain activity. This limitation prevents the capture of dynamic evolution and reconfiguration of brain activity [51,52]. Thus, *time-resolved* analysis of brain activity has been developed, which allows for the study of the inherently dynamic nature of brain activity.

The studies included in this thesis focus on exploring the dynamics of functional reorganization in patients with NMDARE with the objective to advance our understanding of altered brain dynamics in this patient population.

The following sections will give an introduction to the methodologies of time-resolved analysis of intrinsic brain activity, discuss their behavioral and clinical significance, and outline the theoretical and methodological framework that was employed to study brain dynamics in patients with NMDARE.

1.3. From minutes to seconds: time-resolved analysis of spontaneous brain activity

Time-resolved analysis of resting-state fMRI has emerged as the next frontier in functional brain imaging [53,54]. By increasing the temporal resolution from minutes to seconds, new models of brain function have been developed that provide novel insights into regional and network interactions. As a result, our understanding of healthy brain function and pathological conditions has significantly advanced [47,52–56].

One line of research studies the functional dynamics of BOLD activity as the variance or standard deviation of moment-to-moment fluctuations in the signal, providing information on regional BOLD variability [57]. Moreover, several analytical frameworks have been developed to capture functional variations in BOLD activity, including time-resolved signal complexity [56], time-frequency analyses [54], co-activation patterns [58,59], BOLD cofluctuation magnitude based on edge time series [60], and biophysical modeling of nonlinear brain dynamics [61].

On the other hand, to describe *connectivity* dynamics among brain regions, the concept of *time-varying* functional network interaction has been proposed – the functional 'chronnectome' [53]. This framework allows for the identification of transient FC states, which manifest as distinct recurrent patterns of whole-brain FC [62]. The focus of the present thesis is to model brain dynamics by studying these functional brain states and examining the transitions that occur between them (see section 2.1. & section 2.3. for more detail).

1.3.1. Clinical and behavioral relevance of time-resolved spontaneous brain activity

Time-resolved resting-state analyses offer a promising approach to better capture the inherently dynamic aspects of cognition and behavior [63]. Indeed, numerous studies have provided strong evidence linking moment-to-moment fluctuations in brain activity to cognititive processes and behavior: For instance, Gonzalez-Castillo *et al.* [64]

conducted a study where they scanned participants engaged in several cognitive tasks, and they found that the patterns of functional configurations during each task differed among participants and accurately reflected the individual's level of task engagement and cognitive ability [64]. Furthermore, it is possible to predict how well a person is performing a task by analyzing the continuous patterns of brain function. For example, if the connectivity between the default mode and sensory networks in the brain is weak, participants are more likely to fail to perceive a faint sound [65]. Similarly, ongoing connectivity patterns linked to the state of vigilance predicted intra-individual variations in response speed [66].

Task-*independent* ongoing mental states are influenced by the intrinsic activity of the brain, which is assumed to be more variable and less consistent across individuals and time points, and not driven by external demands. Despite this, resting-state brain dynamics have been linked to interindividual differences in general cognitive performance: For example, higher standard deviation of BOLD signal indicated better overall performance in working memory [67], cognitive flexibility [68], and response speed [69]. However, brain signal variability can also have differential effects: for example, higher BOLD signal variability can enhance cognitive flexibility but impair cognitive stability [68].

Moreover, functional dynamics also change across the lifespan: Garrett *et al.* demonstrated that BOLD variability decreases with age, and that signal variability has five times greater predictive power for age than mean-based BOLD measures [57]. Importantly, those regions that were most predictive of age remained undetected with conventional average measures, suggesting that Garrett *at al*. revealed a subset of previously unknown age-related regions using variability measures [57]. Importantly, the relationship between age, cognition, and brain dynamics also extends to other conceptualizations of BOLD variability, such as time-resolved entropy [56].

Finally, time-resolved approaches have inspired efforts to further our understanding of psychiatric and neurological conditions. Although it is unclear whether changes in dynamic network properties are the cause or consequence of the disease, these properties are increasingly regarded as novel biomarkers for disorders, as they seem to be related to many clinical dysfunctions [52]. The analysis of FC states in people with schizophrenia showed a pronounced shift in their state preference, indicating changes of whole-brain activity configurations [70]. Moreover, these patients exhibited increased overall transition frequencies between states [71].

A different pattern was reported for patients with acute ischaemic stroke by Bonkhoff *et al.* [72]: Here, patients exhibited distinct state-wise FC alterations in sensori-motor networks that were accompanied by characteristic changes in temporal properties of network interactions. Remarkably, the extent and nature of the changes varied with the severity of the motor deficits [72].

In people with major depression, a prominent finding was decreased variability in FC, accompanied by extended dwell times in the dominant state which showed low overall connectivity. Changes in FC dynamics were correlated with symptoms such as sadness, and disease severity, potentially reflecting negative, slow, and ruminative thinking [73–76]. Patients with Alzheimer's disease demonstrated more volatile state transitions and spent more time in usually infrequent, functionally segregated states compared to healthy controls [77,78].

Patients with multiple sclerosis exhibited a complex pattern of unstable network dynamics that was topologically constrained to pericentral, limbic and subcortical areas. These dynamics were associated with measures of clinical disability [79,80].

These examples demonstrate the potential of functional dynamics to uncover new perspectives on brain pathology that may not be detected through traditional static analyses. Additionally, studying brain dynamics may reconcile conflicting evidence from traditional resting-state approaches, leading to a more holistic understanding of brain function in health and disease. With this in mind, the current thesis applies these novel methodological advancements to investigate functional dynamics and its clinical relevance in people with NMDARE.

2. Methodological background & Framework

2.1. Identifying brain states

One fundamental approach to assess time-resolved connectivity dynamics involves quantifying distinct functional brain states. These states correspond to transient whole-brain patterns of inter-regional coupling [62].

Methodologically, brain states in resting-state fMRI are most commonly estimated from sliding window correlations. In this simple, yet powerful approach, BOLD time series are subdivided into temporal windows of equal length that can be either overlapping or non-overlapping (Fig 3A). The length of these windows represents an important methodological choice that determines the tradeoff between temporal resolution (tracking fast temporal changes in FC) and estimation accuracy (enhancing signal-to-noise ratio) [81]. Within each window, pairwise correlations of BOLD time series are computed among brain regions, resulting in window-wise FC matrices which represent a time-resolved account of covarying brain activity (Fig 3B). Subsequently, clustering algorithms are applied to group windows with similar connectivity patterns together. Thereby, each window is assigned to a particular functional brain state based on a predetermined target measure (Fig 3C). The present thesis applies two of the leading clustering methods to derive these functional brain states: *k*-means clustering of network connectivity (*Study I*) and temporal meta-states (*Study II*), as shown in Fig 3 and detailed in the following sections.

2.2. Mapping the functional connectome with graph theory

To investigate the multi-faceted organization of brain activity, researchers have widely adopted tools from network neuroscience [82], with a special emphasis on graph theory. Within this framework, the brain can be represented as a graph, where “nodes” represent specific brain regions, and “edges” represent the connections between them (e.g., FC) [83]. This approach allows for a robust abstraction of brain regions and how they interact.

One critical feature of brain organization is network efficiency. Network efficiency refers to how efficiently information flows through a network via the connections between different regions of the brain. In the context of brain activity, network efficiency involves both information integration and segregation [84].

Information integration refers to the ability of a network to transmit information between nodes. In the brain, this can be thought of as how easily information can be transmitted across different brain regions that are not necessarily directly connected [85].

Information segregation refers to the ability of a network to create groups of nodes that are highly interconnected with each other. In the brain, this can be thought of as clusters of regions that work together to perform specific functions [85].

This organizational property is closely linked to modularity. Modularity refers to the presence of groups, modules or subnetworks within a larger network that have a relatively higher density of connections between them compared to connections outside the group [86,87]. In the context of the brain, modularity refers to the existence of subnetworks, i.e., modules, of brain regions. These modules closely resemble canonical resting-state networks and reinforce the idea of network organization in brain function – see section 1.2. [31].

The combination of network efficiency and modularity in the brain allows for parallel information processing across distributed domains, while balancing cost-intensive functional integration and cost-efficient functional segregation [33,88].

Building on this background, the current work applies graph analysis in two ways. In *Study I*, it is used to describe spatial characteristics of functional states (i.e., differences in FC across states). In *Study II*, graph analysis is applied to study the spatiotemporal organization of transitions between temporal states (i.e., how the brain transitions between different functional states over time). For more details, please refer to Fig 3 & section 2.3.

2.3. Frameworks for Study I and Study II

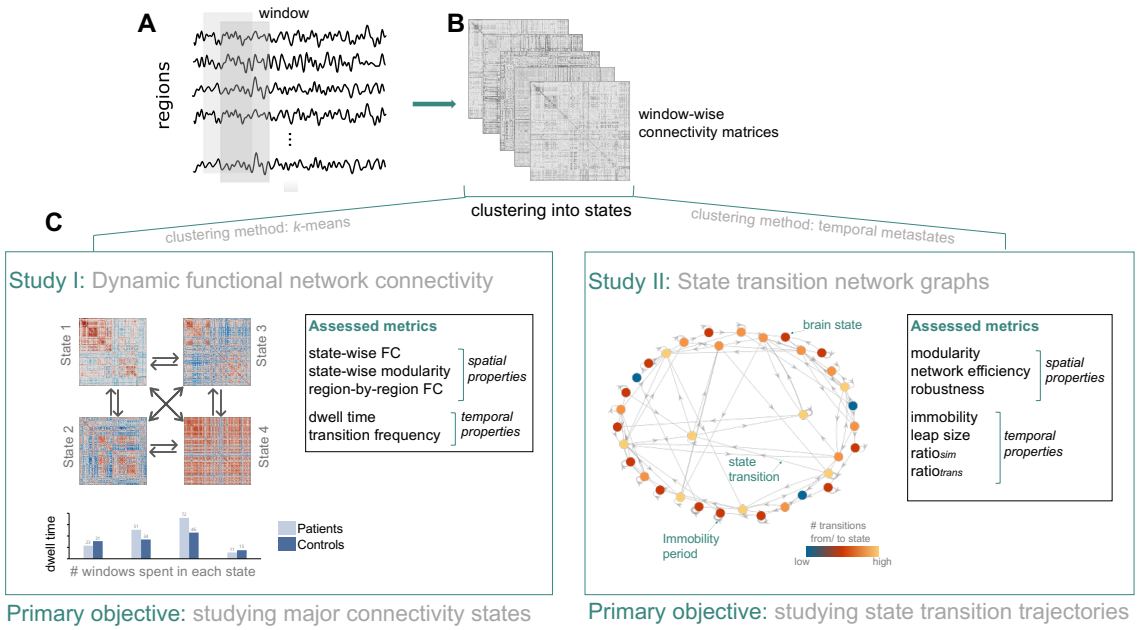

Figure 3: Schematic overview of the methodological and theoretical frameworks applied to explore FC dynamics in patients with NMDARE in Study I and Study II.

In both studies, we applied a sliding window approach, where regional time series of resting-state data are segmented into smaller windows (Fig 3A), with a connectivity matrix obtained for each window (Fig 3B). These matrices are then clustered into temporal patterns of connectivity (Fig 3C).

In *Study I*, four FC states were identified that represent the major connectivity patterns. The approach allowed for the assessment of state-wise characteristics, such as region-by-region differences in FC, average connectivity and modularity, as well as number of windows spent in a given state (dwell time), and transition frequencies between states (indicated with arrows).

In *Study II*, 35-55 temporal states were obtained, and a time-resolved transition network graph was created to analyze transition trajectories between states. The organizational properties of state sequences were assessed with modularity, network efficiency, and robustness, as well as immobility (indicated with self-referenced arrows) and leap size.

A more detailed prescription of the framworks is provided in the next two sections.

2.3.1. Framework *Study I*: Dynamic functional network connectivity – estimating recurrent patterns of FC

Connectivity states quantified within the framework of *dynamic functional network connectivity* reflect major, quasistable connectivity patterns that participants systematically revisit throughout the scan [53,62]. This approach has been validated many times [89], with most studies converging on a sliding window length between 30 and 60 seconds and identifying 4-6 distinct FC states [52,62,70–72,90]. These temporal states are hierarchically organized along varying connectivity levels: from a most frequently visited low-connectivity state to a least frequently visited high-connectivity state, with some intermediate states (also see results of *Study I*) [62,70,91]. While high-connectivity states may reflect moments of cost-intensive functional integration between networks, low-connectivity states show high functional segregation between networks, potentially reflecting a cost-efficient 'default state' [92]. Interestingly, these findings are consistent with our recent work on the complexity of regional BOLD dynamics [56].

Analyses of FC states yield obvious information beyond a static account of brain activity: First, the functional topology of each state can be analyzed individually. This includes the degree of functional integration and segregation (as measured with modularity, for example), overall connectivity, and region-by-region differences in FC. Second, state-wise temporal properties can be quantified to describe how functional coupling evolves over time, assessed with measures such as dwell time (time spent in a given state once entered). Third, across-state functional dynamics can be quantified as transition frequencies (number of switches between each pair of state). For a schematic overview, see Fig 3 and Table 2 for details on these metrics.

2.3.2. Framework *Study II*: Tracking state transitions – a systematic exploration of the brain's functional repertoire

The framework applied in *Study I* is particularly useful to examine spatial characteristics, such as region-by-region connectivity differences within and across the major FC patterns. However, only a few primary brain states are identified with this method which limits its ability to track fast temporal changes in FC [92,93]. *Study II* addresses this limitation and uses a considerably greater number of states, estimated based on shorter windows of 2 to 4 seconds. To track the progression of state transitions effectively, most studies suggest the use of 30-55 states [48,54–56].

Previous research on state transition dynamics has shown that functional state transitions follow a non-random, structured sequential order [94,95], potentially reflecting a systemic exploration of the brain's functional repertoire [93]. Interestingly, sequences of brain states seem to be organized in a modular manner: brain states are clustered into modules of akin states, that show higher transition frequencies amongst each other as compared to states from different modules [95]. This may ensure stable information representation, while maintaining flexibility of responsiveness [88].

Analogous to the connectome, state transitions are hierarchically organized in time [92], following the principal gradient of cortical organization [40]. Accordingly, brain activity cycles between two sets of states with inverse activity profiles. One end of this gradient is associated with lower-order unimodal systems (visual and sensori-motor), while the opposing end is associated with higher-order transmodal systems (default-mode, fronto-parietal) [92]. Traversing along this hierarchical gradient is thought to minimize metabolic demand while enabling systematic state exploration [96]. Remarkably, this principle is highly reproducible across samples and species [95,97].

Finally, prior studies demonstrated that spatiotemporal dynamics of state transitions are related to cognition and behavior [94]. This indicates that aberrant brain transition dynamics may contribute to cognitive or behavioral deficits in neuropsychiatric conditions. To capture these complex organizing principles of transition trajectories, Ramirez-Mahaluf *et al.* recently developed a framework where nodes in a graph represent brain states, and edges represent transitions between those states [94]. This *transition graph* is constructed form the temporal succession of functional brain states. Subsequently, graph theoretical metrics can be used to quantify the spatiotemporal organization of brain state transitions (see Fig 3, and for details on metrics, see Table 4).

3. Research questions

3.1. Brain states and transitions: a new perspective on functional reorganization in NMDARE

This work builds upon earlier studies on static FC in NMDARE by examining the spatiotemporal dynamics of brain connectivity patterns in this patient population. The goal is to uncover the dynamic network alterations associated with the wide range of neuropsychiatric symptoms observed in this condition. To this end, two studies were conducted:

In *Study I*, we performed *dynamic functional network connectivity* analysis [62] to obtain discrete functional brain states (see section 2.3.1) in people with NMDARE and healthy controls. Based on these states, we (i) assessed state-wise group differences in FC and state dynamics, (ii) explored the relationship between state dynamics, disease severity, and duration, and (iii) employed an unsupervised machine learning approach to evaluate the potential of each brain state to discriminate patients from controls in a predictive classification framework.

In *Study II*, we studied *transition trajectories of brain state exploration* in NMDARE, using the recently developed analysis framework introduced in section 2.3.2 [94]. Based on the transition networks, we (i) assessed group differences in the spatial topology of transition networks using graph theoretical measures, (ii) conducted between-group comparisons for two measures that aim to represent the biological costs of state transitions (leap size and immobility), and (iii) explored the relationship between state transition properties and disease severity in patients with NMDARE.

4. Methods & Results for *Study I* and *Study II*

4.1. *Study I*: State-dependent signatures of NMDARE

4.1.1. Methods & materials

This section summarizes the main methods & materials used in von Schwanenflug *et al*. [91]. For more comprehensive information on the analyses, please refer to the dedicated Methods section therein.

Participants:

For this study, we collected resting-state fMRI data from a large sample size of 57 patients with NMDARE and 61 healthy controls with no statistical difference between groups regarding age & sex. NMDARE diagnosis was based on clinical presentation and the presence of IgG NMDA receptor antibodies in cerebrospinal fluid. Patients were in the post-acute stage, with a median of 2.43 years from disease onset to MRI, and a median disease severity of mRS 1.00 at the time of the scan. Controls had no history of neurological or psychiatric conditions. Sample characteristics are summarized in Table 1. All participants provided written consent, and the study was approved by the local ethics committee. Further information on treatment and medication during the disease course can be found in von Schwanenflug *et al.* [91], Supplementary Table 1.

Table 1: Demographic variables and clinical measures of the participants in *Study I*. Table from von Schwanenflug *et al.* [91].

		Patients	Healthy Controls
N		57	61
Sex	♀ / ♂	50/7	54/7
Age (years)	Median ± IQR	25.00 ± 14.50	26.00 ± 11.00
mRS at scan	Median ± IQR	1.00 ± 1.00	..
Disease duration	Median ± IQR	62.00 ± 59.50	..
Time between disease onset and scan (years)	Median ± IQR	2.43 ± 2.95	..

Table lists median and interquartilerange (IQR) of age, mRS at day of scan, and disease duration. mRS = modified Rankin Scale [0-4], higher scores indicate higher disease severity; disease duration = days in acute care; N = number of participants.

MRI data acquisition and analysis:
MRI data was acquired using a 20-channel head coil and a 3T Trim Trio scanner. An echoplanar imaging sequence (repetition time [TR] = 2.25 s, echo time [TE] = 30 ms, 260 volumes, voxel size = 3.4 × 3.4 × 3.4 mm^3) was used for resting-state fMRI data and a high-resolution T1-weighted magnetization-prepared rapid gradient echo sequence (voxel size = 1 × 1 × 1 mm^3) was used for structural scans. Preprocessing of the resting-state fMRI data included discarding the first five volumes, slice time correction, realignment, spatial normalization, and spatial smoothing using a 6-mm kernel. A dedicated MATLAB toolbox was used for group independent component analysis, resulting in a parcellation of 39 regions of interest that were subsequently assigned to functional resting-state networks [33].

Static and dynamic functional network connectivity analysis:
For each participant, sliding window correlation (see section 2.1.) was applied to obtain functional dynamics. Thus, the functional time series of each region of interest was divided into consecutive overlapping time-windows of 67.5 seconds length that slid in steps of 2.25 seconds. Within each window, Pearson's correlation between all region pairs was computed. Subsequently, four discrete functional network connectivity states were defined with *k*-means clustering as described in section 2.3.1, resulting in average whole-brain correlation matrices for both static FC and each dynamic state.

Group differences in static and dynamic functional network connectivity:
First, we analyzed the spatial topology of static FC and each state (dynamic FC).

This involved evaluating whole-brain modularity and overall connectivity (a), as well as FC for all region pairs for static and state-wise connectivity matrices (b). To estimate group differences in modularity and overall connectivity (a), a permutation-based t-test was conducted for the static analysis. For the state analyses, a two-way ANOVA was employed to estimate group- and state-wise effects. Post-hoc analyses were conducted using a Kruskal-Wallis test. To assess group differences in FC between all region pairs for the static and state-wise connectivity matrices (b), non-parametric t-tests were used and adjusted to correct for multiple comparisons [98].

Second, we analyzed the temporal state dynamics using dwell time and transition frequency. Here, a two-way ANOVA was used to estimate group- and state-wise

effects. Post-hoc comparisons were evaluated using either a non-parametric t-test or a Tukey's test depending on data characteristics.

For a detailed explanation of the spatial and temporal metrics used in the analysis, please refer to Table 2.

Correlation with clinical variables:

We conducted post-hoc Pearson's correlation analyses to investigate the relationship between disease severity variables (i.e., acute days in hospitalization and modified Rankin Scale (mRS) scores at the time of the scan), and dynamic metrics (i.e., dwell time and transition frequency).

Table 2: Description of spatial and temporal metrics assessed for between-group comparisons between NMDARE patients and healthy controls.

Metric	Definition
Modularity [85,99]	In *Study I*, modularity defines the degree to which the static FC matrix and each state can be subdivided into modules with maximally high FC within modules and maximally low FC between modules. In the dynamic analyses, modularity was calculated for all windows in each state and then averaged for each subject. Measure of functional segregation.
Overall connectivity	Calculated as the absolute mean connectivity of the static FC matrix or of each state. In the dynamic analyses, overall connectivity was calculated for all windows in each state and then averaged for each subject.
Pairwise FC differences	Group differences in FC between all region pairs with respect to connectivity strength. This was done for the static connectivity matrix as well as each state in the dynamic network analysis.
Dwell time	Average number of windows a participant spends in a particular state once entered.
Transition frequency	Absolute number of transitions between each pair of states.

State-wise classification:

Lastly, we evaluated the ability of static and dynamic FC (encompassing the the four dynamic states) to distinguish between patients and controls utilizing a supervised binary classification approach. Following previous work from Peer *et al.* [49], FC of the visual, fronto-parietal, and default-mode network areas were considered as input features. For each state, as well as for the static connectivity matrix, logistic regression

models were trained to predict group status (patients vs. healthy controls) in a leave-one-out cross validation scheme.

4.1.2. Results

The key findings of the study are displayed in Fig 4 and summarized below. Please refer to von Schwanenflug *et al.* [91] for a detailed report of the results.

i. Clustering analyses identified four major FC states (Fig 4A). While the global spatial topologies (i.e., modularity and overall connectivity) did not differ between groups, they differed considerably between states: the dominant (i.e., most frequently visited) state 1 closely resembled the static FC pattern exhibiting low overall connectivity and moderate modularity. States 2 and 3 both displayed elevated overall connectivity, yet only state 2 had a notably segregated structure (i.e., high modularity). Unlike state 3, which showed highly integrated and interconnected connectivity patterns, state 4 showed high modularity but reduced overall connectivity (see Fig 4A+B and von Schwanenflug *et al.* [91] Supplementary Tables 3-8 for detailed test statistics).
ii. Region-by-region group comparison in FC yielded characteristic patterns of FC alterations in 3 out of 4 states in patients compared to controls (Fig 4A, detailed test statistics can be found in von Schwanenflug *et al.* [91]: Table 1 and Table 2).
    a. In the dominant (i.e., most visited) state, we observed a significant reduction in FC between the hippocampus and the mPFC ($t = 4.01$, $p_{FDR} = 0.0016$). Interestingly, this finding closely aligns with the patterns observed in the static FC analyses ($t = 4.36$, $p_{FDR} < 0.001$; refer to Fig 1 in von Schwanenflug *et al.* [91]). Consequently, our results support and validate previous observations, and appear to drive findings in static analyses.
    b. In addition, these findings are complemented by widespread disruptions in FC in state 2 and 3, including FC changes within the default-mode network, and between frontal and visual regions as well as subcortical areas – findings that went unnoticed in static FC analysis.
    c. Interestingly, in state 2, higher disease severity was significantly associated with a decrease in FC between mPFC and angular gyrus ($r = -0.37$, $p = 0.019$).

iii. Patients showed increased dwell time in state 2 (d = -0.42, p = 0.032), while at the same time showing decreased dwell time in state 1 (d = 0.40, p = 0.020) compared to controls (Fig 4C). This indicates a systematic shift in state preference in patients from the dominant state 1 to the less frequent, but highly segregated state 2.

iv. Furthermore, patients exhibited increased transition frequency between states with low (state 1) and high (state 2) functional segregation (d = -0.50, p = 0.0063) and between states with high (state 3) and low (state 4) overall FC (d = -0.34, p = 0.043, Fig 4C).

   a. Remarkably, increased transition frequency between state 1 and 2 was associated with higher disease severity (r = 0.34, p = 0.012).

v. Lastly, a supervised classification approach further emphasizes the benefit of increasing temporal resolution: the power to predict group status varied and reached up to 78.6% (Fig 4D), exceeding the performance of the static classification (72%, von Schwanenflug *et al.* [91]), and highlighting the uniqueness of each state.

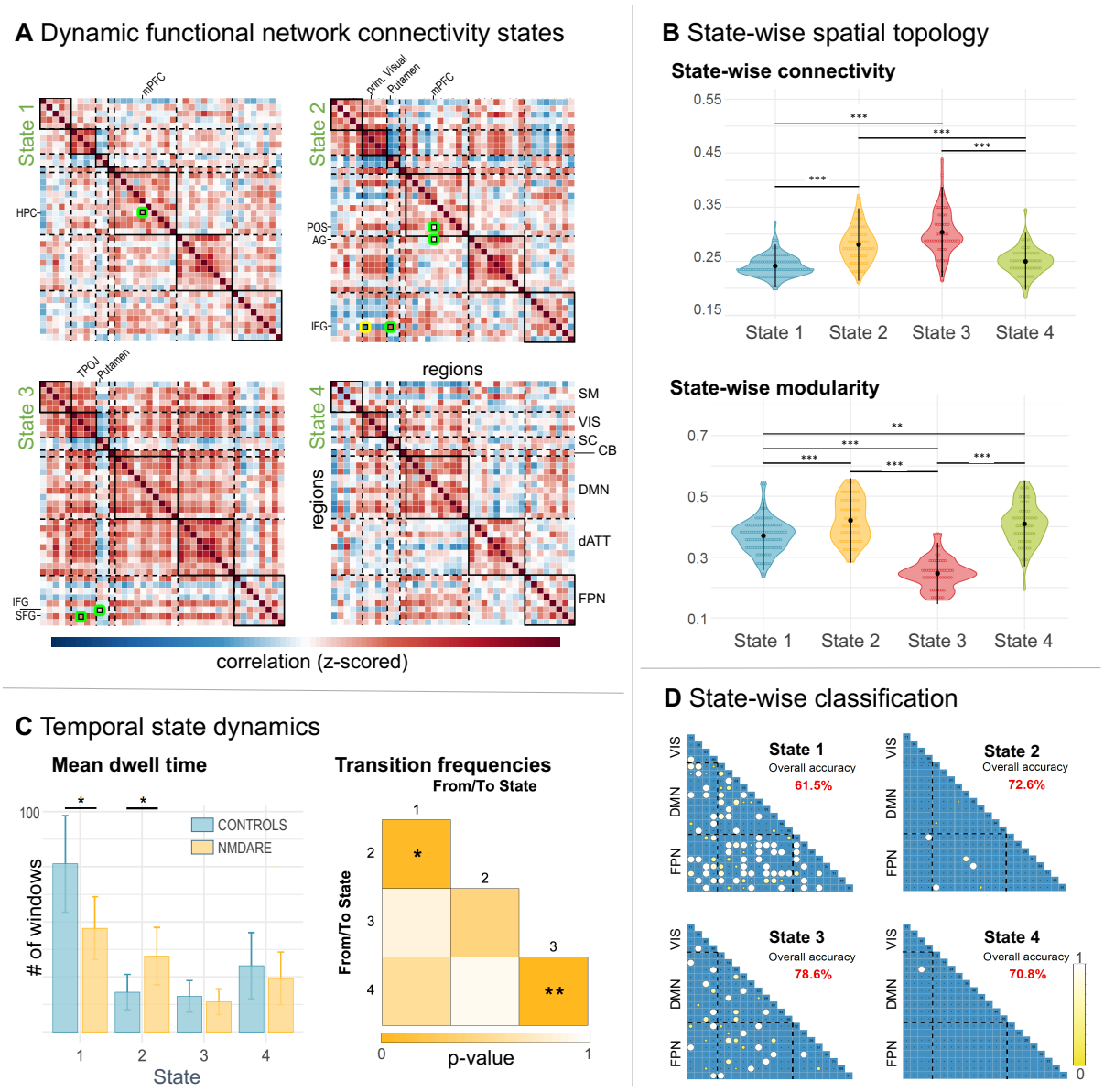

Figure 4: Results *Study I* – Dynamic functional network connectivity. A Dynamic functional network connectivity states. Each matrix displays the mean FC matrix for each state across patients and healthy controls, with darker red colors indicating stronger correlation and darker blue colors indicating stronger anti-correlation between regions. Green and yellow circles denote significantly lower and higher correlation values, respectively, in patients compared to controls. The diagonal rectangles represent functional networks. **B State-wise spatial topology.** State-wise comparison of average connectivity and modularity revealed significant differences between states but not between groups. States 2 and 3 exhibited stronger overall connectivity than States 1 and 4, while States 2 and 4 showed higher modularity than States 1 and 3. Black dots and vertical lines represent mean and standard deviation. **C Temporal state dynamics.** Group differences in average dwell time (left) and transition frequencies between states (right). Patients had lower dwell times in State 1 and longer dwell times in State 2, as well as higher transition frequencies between States 1 and 2, and between States 3 and 4, compared to controls. For transition frequencies, the direction of transition was ignored. **D State-wise classification.** State-wise feature selection matrices indicate the importance for each feature for predicting group status, with bigger and brighter circles indicating higher importance. Classification accuracy for each state is denoted in red.
Statistical significance was denoted by $*p < 0.05$, $**p < 0.01$, or $***p < 0.001$, with temporal state dynamics not corrected for multiple comparisons. CB = cerebellar network, DMN = default-mode network, dATT = dorsal attention network, FPN = fronto-parietal network, SM = sensori-motor network, VIS = visual network; AG = angular gyrus, HPC = hippocampus, IFG = inferior frontal gyrus, mPFC = medial prefrontal cortex, POS = parieto-occipital gyrus, SFG = superior frontal gyrus, TPOJ = temporo-parieto-occipital junction. Figure and captions adapted from von Schwanenflug *et al*. [91].

4.2. *Study II*: Reduced resilience of state transitions in NMDARE

4.2.1. Methods & materials

This section summarizes the main methods & materials used in von Schwanenflug *et al*. [100].

Participants:

This study included a large sample size of 73 patients with NMDARE and 73 healthy controls with no statistical difference between groups regarding age & sex. NMDARE diagnosis was confirmed by clinical presentation and the detection of IgG NMDA receptor antibodies in cerebrospinal fluid. Patients were in the post-acute stage, with a median of 2.97 years from disease onset to MRI, and a median disease severity of mRS 1.00 at the time of the scan. Controls had no history of neurological or psychiatric disorders. Clinical and demographic details are summarized in Table 3. All participants gave written consent, and the study was approved by the local ethics committee. Additional treatment information is available in von Schwanenflug *et al.* [100], Table 1 & Supplementary Table S1.

Table 3: Demographic variables and clinical measures of the participants in *Study II*. Table from von Schwanenflug *et al.* [100].

		Patients	Healthy Controls
N		73	73
Sex	female/male	62/11	62/11
Age (years)	Median ± IQR (N)	28.55 +/- 8.7 (73)	28.50 ± 8.5 (73)
mRS at scan	Median ± IQR (N)	1.00 ± 1.5 (70)	..
Disease duration (hospitalization time)	Median ± IQR (N)	67.50 ± 72.00 (68)	..
Years between disease onset and study	Mean ± SD (N)	2.97 ± 2.48 (71)	..

Table lists median and interquartile range (IQR) of age, mRS at scan, disease duration, and time between scan and diagnosis. Disease duration = days in acute care; N = number of participants; mRS = modified Rankin Scale.

MRI data acquisition and analysis:

MRI data was acquired using a 20-channel head coil and a 3T Trim Trio scanner. An echoplanar imaging sequence (repetition time [TR] = 2.25 s, echo time [TE] = 30 ms, 260 volumes, voxel size = 3.4 × 3.4 × 3.4 mm^3) was used for resting-state fMRI data and a high-resolution T1-weighted magnetization-prepared rapid gradient echo sequence (voxel size = 1 × 1 × 1 mm^3) was used for structural scans. Preprocessing of functional images included removal of the first 4 volumes, slice-timing correction, realignment, detrending, intensity normalization, spatial smoothing, ICA-AROMA for head motion correction, regression of white matter and cerebrospinal fluid time series, demeaning, and band-pass filtering according to Parkes *et al.* [101].

Meta-state estimation and transition network construction:

To further analyze the functional data, we extracted the time-series of 638 regions of interest based on a functional atlas template as previously described [39,94]. Then, for each participant, we divided the time series of each region into non-overlapping windows of ~5 seconds length, and computed FC within each window between any two regions using Multiplication of Temporal Derivatives [77]. These FC values were then clustered into 35 to 55 brain states, resulting in a time-resolved transition network graph with brain states as nodes and transitions between brain states as weighted, directed edges (Fig 5A).

Group comparisons of transition network properties:

The organization of transition networks was assessed using modularity, network efficiency, and robustness. To evaluate the temporal properties of state transitions, leap size, immobility, and overall transition frequency were calculated. Additionally, the within-to-between module state similarity ratio ($ratio_{sim}$) and the within-to-between module transitions ratio ($ratio_{trans}$) were computed for each participant. All metrics are described in detail in Table 4.

General linear models were used to compare graph metrics, transition frequencies, $ratio_{sim}$, and $ratio_{trans}$ between groups, with head motion, framewise displacement, age, and sex as nuisance variables for each metric separately.

Correlation of network properties with disease severity:

Next, the relationship between metrics and disease severity was investigated. To this end, we calculated a composite z-score for each patient, which reflected disease severity based on the patients' mRS scores at the day of the scan and disease duration (days in acute care). Subsequently, Pearson's correlation between network properties and disease severity was computed and corrected for multiple comparisons [98].

Table 4: Description of network properties assessed in *Study II* for between-group comparisons between NMDARE patients and healthy controls. Table from von Schwanenflug *et al.* [100].

Metric	Definition
Modularity [85,99]	This network parameter quantifies the degree to which the transition network can be subdivided into clearly defined groups or modules of states with maximally possible number of within-module transitions and minimally possible number of between-module transitions. A high modularity indicates that states within a module show particularly high transition frequencies compared to states from different modules.
Global efficiency [85,102,103]	The global efficiency quantifies the average number of transitions necessary to reach one state from any other states in the network.
Local efficiency [85,102,103]	The local efficiency is the global efficiency (see above) computed on a particular state. In a transition network, this measure indicates how well-connected neighboring states are among each other. The local efficiency gets averaged across all states in a transition network.
Immobility [94]	Immobility quantifies the average number of windows a participant remained in the same state before transitioning to a different state.
Leap size [94]	Leap size is the average distance between consecutive states excluding periods of immobility. It is defined as the spatial distance between one state and the next one (1 – correlation coefficient of their connectivity matrices). It therefore measures the magnitude of 'jumps' between states and is thought to reflect metabolic cost of state transitions, assuming that transitions between more distinct states are more costly.
Robustness [104]	Measure of resilience against fragmentation of a network. Nodes (states) of the transition network are randomly removed one by one. A high robustness of a transition network indicates that even in the absence of several nodes (states), transitions among the remaining states are still possible.
Transition frequency	Overall number of transitions between different states excluding the periods of immobility.
$Ratio_{sim}$	The ratio of within-to-between state similarity is defined as the average correlation of states within a module divided by the average correlation of states between modules.

Ratio$_{trans}$	The ratio of within-to-between module transitions is the absolute number of transitions between states within the same module divided by the absolute number of transitions between modules.

Functional topology of brain states:

Lastly, we investigated which regions diverged most in their connectivity strength across states. Following Krohn et al. [56], the distance across meta-states (DAMS) for each pair of regions and for each participant was calculated. A high value of DAMS indicates that the connectivity pattern diverges strongly between brain states, while a low DAMS implies that the connectivity strength between two regions remains constant across all states of a transition network.

4.2.2. Results

The key findings of *Study II* are summarized below. Please refer to von Schwanenflug et al. [100] for a detailed report of the results.

i. Between-group comparison of network properties (Fig 5B) indicated reduced resilience of state transition networks in patients compared to controls, which manifests in
   a. lower local efficiency of the network – fewer transitions between neighboring (and thus similar) states (t = -2.41, p_{FDR} = 0.029, d = 0.40),
   b. higher leap size – transitions between more distinct states (t = 2.18, p_{FDR} = 0.037, d = 0.36), and
   c. reduced robustness of the patients' transition networks against perturbations (t = -2.01, p_{FDR} = 0.048, d = 0.33).
   d. modularity (t = -1.43, p_{FDR} = 0.12, d = 0.27), global efficiency (t = 1.00, p_{FDR} = 0.20, d = 0.17), and immobility (t = -0.32, p_{FDR} = 0.38, d = 0.05) of transitions networks did not differ between groups.

ii. Moreover, patients showed a significantly lower ratio$_{trans}$ and ratio$_{sim}$ compared to controls (ratio$_{trans:}$ t = -2.48, p_{FDR} = 0.026, d = 0.40; ratio$_{sim:}$ t = -2.48, p_{FDR} = 0.026, d = 0.41), while the overall number of transitions did not differ between groups (t = 0.32, p_{FDR} = 0.377, d = 0.05). This suggests that patients more frequently move

between states from different modules compared to controls, possibly reflecting a dissolved architecture of transition networks in NMDARE.

iii. Significant network properties correlated with disease severity (Fig 5C), highlighting the clinical relevance of our findings. Specifically, we found that higher disease severity was associated with
   a. higher leap size (Pearson's r = 0.37, p_{FDR} = 0.0030),
   b. decreased robustness (Pearson's r = -0.37, p_{FDR} = 0.0030),
   c. lower $ratio_{sim}$ (Pearson's r = -0.40, p_{FDR} = 0.0030),
   d. and lower $ratio_{trans}$ (Pearson's r = -0.33, p_{FDR} = 0.0064).

iv. Lastly, in both groups the divergence in connectivity across states were most pronounced in visual and sensori-motor areas, suggesting that state transitions are mainly initiated by connectivity changes in unimodal networks. Patients exhibited even greater divergence in connectivity within these networks compared to controls, potentially explaining the increased temporal instability in brain state transitions (Fig 5D).

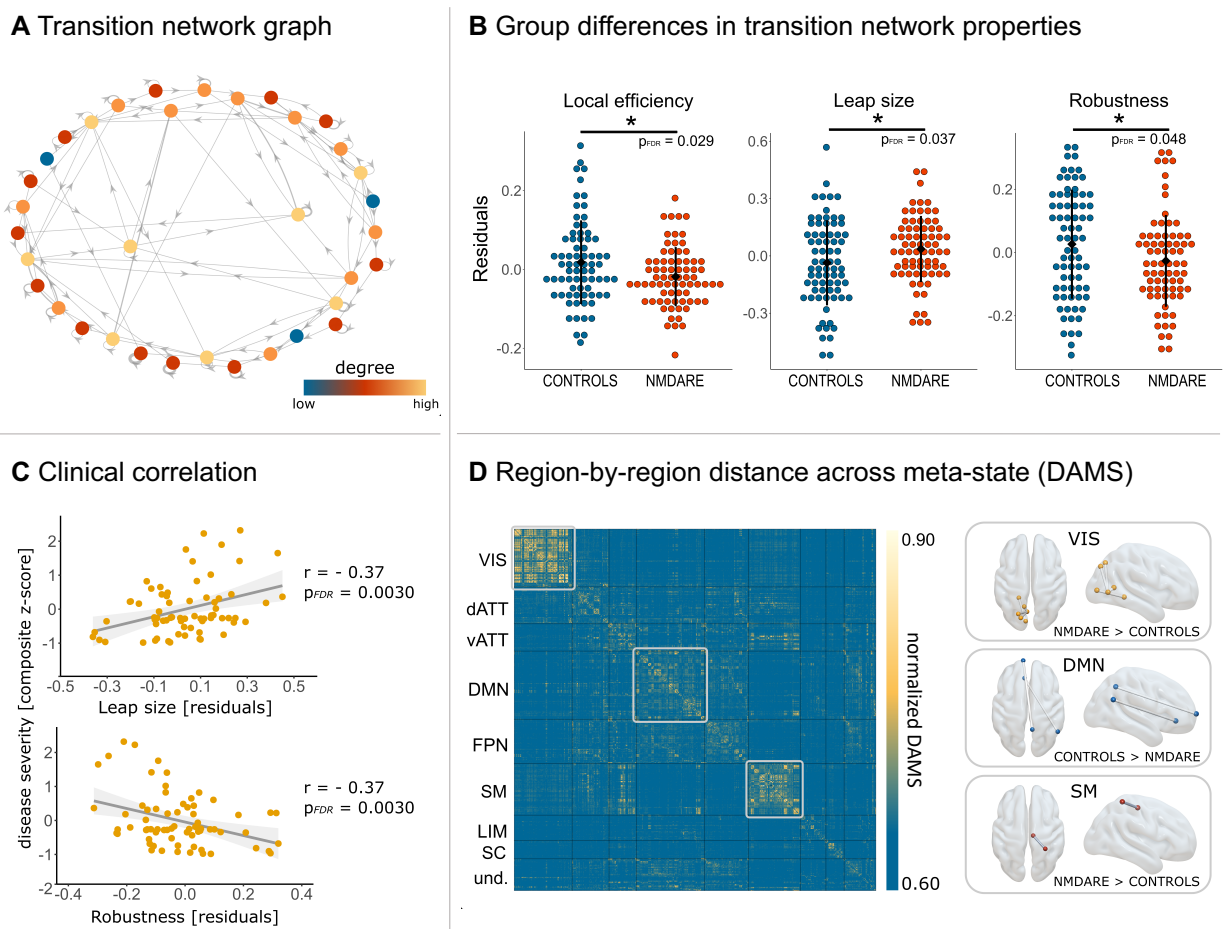

Figure 5: Results *Study II* – Temporal meta-state analysis. **A Transition network graph of an exemplary participant.** In this state transition network visualization, nodes (i.e., brain states) are colored based on their degree, i.e., the number of transitions to/ from that state. The distance between two nodes represents their transition cost (1 minus correlation). The thickness of the edges indicates the number of transitions between the nodes, and the arrows indicate the direction of the transition. Self-connections indicate immobility periods, where there were no changes in meta-states between two consecutive time windows. **B Group differences in transition network properties.** Between-group comparisons of graph theoretical measures. Only significant metrics are shown. Coloured dots represent the residuals after nuisance regression. Black dots and whiskers represent the mean and standard deviation. **C Clinical correlation.** Correlation between disease severity (composite z-score) and altered network properties (residuals after nuisance regression). Correlation plots for local efficiency, $ratio_{sim}$ and $ratio_{trans}$ are shown in Supplementary Figure 3 in von Schwanenflug *et al.* [100]. **D Region-by-region distance across meta-states (DAMS).** The DAMS matrix displays how coupling strength varies between brain regions across meta-states. High DAMS values (yellow) indicate strong differences in connectivity strength across meta-states, while low DAMS values (blue) indicate more consistent connectivity strength. Brain plots on the right show group differences within functional networks. Differences in DAMS between patients and controls were found in edges within the visual, default-mode, and sensori-motor networks. VIS = visual network, dATT = dorsal attention network, vATT = ventral attention network, DMN = default mode network, FPN = fronto-parietal network, SM = sensori-motor network, LIM = limbic network, SC = subcortical network, und. = undefined.
* indicates significant difference with $p_{FDR} < .05$.
Figure and captions adapted from von Schwanenflug *et al*. [100].

5. Discussion

5.1. Scope of the present thesis and summary of findings

NMDARE is a severe antibody-mediated inflammatory disease with a characteristic neuropsychiatric syndrome [6]. Despite the severe disease course, standard clinical structural MRI shows no or only mild abnormalities in most patients [22,23], motivating the search for functional signatures of the disease. Indeed, conventional static FC analyses have identified widespread alterations in connectivity linked to cognitive and psychiatric symptom severity [23,49,50,105]. However, these results are based on overly simplistic, static models of brain function. As brain activity is intrinsically dynamic [54], models that integrate time-dependent properties of connectivity are crucial to understand functional reorganization in NMDARE.

To close this gap, the present thesis studied alterations in the *temporal dynamics* of functional brain organization in patients with NMDARE. To this end, FC dynamics in NMDARE were compared to healthy control particpants from two perspectives:

First, spatial and temporal patterns of major FC states were identified and compared between groups in a well-established neuroimaging framework [62]. In the second study, an innovative method [94] was applied to investigate alterations in the sequence of state exploration – measured as temporal transitions between patterns of spontaneous brain activity.

In the first study, patients showed state-specific impairments of FC in three out of four states, along with a systematic shift in dwell time from the dominant, low-connectivity state to a less frequent, but highly segregated state. In addition, patients exhibited an increased volatility of overall state transitions. These findings were associated with measures of disease severity. Furthermore, a supervised machine learning approach showed higher predictive power in dynamic in contrast to static FC models. While these findings reveal state-dependent changes in FC and a characteristic dynamic profile of state dynamics in patients with NMDARE, detailed investigation of individualized temporal dynamics and transition trajectories was limited due to a comparatively low spatial and temporal resolution.

Therefore, the second study extended these findings and investigated alterations in patterns of state exploration. By employing a graph-analytical framework, we identified reduced stability of functional state transitions and a disrupted architecture

of transition networks in patients with NMDARE that was again related to disease severity.

Together, our analyses show that NMDARE is associated with a clinically relevant destabilization of brain state transitions, thereby offering new perspectives on the functional reorganization of brain dynamics in the disease. Our results moreover demonstrate the potential of time-resolved FC analyses for the identification of biomarkers in NMDARE and other neuropsychiatric disorders.

5.2. Implications of the findings

Together, the findings of our studies show that NMDARE is characterized by an increased volatility of temporal brain states. These changes in brain dynamics reflect *functional* reorganization and aligns well with the clinico-radiological paradox detailed in section 1.1.

Prior research has indicated that the efficiency of transitioning between states is closely linked with cognitive performance and motor abilities [94]. This suggests that an irregular pattern of state exploration in NMDARE underpins some of the identified dysfunctions [52,93] and aligns well with the clinical correlations observed in this thesis. Overall, this indicates that the clinical symptoms of NMDARE might be more accurately attributed to functional reorganization — possibly as an expression of NMDA hypoactivity — than purely structural damage.

In patients with NMDARE, the internalization of the NMDA receptor triggered by autoantibodies leads to a decrease in receptor density [13]. This likely impacts glutamatergic neurotransmission, which drive transient fluctuations in neural oscillations [106,107]. Alterations in these neural dynamics could compromise the temporal coordinations of brain regions. Such disruptions might disturb the balance of brain activity patterns, so that NMDA receptor hypofunction potentially results in excessively unstable state transitions [108,109], which are generally thought to facilitate the exploration of the functional repertoire [110].

The present thesis supports this view and highlights the key role of functional brain dynamics in the functional reorganization in NMDARE.

5.3. Limitations of the present thesis and open questions in the study of dynamic FC

Some limitations of the current work deserve mentioning: First, the sliding window approach requires a pre-specification of the window length. As it is likely that the brain operates on different temporal scales, the window size inherently limits the temporal spectrum that can be captured. Hence, the optimal choice of this parameter depends on the scientific question and is a matter of ongoing debate. Methodological improvements try to address these shortcomings and propose windowless approaches such as time-frequency analysis [54,111] or hidden Markov models [92]. However, these methods have their own weaknesses and assumptions [63].

Second, the current studies are based on the *connectivity* between brain regions, which is by definition a relational measure of the activity between two brain regions. However, it is crucial to consider time-varying properties of the brain regions themselves, as their activity ultimately shape the inter-regional relations, functional hierarchy and temporal dynamics of the brain. As such, measures such as time-varying complexity or edge-time series may give deeper insights into the processes that give rise to the phenomenon of dynamic network connectivity [56,112].

Third, *k*-means clustering enforces the extraction of a predefined *k* number of states. While this ensures comparability between participants and groups, it may not mirror the actual number of states present in the current data set. Yet, for the dynamic functional network connectivity as applied in *Study I*, the replicability of states has been demonstrated to be high within and between participants [89]. For the temporal meta-state analysis as applied in *Study II*, we scrutinized our analysis across multiple *k* meta-states to ensure that parameter choices did not bias the observed results (see von Schwanenflug *et al.* [100]).

Forth, direct implications for clinical practice are limited due to the lack of statistical power in neuroimaging studies to identify reliable individual markers of dynamic change, complex processing pipelines and the limited amount of available data. Nevertheless, our findings provide important new insights into the functional brain reorganization in NMDARE and strengthen the foundation needed to ultimately develop practical implementations.

5.4. Future directions: functional dynamics as the next frontier in the brain sciences

Psychiatric disorders often share similar characteristics to NMDARE including clinical and cognitive symptoms, neurotransmitter dysfunctions, or genetic risk factors. Identifying FC markers sensitive enough to complement existing criteria and symptom checklists would greatly benefit the clinical setting, facilitating faster initial diagnosis and enhanced differential diagnosis. In the case of NMDARE, there have been consistent findings of marked disruptions in FC, making it a potential neuroimaging marker [23,49,50,91,100]. Further investigating brain dynamics (that is, including the dimension of time in describing functional signals) opens up new opportunities to identify more precise characteristics of brain functioning and pathology. Indeed, our studies demonstrate that some states are more relevant to disease expression than others, and dynamic features of FC enhance classification performance compared to static accounts of FC [71,113]. This exciting finding suggests that dynamic state analyses can be useful in distinguishing disease, disease stage, or prognostic outcome.

NMDARE in particular provides remarkable opportunities to identify transdiagnostic characteristics, as the condition shares dynamic network alterations that are associated with NMDAR dysfunction with other pathologies – first and foremost schizophrenia [114]. Given the large overlap in psychiatric symptomatology in these diseases, NMDA receptor hypofunction is further strengthened as the hypothesized pathophysiological basis for cognitive and psychiatric symptoms in both diseases [18]. Recent studies on time-resolved FC in schizophrenia have shown notable convergence with our findings, including a shift in state preference [70], increased overall transition frequencies [71], and altered modular network structure [115]. The extent to which these dynamic features are indeed transdiagnostic must therefore be investigated in specifically designed comparative studies.

Computational models that go beyond diagnosis and biomarkers simulate neuronal and neurotransmitter systems for treatment purposes. These models suggest that interventions using pharmacological and electromagnetic methods have the potential to rebalance perturbed state dynamics by inducing state transitions [93,97,116]. Similar to our study, they suggest that state transitions can be initiated by specific regions, making them promising treatment targets [93]. Other studies using deep-brain stimulation have identified targets that can rebalance and elicit changes in brain

connectivity, alleviating symptoms in neuropsychiatric and motor disorders that are otherwise resistant to treatment [93].

To advance its clinical potential and bring brain dynamics into practice, a key goal of the next years is to gain a comprehensive understanding on human brain dynamics. Only if we identify unifying principles, can we advance our understanding of neurological and psychiatric disorders and enable functional dynamics to ultimately serve as risk, diagnostic, and prognostic markers.

5.5. Conclusion

The studies presented in the current thesis are the first to investigate the temporal dynamics of brain activity in patients with NMDARE. Overall, the results suggest that the clinical manifestations of NMDARE may be more closely tied to (dynamic) functional reorganization than to structural damage. Using state-of-the art methodologies in contemporary human neuroimaging, both studies suggested a clinically relevant increase in the volatility of brain dynamics and reduced resilience of brain state transitions, emphasizing the importance of brain dynamics in the manifestation of the disease. These results highlight that, by increasing the temporal resolution from minutes to seconds, time-resolved FC analyses add clinically valuable information and provide new insights beyond traditional FC analyses. Converging findings in other neuropsychiatric disorders furthermore strengthen the importance of spatiotemporal dynamics for improved characterization and understanding of functional reorganization in these diseases. Critically, association with measures of disease severity stresses the potential of time-resolved FC measures as novel disease biomarkers and treatment targets in NMDARE.

References

1 Dalmau J, Tüzün E, Wu H, Masjuan J, Rossi JE, Voloschin A, Baehring JM, Shimazaki H, Koide R, King D, Mason W, Sansing LH, Dichter MA, Rosenfeld MR, Lynch DR. Paraneoplastic anti-N-methyl-D-aspartate receptor encephalitis associated with ovarian teratoma. *Ann Neurol*. 2007;61:25–36. https://doi.org/10.1002/ana.21050

2 Dubey D, Pittock SJ, Kelly CR, McKeon A, Lopez-Chiriboga AS, Lennon VA, Gadoth A, Smith CY, Bryant SC, Klein CJ, Aksamit AJ, Toledano M, Boeve BF, Tillema J-M, Flanagan EP. Autoimmune encephalitis epidemiology and a comparison to infectious encephalitis: Autoimmune Encephalitis. *Ann Neurol*. 2018;83:166–77. https://doi.org/10.1002/ana.25131

3 Dalmau J, Graus F. Antibody-Mediated Encephalitis. *N Engl J Med*. 2018;378:840–51. https://doi.org/10.1056/NEJMra1708712

4 Al-Diwani A, Handel A, Townsend L, Pollak T, Leite MI, Harrison PJ, Lennox BR, Okai D, Manohar SG, Irani SR. The psychopathology of NMDAR-antibody encephalitis in adults: a systematic review and phenotypic analysis of individual patient data. *Lancet Psychiatry*. 2019;6:235–46. https://doi.org/10.1016/S2215-0366(19)30001-X

5 Dalmau J, Armangué T, Planagumà J, Radosevic M, Mannara F, Leypoldt F, Geis C, Lancaster E, Titulaer MJ, Rosenfeld MR, Graus F. An update on anti-NMDA receptor encephalitis for neurologists and psychiatrists: mechanisms and models. *Lancet Neurol*. 2019;18:1045–57. https://doi.org/10.1016/S1474-4422(19)30244-3

6 Kayser MS, Dalmau J. Anti-NMDA receptor encephalitis, autoimmunity, and psychosis. *Schizophr Res*. 2016;176:36–40. https://doi.org/10.1016/j.schres.2014.10.007

7 Titulaer MJ, McCracken L, Gabilondo I, Armangué T, Glaser C, Iizuka T, Honig LS, Benseler SM, Kawachi I, Martinez-Hernandez E, Aguilar E, Gresa-Arribas N, Ryan-Florance N, Torrents A, Saiz A, Rosenfeld MR, Balice-Gordon R, Graus F, Dalmau J. Treatment and prognostic factors for long-term outcome in patients with anti-NMDA receptor encephalitis: an observational cohort study. *Lancet Neurol*. 2013;12:157–65. https://doi.org/10.1016/S1474-4422(12)70310-1

8 McKeon GL, Scott JG, Spooner DM, Ryan AE, Blum S, Gillis D, Langguth D, Robinson GA. Cognitive and Social Functioning Deficits after Anti-N-Methyl-D-Aspartate Receptor Encephalitis: An Exploratory Case Series. *J Int Neuropsychol Soc*. 2016;22:828–38. https://doi.org/10.1017/S1355617716000679

9 Finke C, Kopp UA, Prüss H, Dalmau J, Wandinger K-P, Ploner CJ. Cognitive deficits following anti-NMDA receptor encephalitis. *J Neurol Neurosurg Psychiatry*. 2012;83:195–8. https://doi.org/10.1136/jnnp-2011-300411

10 Heine J, Kopp UA, Klag J, Ploner CJ, Prüss H, Finke C. Long-term cognitive outcome in ANTI-NMDA receptor encephalitis. *Ann Neurol*. 2021;ana.26241. https://doi.org/10.1002/ana.26241

11 Bartels F, Krohn S, Nikolaus M, Johannsen J, Wickström R, Schimmel M, Häusler M, Berger A, Breu M, Blankenburg M, Stoffels J, Hendricks O, Bernert G, Kurlemann G, Knierim E, Kaindl A, Rostásy K, Finke C. Clinical and Magnetic Resonance Imaging Outcome Predictors in Pediatric ANTI–N-METHYL-D-ASPARTATE Receptor Encephalitis. *Ann Neurol*. 2020;88:148–59. https://doi.org/10.1002/ana.25754

12 Armangue T, Leypoldt F, Málaga I, Raspall-Chaure M, Marti I, Nichter C, Pugh J, Vicente-Rasoamalala M, Lafuente-Hidalgo M, Macaya A, Ke M, Titulaer MJ, Höftberger R, Sheriff H, Glaser C, Dalmau J. Herpes simplex virus encephalitis is a trigger of brain autoimmunity: HSV Triggers Brain Autoimmunity. *Ann Neurol*. 2014;75:317–23. https://doi.org/10.1002/ana.24083

13 Dalmau J, Lancaster E, Martinez-Hernandez E, Rosenfeld MR, Balice-Gordon R. Clinical experience and laboratory investigations in patients with anti-NMDAR encephalitis. *Lancet Neurol*. 2011;10:63–74. https://doi.org/10.1016/S1474-4422(10)70253-2

14 Lang K, Prüß H. Anti-NMDA-Rezeptor Enephalitis - eine wichtige Differenzialdiagnose. *InFo Neurologie*. 2016;18:40–8. https://doi.org/10.1007/s15005-016-1780-y

15 Palomero-Gallagher N, Amunts K, Zilles K. Transmitter Receptor Distribution in the Human Brain. *Brain Mapping*. Elsevier 2015:261–75. https://doi.org/10.1016/B978-0-12-397025-1.00221-9

16 Monaghan D, Cotman C. Distribution of N-methyl-D-aspartate-sensitive L-[3H]glutamate-binding sites in rat brain. *J Neurosci*. 1985;5:2909–19. https://doi.org/10.1523/JNEUROSCI.05-11-02909.1985

17 Zhu S, Stein RA, Yoshioka C, Lee C-H, Goehring A, Mchaourab HS, Gouaux E. Mechanism of NMDA Receptor Inhibition and Activation. *Cell*. 2016;165:704–14. https://doi.org/10.1016/j.cell.2016.03.028

18 Moghaddam B, Javitt D. From revolution to evolution: the glutamate hypothesis of schizophrenia and its implication for treatment. *Neuropsychopharmacol Off Publ Am Coll Neuropsychopharmacol*. 2012;37:4–15.

https://doi.org/10.1038/npp.2011.181

19 Stein H, Barbosa J, Rosa-Justicia M, Prades L, Morató A, Galan-Gadea A, Ariño H, Martinez-Hernandez E, Castro-Fornieles J, Dalmau J, Compte A. Reduced serial dependence suggests deficits in synaptic potentiation in anti-NMDAR encephalitis and schizophrenia. *Nat Commun*. 2020;11:4250. https://doi.org/10.1038/s41467-020-18033-3

20 Ghasemi M, Phillips C, Trillo L, De Miguel Z, Das D, Salehi A. The role of NMDA receptors in the pathophysiology and treatment of mood disorders. *Neurosci Biobehav Rev*. 2014;47:336–58. https://doi.org/10.1016/j.neubiorev.2014.08.017

21 Gresa-Arribas N, Titulaer MJ, Torrents A, Aguilar E, McCracken L, Leypoldt F, Gleichman AJ, Balice-Gordon R, Rosenfeld MR, Lynch D, Graus F, Dalmau J. Antibody titres at diagnosis and during follow-up of anti-NMDA receptor encephalitis: a retrospective study. *Lancet Neurol*. 2014;13:167–77. https://doi.org/10.1016/S1474-4422(13)70282-5

22 Graus F, Titulaer MJ, Balu R, Benseler S, Bien CG, Cellucci T, Cortese I, Dale RC, Gelfand JM, Geschwind M, Glaser CA, Honnorat J, Höftberger R, Iizuka T, Irani SR, Lancaster E, Leypoldt F, Prüss H, Rae-Grant A, Reindl M, Rosenfeld MR, Rostásy K, Saiz A, Venkatesan A, Vincent A, Wandinger K-P, Waters P, Dalmau J. A clinical approach to diagnosis of autoimmune encephalitis. *Lancet Neurol*. 2016;15:391–404. https://doi.org/10.1016/S1474-4422(15)00401-9

23 Heine J, Prüss H, Bartsch T, Ploner CJ, Paul F, Finke C. Imaging of autoimmune encephalitis – Relevance for clinical practice and hippocampal function. *Neuroscience*. 2015;309:68–83. https://doi.org/10.1016/j.neuroscience.2015.05.037

24 Huettel SA, Song AW, McCarthy G. *Functional magnetic resonance imaging*. 2nd ed. Sunderland, Mass: Sinauer Associates 2008.

25 Hillman EMC. Coupling Mechanism and Significance of the BOLD Signal: A Status Report. *Annu Rev Neurosci*. 2014;37:161–81. https://doi.org/10.1146/annurev-neuro-071013-014111

26 Cipolla M. Control of Cerebral Blood Flow. *The Cerebral Circulation*. Morgan & Claypool Life Sciences 2009. https://www.ncbi.nlm.nih.gov/books/NBK53082/?report=classic

27 Fox MD, Raichle ME. Spontaneous fluctuations in brain activity observed with functional magnetic resonance imaging. *Nat Rev Neurosci*. 2007;8:700–11. https://doi.org/10.1038/nrn2201

28 Buzsáki G, Draguhn A. Neuronal Oscillations in Cortical Networks. *Science*.

2004;304:1926–9. https://doi.org/10.1126/science.1099745

29 Uddin LQ. Bring the Noise: Reconceptualizing Spontaneous Neural Activity. *Trends Cogn Sci*. 2020;24:734–46. https://doi.org/10.1016/j.tics.2020.06.003

30 Biswal B, Zerrin Yetkin F, Haughton VM, Hyde JS. Functional connectivity in the motor cortex of resting human brain using echo-planar mri. *Magn Reson Med*. 1995;34:537–41. https://doi.org/10.1002/mrm.1910340409

31 Power JD, Cohen AL, Nelson SM, Wig GS, Barnes KA, Church JA, Vogel AC, Laumann TO, Miezin FM, Schlaggar BL, Petersen SE. Functional Network Organization of the Human Brain. *Neuron*. 2011;72:665–78. https://doi.org/10.1016/j.neuron.2011.09.006

32 Power JD, Schlaggar BL, Petersen SE. Studying Brain Organization via Spontaneous fMRI Signal. *Neuron*. 2014;84:681–96. https://doi.org/10.1016/j.neuron.2014.09.007

33 Yeo BT, Krienen FM, Sepulcre J, Sabuncu MR, Lashkari D, Hollinshead M, Roffman JL, Smoller JW, Zöllei L, Polimeni JR, Fischl B, Liu H, Buckner RL. The organization of the human cerebral cortex estimated by intrinsic functional connectivity. *J Neurophysiol*. 2011;106:1125–65. https://doi.org/10.1152/jn.00338.2011

34 Biswal BB, Mennes M, Zuo X-N, Gohel S, Kelly C, Smith SM, Beckmann CF, Adelstein JS, Buckner RL, Colcombe S, Dogonowski A-M, Ernst M, Fair D, Hampson M, Hoptman MJ, Hyde JS, Kiviniemi VJ, Kotter R, Li S-J, Lin C-P, Lowe MJ, Mackay C, Madden DJ, Madsen KH, Margulies DS, Mayberg HS, McMahon K, Monk CS, Mostofsky SH, Nagel BJ, Pekar JJ, Peltier SJ, Petersen SE, Riedl V, Rombouts SARB, Rypma B, Schlaggar BL, Schmidt S, Seidler RD, Siegle GJ, Sorg C, Teng G-J, Veijola J, Villringer A, Walter M, Wang L, Weng X-C, Whitfield-Gabrieli S, Williamson P, Windischberger C, Zang Y-F, Zhang H-Y, Castellanos FX, Milham MP. Toward discovery science of human brain function. *Proc Natl Acad Sci*. 2010;107:4734–9. https://doi.org/10.1073/pnas.0911855107

35 Smith SM, Vidaurre D, Beckmann CF, Glasser MF, Jenkinson M, Miller KL, Nichols TE, Robinson EC, Salimi-Khorshidi G, Woolrich MW, Barch DM, Uğurbil K, Van Essen DC. Functional connectomics from resting-state fMRI. *Trends Cogn Sci*. 2013;17:666–82. https://doi.org/10.1016/j.tics.2013.09.016

36 Petersen SE, Sporns O. Brain Networks and Cognitive Architectures. *Neuron*. 2015;88:207–19. https://doi.org/10.1016/j.neuron.2015.09.027

37 Raichle ME, MacLeod AM, Snyder AZ, Powers WJ, Gusnard DA, Shulman GL. A default mode of brain function. *Proc Natl Acad Sci*. 2001;98:676–82.

https://doi.org/10.1073/pnas.98.2.676

38 Sporns O. The human connectome: a complex network: The human connectome. *Ann N Y Acad Sci*. 2011;1224:109–25. https://doi.org/10.1111/j.1749-6632.2010.05888.x

39 Crossley NA, Mechelli A, Vertes PE, Winton-Brown TT, Patel AX, Ginestet CE, McGuire P, Bullmore ET. Cognitive relevance of the community structure of the human brain functional coactivation network. *Proc Natl Acad Sci*. 2013;110:11583–8. https://doi.org/10.1073/pnas.1220826110

40 Margulies DS, Ghosh SS, Goulas A, Falkiewicz M, Huntenburg JM, Langs G, Bezgin G, Eickhoff SB, Castellanos FX, Petrides M, Jefferies E, Smallwood J. Situating the default-mode network along a principal gradient of macroscale cortical organization. *Proc Natl Acad Sci*. 2016;113:12574–9. https://doi.org/10.1073/pnas.1608282113

41 Finn ES, Shen X, Scheinost D, Rosenberg MD, Huang J, Chun MM, Papademetris X, Constable RT. Functional connectome fingerprinting: identifying individuals using patterns of brain connectivity. *Nat Neurosci*. 2015;18:1664–71. https://doi.org/10.1038/nn.4135

42 Rosenberg MD, Finn ES, Scheinost D, Papademetris X, Shen X, Constable RT, Chun MM. A neuromarker of sustained attention from whole-brain functional connectivity. *Nat Neurosci*. 2016;19:165–71. https://doi.org/10.1038/nn.4179

43 Avery EW, Yoo K, Rosenberg MD, Greene AS, Gao S, Na DL, Scheinost D, Constable TR, Chun MM. Distributed Patterns of Functional Connectivity Predict Working Memory Performance in Novel Healthy and Memory-impaired Individuals. *J Cogn Neurosci*. 2020;32:241–55. https://doi.org/10.1162/jocn_a_01487

44 Mantwill M, Gell M, Krohn S, Finke C. Brain connectivity fingerprinting and behavioural prediction rest on distinct functional systems of the human connectome. *Commun Biol*. 2022;5:261. https://doi.org/10.1038/s42003-022-03185-3

45 Fornito A, Zalesky A, Breakspear M. The connectomics of brain disorders. *Nat Rev Neurosci*. 2015;16:159–72. https://doi.org/10.1038/nrn3901

46 Braun U, Muldoon SF, Bassett DS. On Human Brain Networks in Health and Disease. In: John Wiley & Sons Ltd, ed. *eLS*. Chichester, UK: John Wiley & Sons, Ltd 2015:1–9. https://doi.org/10.1002/9780470015902.a0025783

47 Uhlhaas PJ, Singer W. Neuronal Dynamics and Neuropsychiatric Disorders:

Toward a Translational Paradigm for Dysfunctional Large-Scale Networks. *Neuron*. 2012;75:963–80. https://doi.org/10.1016/j.neuron.2012.09.004

48 Horn A, Fox MD. Opportunities of connectomic neuromodulation. *NeuroImage*. 2020;221:117180. https://doi.org/10.1016/j.neuroimage.2020.117180

49 Peer M, Prüss H, Ben-Dayan I, Paul F, Arzy S, Finke C. Functional connectivity of large-scale brain networks in patients with anti-NMDA receptor encephalitis: an observational study. *Lancet Psychiatry*. 2017;4:768–74. https://doi.org/10.1016/S2215-0366(17)30330-9

50 Finke C, Kopp UA, Scheel M, Pech L-M, Soemmer C, Schlichting J, Leypoldt F, Brandt AU, Wuerfel J, Probst C, Ploner CJ, Prüss H, Paul F. Functional and structural brain changes in anti-N-methyl-D-aspartate receptor encephalitis: Finke et al: MRI in Anti-NMDAR Encephalitis. *Ann Neurol*. 2013;n/a-n/a. https://doi.org/10.1002/ana.23932

51 Deco G, Jirsa VK, McIntosh AR. Emerging concepts for the dynamical organization of resting-state activity in the brain. *Nat Rev Neurosci*. 2011;12:43–56. https://doi.org/10.1038/nrn2961

52 Hutchison RM, Womelsdorf T, Allen EA, Bandettini PA, Calhoun VD, Corbetta M, Della Penna S, Duyn JH, Glover GH, Gonzalez-Castillo J, Handwerker DA, Keilholz S, Kiviniemi V, Leopold DA, de Pasquale F, Sporns O, Walter M, Chang C. Dynamic functional connectivity: Promise, issues, and interpretations. *NeuroImage*. 2013;80:360–78. https://doi.org/10.1016/j.neuroimage.2013.05.079

53 Calhoun VD, Miller R, Pearlson G, Adalı T. The Chronnectome: Time-Varying Connectivity Networks as the Next Frontier in fMRI Data Discovery. *Neuron*. 2014;84:262–74. https://doi.org/10.1016/j.neuron.2014.10.015

54 Chang C, Glover GH. Time–frequency dynamics of resting-state brain connectivity measured with fMRI. *NeuroImage*. 2010;50:81–98. https://doi.org/10.1016/j.neuroimage.2009.12.011

55 Preti MG, Bolton TA, Van De Ville D. The dynamic functional connectome: State-of-the-art and perspectives. *NeuroImage*. 2017;160:41–54. https://doi.org/10.1016/j.neuroimage.2016.12.061

56 Krohn S, von Schwanenflug N, Waschke L, Romanello A, Gell M, Garrett DD, Finke C. A spatiotemporal complexity architecture of human brain activity. *Sci Adv*. 2023;9:eabq3851. https://doi.org/10.1126/sciadv.abq3851

57 Garrett DD, Kovacevic N, McIntosh AR, Grady CL. Blood Oxygen Level-

Dependent Signal Variability Is More than Just Noise. *J Neurosci*. 2010;30:4914–21. https://doi.org/10.1523/JNEUROSCI.5166-09.2010

58 Chen JE, Chang C, Greicius MD, Glover GH. Introducing co-activation pattern metrics to quantify spontaneous brain network dynamics. *NeuroImage*. 2015;111:476–88. https://doi.org/10.1016/j.neuroimage.2015.01.057

59 Liu X, Zhang N, Chang C, Duyn JH. Co-activation patterns in resting-state fMRI signals. *NeuroImage*. 2018;180:485–94. https://doi.org/10.1016/j.neuroimage.2018.01.041

60 Esfahlani F, Jo Y, Faskowitz J, Byrge L, Kennedy DP, Sporns O, Betzel RF. High-amplitude cofluctuations in cortical activity drive functional connectivity. *Proc Natl Acad Sci*. 2020;117:28393–401. https://doi.org/10.1073/pnas.2005531117

61 Roberts JA, Gollo LL, Abeysuriya RG, Roberts G, Mitchell PB, Woolrich MW, Breakspear M. Metastable brain waves. *Nat Commun*. 2019;10:1056. https://doi.org/10.1038/s41467-019-08999-0

62 Allen EA, Damaraju E, Plis SM, Erhardt EB, Eichele T, Calhoun VD. Tracking whole-brain connectivity dynamics in the resting state. *Cereb Cortex N Y N 1991*. 2014;24:663–76. https://doi.org/10.1093/cercor/bhs352

63 Lurie DJ, Kessler D, Bassett DS, Betzel RF, Breakspear M, Kheilholz S, Kucyi A, Liégeois R, Lindquist MA, McIntosh AR, Poldrack RA, Shine JM, Thompson WH, Bielczyk NZ, Douw L, Kraft D, Miller RL, Muthuraman M, Pasquini L, Razi A, Vidaurre D, Xie H, Calhoun VD. Questions and controversies in the study of time-varying functional connectivity in resting fMRI. *Netw Neurosci*. 2020;4:30–69. https://doi.org/10.1162/netn_a_00116

64 Gonzalez-Castillo J, Hoy CW, Handwerker DA, Robinson ME, Buchanan LC, Saad ZS, Bandettini PA. Tracking ongoing cognition in individuals using brief, whole-brain functional connectivity patterns. *Proc Natl Acad Sci*. 2015;112:8762–7. https://doi.org/10.1073/pnas.1501242112

65 Sadaghiani S, Poline J-B, Kleinschmidt A, D'Esposito M. Ongoing dynamics in large-scale functional connectivity predict perception. *Proc Natl Acad Sci*. 2015;112:8463–8. https://doi.org/10.1073/pnas.1420687112

66 Wang C, Ong JL, Patanaik A, Zhou J, Chee MWL. Spontaneous eyelid closures link vigilance fluctuation with fMRI dynamic connectivity states. *Proc Natl Acad Sci*. 2016;113:9653–8. https://doi.org/10.1073/pnas.1523980113

67 Garrett DD, Nagel IE, Preuschhof C, Burzynska AZ, Marchner J, Wiegert S, Jungehülsing GJ, Nyberg L, Villringer A, Li S-C, Heekeren HR, Bäckman L,

Lindenberger U. Amphetamine modulates brain signal variability and working memory in younger and older adults. *Proc Natl Acad Sci*. 2015;112:7593–8. https://doi.org/10.1073/pnas.1504090112

68 Armbruster-Genç DJN, Ueltzhöffer K, Fiebach CJ. Brain Signal Variability Differentially Affects Cognitive Flexibility and Cognitive Stability. *J Neurosci*. 2016;36:3978–87. https://doi.org/10.1523/JNEUROSCI.2517-14.2016

69 Garrett DD, Kovacevic N, McIntosh AR, Grady CL. The Modulation of BOLD Variability between Cognitive States Varies by Age and Processing Speed. *Cereb Cortex*. 2013;23:684–93. https://doi.org/10.1093/cercor/bhs055

70 Damaraju E, Allen EA, Belger A, Ford JM, McEwen S, Mathalon DH, Mueller BA, Pearlson GD, Potkin SG, Preda A, Turner JA, Vaidya JG, van Erp TG, Calhoun VD. Dynamic functional connectivity analysis reveals transient states of dysconnectivity in schizophrenia. *NeuroImage Clin*. 2014;5:298–308. https://doi.org/10.1016/j.nicl.2014.07.003

71 Rashid B, Damaraju E, Pearlson GD, Calhoun VD. Dynamic connectivity states estimated from resting fMRI Identify differences among Schizophrenia, bipolar disorder, and healthy control subjects. *Front Hum Neurosci*. 2014;8. https://doi.org/10.3389/fnhum.2014.00897

72 Bonkhoff AK, Espinoza FA, Gazula H, Vergara VM, Hensel L, Michely J, Paul T, Rehme AK, Volz LJ, Fink GR, Calhoun VD, Grefkes C. Acute ischaemic stroke alters the brain's preference for distinct dynamic connectivity states. *Brain*. 2020;143:1525–40. https://doi.org/10.1093/brain/awaa101

73 Demirtaş M, Tornador C, Falcón C, López-Solà M, Hernández-Ribas R, Pujol J, Menchón JM, Ritter P, Cardoner N, Soriano-Mas C, Deco G. Dynamic functional connectivity reveals altered variability in functional connectivity among patients with major depressive disorder: Dynamic Functional Connectivity in Major Depression. *Hum Brain Mapp*. 2016;37:2918–30. https://doi.org/10.1002/hbm.23215

74 Marchitelli R, Paillère-Martinot M-L, Bourvis N, Guerin-Langlois C, Kipman A, Trichard C, Douniol M, Stordeur C, Galinowski A, Filippi I, Bertschy G, Weibel S, Granger B, Limosin F, Cohen D, Martinot J-L, Artiges E. Dynamic Functional Connectivity in Adolescence-Onset Major Depression: Relationships With Severity and Symptom Dimensions. *Biol Psychiatry Cogn Neurosci Neuroimaging*. 2021;S2451902221001439. https://doi.org/10.1016/j.bpsc.2021.05.003

75 Kaiser RH, Whitfield-Gabrieli S, Dillon DG, Goer F, Beltzer M, Minkel J, Smoski M, Dichter G, Pizzagalli DA. Dynamic Resting-State Functional Connectivity in

Major Depression. *Neuropsychopharmacology*. 2016;41:1822–30. https://doi.org/10.1038/npp.2015.352

76 Yao Z, Shi J, Zhang Z, Zheng W, Hu T, Li Y, Yu Y, Zhang Z, Fu Y, Zou Y, Zhang W, Wu X, Hu B. Altered dynamic functional connectivity in weakly-connected state in major depressive disorder. *Clin Neurophysiol*. 2019;130:2096–104. https://doi.org/10.1016/j.clinph.2019.08.009

77 Fu Z, Caprihan A, Chen J, Du Y, Adair JC, Sui J, Rosenberg GA, Calhoun VD. Altered static and dynamic functional network connectivity in Alzheimer's disease and subcortical ischemic vascular disease: shared and specific brain connectivity abnormalities. *Hum Brain Mapp*. 2019;40:3203–21. https://doi.org/10.1002/hbm.24591

78 Gu Y, Lin Y, Huang L, Ma J, Zhang J, Xiao Y, Dai Z, Alzheimer's Disease Neuroimaging Initiative. Abnormal dynamic functional connectivity in Alzheimer's disease. *CNS Neurosci Ther*. 2020;26:962–71. https://doi.org/10.1111/cns.13387

79 Von Schwanenflug N, Koch SP, Krohn S, Broeders TAA, Lydon-Staley DM, Bassett DS, Schoonheim MM, Paul F, Finke C. Increased flexibility of brain dynamics in patients with multiple sclerosis. *Brain Commun*. 2023;fcad143. https://doi.org/10.1093/braincomms/fcad143

80 Romanello A, Krohn S, Von Schwanenflug N, Chien C, Bellmann-Strobl J, Ruprecht K, Paul F, Finke C. Functional connectivity dynamics reflect disability and multi-domain clinical impairment in patients with relapsing-remitting multiple sclerosis. *NeuroImage Clin*. 2022;36:103203. https://doi.org/10.1016/j.nicl.2022.103203

81 Savva AD, Mitsis GD, Matsopoulos GK. Assessment of dynamic functional connectivity in resting-state fMRI using the sliding window technique. *Brain Behav*. 2019;9:e01255. https://doi.org/10.1002/brb3.1255

82 Bullmore E, Sporns O. Complex brain networks: graph theoretical analysis of structural and functional systems. *Nat Rev Neurosci*. 2009;10:186–98. https://doi.org/10.1038/nrn2575

83 Bullmore ET, Bassett DS. Brain Graphs: Graphical Models of the Human Brain Connectome. *Annu Rev Clin Psychol*. 2011;7:113–40. https://doi.org/10.1146/annurev-clinpsy-040510-143934

84 Watts DJ, Strogatz SH. Collective dynamics of 'small-world' networks. *Nature*. 1998;393:440–2. https://doi.org/10.1038/30918

85 Rubinov M, Sporns O. Complex network measures of brain connectivity: Uses and interpretations. *NeuroImage*. 2010;52:1059–69. https://doi.org/10.1016/j.neuroimage.2009.10.003

86 Bertolero MA, Yeo BTT, D'Esposito M. The modular and integrative functional architecture of the human brain. *Proc Natl Acad Sci*. 2015;112:E6798–807. https://doi.org/10.1073/pnas.1510619112

87 Sporns O, Betzel RF. Modular Brain Networks. *Annu Rev Psychol*. 2016;67:613–40. https://doi.org/10.1146/annurev-psych-122414-033634

88 Bullmore E, Sporns O. The economy of brain network organization. *Nat Rev Neurosci*. 2012;13:336–49. https://doi.org/10.1038/nrn3214

89 Abrol A, Damaraju E, Miller RL, Stephen JM, Claus ED, Mayer AR, Calhoun VD. Replicability of time-varying connectivity patterns in large resting state fMRI samples. *NeuroImage*. 2017;163:160–76. https://doi.org/10.1016/j.neuroimage.2017.09.020

90 Leonardi N, Van De Ville D. On spurious and real fluctuations of dynamic functional connectivity during rest. *NeuroImage*. 2015;104:430–6. https://doi.org/10.1016/j.neuroimage.2014.09.007

91 von Schwanenflug N, Krohn S, Heine J, Paul F, Prüss H, Finke C. State-dependent signatures of anti- *N* -methyl- D -aspartate receptor encephalitis. *Brain Commun*. 2022;4:fcab298. https://doi.org/10.1093/braincomms/fcab298

92 Vidaurre D, Smith SM, Woolrich MW. Brain network dynamics are hierarchically organized in time. *Proc Natl Acad Sci*. 2017;114:12827–32. https://doi.org/10.1073/pnas.1705120114

93 Kringelbach ML, Deco G. Brain States and Transitions: Insights from Computational Neuroscience. *Cell Rep*. 2020;32:108128. https://doi.org/10.1016/j.celrep.2020.108128

94 Ramirez-Mahaluf JP, Medel V, Tepper Á, Alliende LM, Sato JR, Ossandon T, Crossley NA. Transitions between human functional brain networks reveal complex, cost-efficient and behaviorally-relevant temporal paths. *NeuroImage*. 2020;219:117027. https://doi.org/10.1016/j.neuroimage.2020.117027

95 Ma Z, Zhang N. Temporal transitions of spontaneous brain activity. *eLife*. 2018;7:e33562. https://doi.org/10.7554/eLife.33562

96 Zalesky A, Fornito A, Cocchi L, Gollo LL, Breakspear M. Time-resolved resting-state brain networks. *Proc Natl Acad Sci U S A*. 2014;111:10341–6.

https://doi.org/10.1073/pnas.1400181111

97 Gu S, Betzel RF, Mattar MG, Cieslak M, Delio PR, Grafton ST, Pasqualetti F, Bassett DS. Optimal trajectories of brain state transitions. *NeuroImage*. 2017;148:305–17. https://doi.org/10.1016/j.neuroimage.2017.01.003

98 Benjamini Y, Hochberg Y. Controlling the False Discovery Rate: A Practical and Powerful Approach to Multiple Testing. *J R Stat Soc Ser B Methodol*. 1995;57:289–300. https://doi.org/10.1111/j.2517-6161.1995.tb02031.x

99 Blondel VD, Guillaume J-L, Lambiotte R, Lefebvre E. Fast unfolding of communities in large networks. *J Stat Mech Theory Exp*. 2008;2008:P10008. https://doi.org/10.1088/1742-5468/2008/10/P10008

100 von Schwanenflug N, Ramirez-Mahaluf JP, Krohn S, Romanello A, Heine J, Prüss H, Crossley NA, Finke C. Reduced resilience of brain state transitions in anti- *N* -methyl-D-aspartate receptor encephalitis. *Eur J Neurosci*. 2023;57:568–79. https://doi.org/10.1111/ejn.15901

101 Parkes L, Fulcher B, Yücel M, Fornito A. An evaluation of the efficacy, reliability, and sensitivity of motion correction strategies for resting-state functional MRI. *NeuroImage*. 2018;171:415–36. https://doi.org/10.1016/j.neuroimage.2017.12.073

102 Latora V, Marchiori M. Efficient Behavior of Small-World Networks. *Phys Rev Lett*. 2001;87:198701. https://doi.org/10.1103/PhysRevLett.87.198701

103 Fagiolo G. Clustering in complex directed networks. *Phys Rev E*. 2007;76:026107. https://doi.org/10.1103/PhysRevE.76.026107

104 Lhomme S. Analyse spatiale de la structure des réseaux techniques dans un contexte de risques. *Cybergeo*. Published Online First: 20 February 2015. https://doi.org/10.4000/cybergeo.26763

105 Cai L, Liang Y, Huang H, Zhou X, Zheng J. Cerebral functional activity and connectivity changes in anti-N-methyl-D-aspartate receptor encephalitis: A resting-state fMRI study. *NeuroImage Clin*. 2020;25:102189. https://doi.org/10.1016/j.nicl.2020.102189

106 Brunel N, Wang X-J. Effects of Neuromodulation in a Cortical Network Model of Object Working Memory Dominated by Recurrent Inhibition. *J Comput Neurosci*. 2001;11:63–85. https://doi.org/10.1023/A:1011204814320

107 Deco G, Jirsa VK. Ongoing cortical activity at rest: criticality, multistability, and ghost attractors. *J Neurosci Off J Soc Neurosci*. 2012;32:3366–75.

https://doi.org/10.1523/JNEUROSCI.2523-11.2012

108 Rolls ET. Glutamate, obsessive–compulsive disorder, schizophrenia, and the stability of cortical attractor neuronal networks. *Pharmacol Biochem Behav*. 2012;100:736–51. https://doi.org/10.1016/j.pbb.2011.06.017

109 Rolls ET. Attractor cortical neurodynamics, schizophrenia, and depression. *Transl Psychiatry*. 2021;11:215. https://doi.org/10.1038/s41398-021-01333-7

110 Kringelbach ML, Cruzat J, Cabral J, Knudsen GM, Carhart-Harris R, Whybrow PC, Logothetis NK, Deco G. Dynamic coupling of whole-brain neuronal and neurotransmitter systems. *Proc Natl Acad Sci*. 2020;117:9566–76. https://doi.org/10.1073/pnas.1921475117

111 Yaesoubi M, Miller RL, Calhoun VD. Mutually temporally independent connectivity patterns: A new framework to study the dynamics of brain connectivity at rest with application to explain group difference based on gender. *NeuroImage*. 2015;107:85–94. https://doi.org/10.1016/j.neuroimage.2014.11.054

112 Betzel RF, Fukushima M, He Y, Zuo X-N, Sporns O. Dynamic fluctuations coincide with periods of high and low modularity in resting-state functional brain networks. *NeuroImage*. 2016;127:287–97. https://doi.org/10.1016/j.neuroimage.2015.12.001

113 Vergara VM, Mayer AR, Kiehl KA, Calhoun VD. Dynamic functional network connectivity discriminates mild traumatic brain injury through machine learning. *NeuroImage Clin*. 2018;19:30–7. https://doi.org/10.1016/j.nicl.2018.03.017

114 Finke C. A transdiagnostic pattern of psychiatric symptoms in autoimmune encephalitis. *Lancet Psychiatry*. 2019;6:191–3. https://doi.org/10.1016/S2215-0366(19)30038-0

115 Alexander-Bloch AF, Gogtay N, Meunier D, Birn R, Clasen L, Lalonde F, Lenroot R, Giedd J, Bullmore ET. Disrupted Modularity and Local Connectivity of Brain Functional Networks in Childhood-Onset Schizophrenia. *Front Syst Neurosci*. 2010;4:147. https://doi.org/10.3389/fnsys.2010.00147

116 Deco G, Kringelbach ML, Jirsa VK, Ritter P. The dynamics of resting fluctuations in the brain: metastability and its dynamical cortical core. *Sci Rep*. 2017;7:3095. https://doi.org/10.1038/s41598-017-03073-5

Statutory declaration

„Ich, Nina Claudia von Schwanenflug, versichere an Eides statt durch meine eigenhändige Unterschrift, dass ich die vorgelegte Dissertation mit dem Thema: *Funktionelle Konnektivitätsdynamik bei Anti-NMDA Rezeptor Enzephalitis / Functional connectivity dynamics in anti-NMDA receptor encephalitis* selbstständig und ohne nicht offengelegte Hilfe Dritter verfasst und keine anderen als die angegebenen Quellen und Hilfsmittel genutzt habe.
Alle Stellen, die wörtlich oder dem Sinne nach auf Publikationen oder Vorträgen anderer Autoren/innen beruhen, sind als solche in korrekter Zitierung kenntlich gemacht. Die Abschnitte zu Methodik (insbesondere praktische Arbeiten, Laborbestimmungen, statistische Aufarbeitung) und Resultaten (insbesondere Abbildungen, Graphiken und Tabellen) werden von mir verantwortet.

Meine Anteile an etwaigen Publikationen zu dieser Dissertation entsprechen denen, die in der untenstehenden gemeinsamen Erklärung mit dem/der Erstbetreuer/in, angegeben sind. Für sämtliche im Rahmen der Dissertation entstandenen Publikationen wurden die Richtlinien des ICMJE (International Committee of Medical Journal Editors; www.icmje.og) zur Autorenschaft eingehalten. Ich erkläre ferner, dass ich mich zur Einhaltung der Satzung der Charité – Universitätsmedizin Berlin zur Sicherung Guter Wissen-schaftlicher Praxis verpflichte.

Weiterhin versichere ich, dass ich diese Dissertation weder in gleicher noch in ähnlicher Form bereits an einer anderen Fakultät eingereicht habe.

Die Bedeutung dieser eidesstattlichen Versicherung und die strafrechtlichen Folgen einer unwahren eidesstattlichen Versicherung (§§156, 161 des Strafgesetzbuches) sind mir bekannt und bewusst.“

Ort, Datum	Unterschrift

Statement of authorship

Nina Claudia von Schwanenflug hatte folgenden Anteil an den folgenden Publikationen:

Publikation 1:

von Schwanenflug, N., Krohn, S., Heine, J., Paul, F., Prüss, H., & Finke, C. (2022). *State-dependent signatures of anti-N-methyl-D-aspartate receptor encephalitis.* Brain Communications, 4(1), fcab298. https://doi.org/10.1093/braincomms/fcab298

Beitrag im Einzelnen: *Leitung zusammen mit CF in der Konzeptualisierung der Studie und des Manuskripts, umfangreiche Literaturrecherche für den Manteltext, Leitung der Datenverarbeitung (Prozessierung, Vorverarbeitung, statische und dynamische Gehirnaktivität), Hypothesengenerierung, statistische Datenanalyse (alle Gruppenvergleiche & Zustandsvergleiche, klinische Korrelationen), Erstellen aller Abbildungen, Erstellen aller Tabellen, Leitung im Verfassen, Einreichen und Überarbeitung des Manuskripts im Peer Review-Prozess.*

IF: 4.8

Publikation 2:

von Schwanenflug, N., Ramirez-Mahaluf, J. P., Krohn, S., Romanello, A., Heine, J., Prüss, H., Crossley, N. A., & Finke, C. (2023). *Reduced resilience of brain state transitions in anti-N-methyl-D-aspartate receptor encephalitis.* European Journal of Neuroscience, 57(3), 568–579. https://doi.org/10.1111/ejn.15901

Beitrag im Einzelnen: *Probandenauswahl & Gruppenmatching*, *erweiterte Literaturrecherche, Datenverarbeitung (Prozessierung, Vorverarbeitung, Erstellung von Übergangsnetzwerken), statistische Datenanalysen (Netzwerkanalysen, alle Gruppenvergleiche, klinische Korrelationen), Erstellen aller Abbildungen, Erstellen aller Tabellen, Leitung im Verfassen, Einreichen und Überarbeitung des Manuskripts im Peer Review-Prozess.*

IF: 3.69

_____

Unterschrift

Excerpt from Journal Summary List: ***Publication I***

This journal is not yet listed in the latest version of the ISI-WEB-List.

Publication I: State-dependent signatures of anti-N-methyl-D-aspartate receptor encephalitis

https://doi.org/10.1093/braincomms/fcab298 BRAIN COMMUNICATIONS 2022: Page 1 of 13 | 1

BRAIN COMMUNICATIONS

State-dependent signatures of anti-*N*-methyl-D-aspartate receptor encephalitis

Nina von Schwanenflug,[1,2] Stephan Krohn,[1,2] Josephine Heine,[1] Friedemann Paul,[1,3,4,5] Harald Prüss[1,6] and Carsten Finke[1,2]*

Traditional static functional connectivity analyses have shown distinct functional network alterations in patients with anti-*N*-methyl-D-aspartate receptor encephalitis. Here, we use a dynamic functional connectivity approach that increases the temporal resolution of connectivity analyses from minutes to seconds. We hereby explore the spatiotemporal variability of large-scale brain network activity in anti-*N*-methyl-D-aspartate receptor encephalitis and assess the discriminatory power of functional brain states in a supervised classification approach. We included resting-state functional magnetic resonance imaging data from 57 patients and 61 controls to extract four discrete connectivity states and assess state-wise group differences in functional connectivity, dwell time, transition frequency, fraction time and occurrence rate. Additionally, for each state, logistic regression models with embedded feature selection were trained to predict group status in a leave-one-out cross-validation scheme. Compared to controls, patients exhibited diverging dynamic functional connectivity patterns in three out of four states mainly encompassing the default-mode network and frontal areas. This was accompanied by a characteristic shift in the dwell time pattern and higher volatility of state transitions in patients. Moreover, dynamic functional connectivity measures were associated with disease severity and positive and negative schizophrenia-like symptoms. Predictive power was highest in dynamic functional connectivity models and outperformed static analyses, reaching up to 78.6% classification accuracy. By applying time-resolved analyses, we disentangle state-specific functional connectivity impairments and characteristic changes in temporal dynamics not detected in static analyses, offering new perspectives on the functional reorganization underlying anti-N-methyl-D-aspartate receptor encephalitis. Finally, the correlation of dynamic functional connectivity measures with disease symptoms and severity demonstrates a clinical relevance of spatiotemporal connectivity dynamics in anti-*N*-methyl-D-aspartate receptor encephalitis.

1 Department of Neurology, Charité—Universitätsmedizin Berlin, Corporate Member of Freie Universität Berlin, Humboldt-Universität zu Berlin, and Berlin Institute of Health, Berlin, Germany
2 Berlin School of Mind and Brain, Humboldt-Universität zu Berlin, Berlin, Germany
3 Experimental and Clinical Research Center, Max-Delbrück Center for Molecular Medicine and Charité—Universitätsmedizin Berlin, Berlin, Germany
4 Berlin Institute of Health, Berlin, Germany
5 NeuroCure Clinical Research Center, Charité—Universitätsmedizin Corporate Member of Freie Universität Berlin, Humboldt-Universität zu Berlin, and Berlin Institute of Health, Berlin, Germany
6 German Centre for Neurodegenerative Diseases, DZNE, Berlin, Germany

*Correspondence to: Carsten Finke
Charitéplatz 1
10117 Berlin,
Germany
E-mail: carsten.finke@charite.de

Keywords: autoimmune encephalitis; NMDA receptor; dynamic functional connectivity; supervised classification

Abbreviations: AG = angular gyrus; CB = cerebellar; dATT = dorsal attention network; DMN = default-mode network; FC = functional connectivity; FDR = false discovery rate; FNC = functional network connectivity; FPN = fronto-parietal network;

Received June 2, 2021. Revised October 13, 2021. Accepted January 3, 2022

HC = healthy controls; HPC = hippocampus; IFG = inferior frontal gyrus; LOOCV = leave-one-out cross-validation; mPFC = medial prefrontal cortex; MPRAGE = Magnetization-Prepared RApid Gradient Echo; mRS = modified Rankin scale; OFG = orbito-frontal gyrus; PC = principal component; PHG = parahippocampal gyrus; POS = parieto-occipital gyrus; prim. Visual = primary visual cortex; rs-fMRI = resting-state functional MRI; SB = subcortical; SFG = superior frontal gyrus SM = sensorimotor; SMA = supplementary motor area; STG = superior temporal gyrus; TE = echo time; TPOJ = temporo-parieto-occipital junction; TR = repetition time

Graphical Abstract

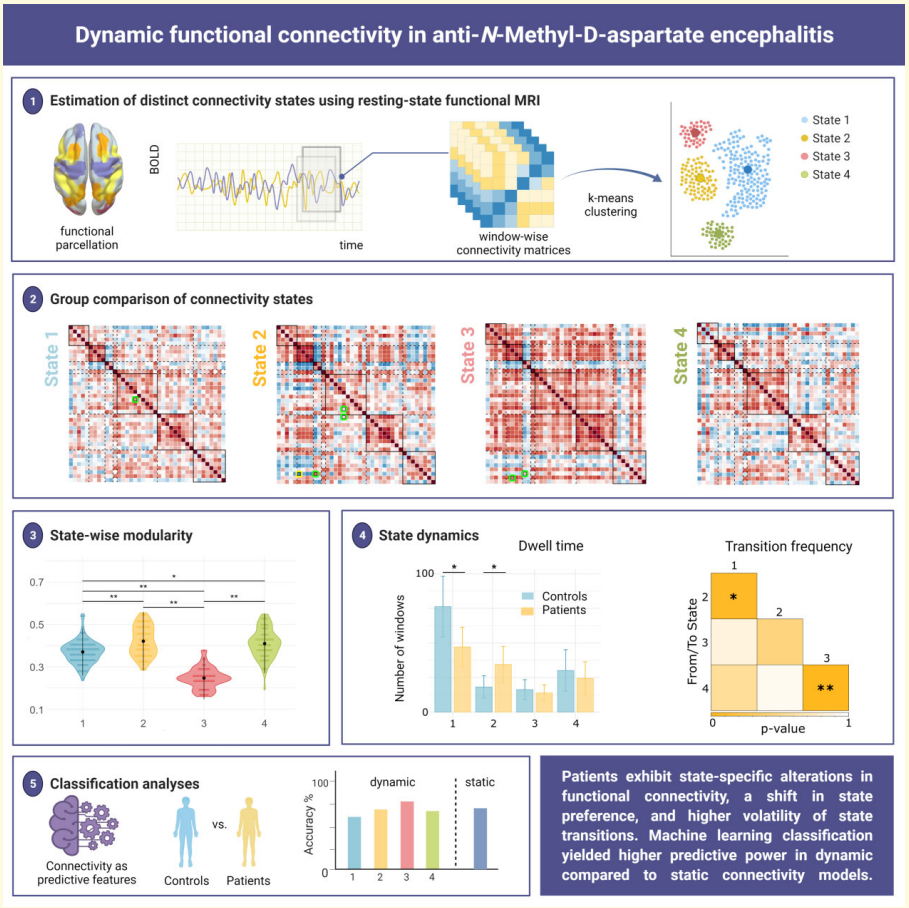

Introduction

Anti-*N*-methyl-D-aspartate (NMDA) receptor encephalitis is a severe autoimmune disorder of the CNS caused by antibodies targeting the NR1 subunit of the NMDA receptor.[1] The disease is characterized by a complex neuropsychiatric syndrome with delusions, hallucinations, movement abnormalities, autonomic dysfunction, decreased levels of consciousness and cognitive dysfunction, e.g. deficits of executive control and memory.[1–6]

Despite the severe disease course, routine clinical MRI reveals no abnormalities in 50–80% of patients.[5,7] In contrast, functional connectivity (FC) is disrupted in distinct functional networks, including medial-temporal, fronto-parietal and visual networks.[8] Specifically, hippocampal connectivity with medial prefrontal regions of the default-mode network

(DMN) is significantly impaired, and these alterations are associated with the severity of memory impairment. Moreover, disruption of fronto-parietal and ventral attention networks correlates with positive and negative schizophrenia-like symptoms.[3,8] These traditional resting-state FC analyses have thus contributed to reveal the mechanisms underlying clinical symptoms in anti-NMDA receptor encephalitis by assessing the coherence of brain activity between distinct regions. However, traditional FC analyses are 'static' in the sense that blood-oxygen-level dependent time series are averaged across a scan with duration of several minutes.

Yet, the brain is a complex dynamic system in which the strength and spatial organization of connectivity patterns can change within seconds, resulting in multiple spatiotemporal organization patterns during one MRI scan.[9–11] 'Dynamic' FC approaches capture these changes of functional brain organization and allow for the investigation of temporal properties, i.e. identification of distinct connectivity states and analysis of transition trajectories between these states—alterations of which may vary with the disease.[9] Indeed, recent studies report intriguing evidence that dynamic FC analyses enable a better characterization of network alterations in psychiatric and neurological diseases compared to static FC approaches.[10] Therefore, dynamic FC measures are increasingly understood as meaningful attributes to describe different disease phenotypes, e.g. in schizophrenia, major depression, stroke and Alzheimer's disease.[12–15]

One common method to analyse dynamic FC applies a clustering algorithm to obtain distinct functional brain states, which are defined as time-varying, but recurrent patterns of FC.[16] This approach provides a specifically promising tool for disentangling the dynamic network changes underlying the diverse neuropsychiatric symptoms in anti-NMDA receptor encephalitis. Here, we used this approach to (i) investigate the spatiotemporal properties of brain states in a large sample of patients with anti-NMDA receptor encephalitis and healthy controls (HC); (ii) explore the relationship between state dynamics, disease severity and duration and psychiatric symptoms and (iii) evaluate the potential of each brain state to discriminate between patients and controls using a supervised machine learning approach.

Materials and methods

Participants

For this study, 57 patients with anti-NMDA receptor encephalitis (female: 50, median age: 25.00 ± 14.50 years) were recruited from the Department of Neurology at Charité-Universitätsmedizin Berlin. The diagnosis was based on clinical presentation and detection of IgG NMDA receptor antibodies in the cerebrospinal fluid. Patients were in the post-acute disease stage, with a median of 2.43 years (± 2.95) between disease onset and MRI data acquisition. The median disease duration, i.e. days spent in hospitalization, was 63 days (± 56.50, $N = 52$). Disease severity at the time of scan was assessed based on the modified Rankin scale (mRS; median mRS: 1.00 ± 1.00, $N = 55$). The control group consisted of 61 age- and sex-matched healthy participants (female: 54, median age: 26.00 ± 11.00 years) with no history of neurological or psychiatric disease. Clinical and demographic characteristics are summarized in Supplementary Table 1. All participants gave written informed consent, and the study was approved by the local ethics committee.

MRI data acquisition

Structural and functional MRI data were acquired at the Berlin Center for Advanced Neuroimaging at Charité-Universitätsmedizin Berlin using a 20-channel head coil and a 3 T Trim Trio scanner (Siemens, Erlangen, Germany). For resting-state functional MRI (rs-fMRI), we employed an echoplanar imaging sequence [repetition time (TR) = 2.25 s, echo time = 30 ms, 260 volumes, voxel size = 3.4 mm × 3.4 mm × 3.4 mm]. High-resolution T_1-weighted structural scans were collected using a Magnetization-Prepared RApid Gradient Echo sequence (MPRAGE; 1 mm × 1 mm × 1 mm).

MRI data analysis

Our processing pipeline followed the procedure of recent related work.[16] Preprocessing of rs-fMRI scans included discarding the first five volumes to account for equilibration effects, slice time correction, realignment to the first volume, spatial normalization to MNI space (voxel size 2 mm × 2 mm × 2 mm) and spatial smoothing with a 6-mm full width at half maximum smoothing kernel using the CONN Toolbox (https://web.conn-toolbox.org/).

Group-independent component analysis

To perform group-independent component analysis and dynamic functional network analysis, we applied the GroupICA fMRI toolbox (GIFT, http://mialab.mrn.org/software/gift/index.html). For each participant, 255 time points were first decomposed into 150 temporally independent principle components (PCs) and subsequently into 100 independent PCs using the *Infomax* algorithm.[17] This procedure was repeated 20 times in ICASSO to estimate the reliability and ensure the stability of the decomposition.[18] For back-reconstruction of individual time courses and spatial maps, *gig-ica* (integrated in the GIFT Toolbox) was applied to the data.[19] The resulting 100 independent components were individually rated as signal or noise by three independent raters (N.v.S., J.H., C.F.). In total, 39 components were assigned to functional networks based on the labels proposed by Thomas Yeo *et al.*[20] For cerebellar

(CB) and subcortical (SB) components, two distinct networks were added. This yielded a total of seven functional resting-state networks including sensorimotor (SM), visual (VIS), SB, CB, DMN, dorsal attention and fronto-parietal network (FPN). Supplementary Fig. 1 shows all functional networks and Supplementary Table 2 contains peak values and coordinates for all components. Finally, we applied additional processing steps including linear, quadratic and cubic detrending, motion regression (12 motion parameters) to reduce motion-related artefacts, high-frequency cut-off at 15 Hz, despiking (identified as framewise displacement > 0.5 mm) and interpolation of time courses using a third-order spline fit.

Static functional network connectivity analysis

To compare the dynamic FC results with conventional 'static' FC, we calculated the average pairwise connectivity between all component pairs across the resting-state scan using Pearson's correlation coefficient r for each subject. Subsequently, age, sex and motion parameters were regressed out, and Fisher z-transformation was applied.

Dynamic functional network connectivity analysis

In order to obtain FC dynamics, FC between all component pairs was calculated over consecutive windowed segments of the time courses (i.e. sliding windows) using a window of 30TR length ($\triangleq$ 67.5 s) that shifted in steps of 1TR ($\triangleq$ 2.25 s). After the correlation matrix was computed on each window (i.e. 225 39×39 matrices per participant), Fisher z-transformation was applied and age, sex and motion parameters were regressed out as nuisance variables. Subsequently, matrices of each participant were concatenated, and k-means clustering was applied with $k = 4$ according to the elbow criterion (see Supplementary Fig. 2). Thus, each window was assigned to one of the four clusters representing discrete network FC states.[16] Squared Euclidean distance was applied for clustering, and the process was repeated 100 times to avoid convergence on local minima.

Statistical analysis for group differences in static and dynamic functional network connectivity

For a global characterization of the static and the state-wise correlation matrices, modularity (as a measure of functional network segregation) and absolute mean connectivity (referred to as 'overall connectivity') were calculated.[21,22] In the static FC analysis, both measures were calculated on each subject's connectivity matrix and subsequent group comparison was performed using a non-parametric t-test as applied in Glerean *et al.*[23] In the dynamic FC analysis, modularity and absolute mean connectivity were calculated for all windows in each state and averaged for each subject. Subsequently, a two-way ANOVA was conducted to estimate group- and state-wise effects as well as their interaction. For *post hoc* analysis, a Kruskal–Wallis test was performed.

Next, we assessed group differences in FC between all component pairs for the static and the dynamic functional network analysis with respect to connectivity strength with a non-parametric t-test. For the dynamic FC analysis, group differences were evaluated for each state separately.

Statistical analysis for state dynamics

Besides the analysis of state-dependent connectivity patterns, estimation of time-varying FC provides the opportunity to capture dynamic metrics. Here, four commonly used metrics were calculated: (i) dwell time (i.e. average number of windows a participant spends in a particular state), (ii) transition frequency (i.e. a participant's number of transitions between each pair of states), (iii) fraction time (i.e. percentage of windows spent in a state) and (iv) state occurrence rate (i.e. number of participants that entered the state over the course of the scan).[12,15] Group differences in occurrence rates were estimated using the z-test for population proportions. For the other metrics, two-way ANOVAs were conducted to estimate group- and state-wise effects as well as their interaction. *Post hoc* comparisons were evaluated with a non-parametric t-test or a Tukey's test.

Between-group comparisons for the modularity and overall connectivity, static and dynamic functional network analysis, dwell time, fraction time and occurrence rates were based only on participants who visited the respective state.

State-wise classification

Finally, group-wise analyses were complemented by a supervised binary classification approach to assess the potential of the static FC markers and the four dynamic FC states to discriminate between patients and controls. As previous work has suggested visual, fronto-parietal and DMN areas to represent the biologically relevant discriminatory features in anti-NMDA receptor encephalitis, these networks were considered as the set of input features.[8] For the static design and each state, logistic regression models were trained on the z-scored FC indices to predict group status (anti-NMDA receptor encephalitis patients versus HC) in a leave-one-out cross-validation (LOOCV) scheme. To facilitate model sparsity and counteract overfitting, embedded feature selection was applied through L1 regularization. Hyperparameter optimization of the regularization strength λ was applied for each state-input matrix (observations-by-connectivity features) by searching a linearly spaced parameter grid that was identical for all four states. Selection probability of each feature was read out as the empirical rate of non-zeroed feature weights over all predictions within a state. Prediction performance was evaluated by standard confusion matrix

measures (i.e. true and false positive and negative rates and overall accuracy). Model training and prediction were implemented in Matlab (The MathWorks, Inc., Natick, MA, USA).

Data availability

The data that support the findings of this study are available upon reasonable request from the corresponding author. The code is available on GitHub (https://github.com/nivons/statedynamicsNMDARE).

Results

Functional network analysis

Static functional network connectivity analysis

We observed pairwise (component-to-component) differences in static FC between anti-NMDA receptor encephalitis patients and HC that clustered in the inter- and intra-connectivity of the DMN (Fig. 1 and Table 1). In line with previous studies,[3,8] anti-NMDA receptor encephalitis patients showed decreased static connectivity between the hippocampus (HPC) and the medial prefrontal cortex (mPFC; $P_{FDR} < 0.05$). In addition, anti-NMDA receptor encephalitis patients exhibited significantly reduced DMN connectivity with the supplementary motor area, temporo-parieto-occiptal junction (TPOJ), the parieto-occipital sulcus (POS) and the superior frontal gyrus (SFG) and increased FC with the orbito-frontal gyrus (OFG) ($P_{uncorr} < 0.001$). There was no significant difference between patients and controls in modularity (*mean* $\pm$ *SD*: 0.35 $\pm$ 0.09 versus 0.33 $\pm$ 0.09; $t = -1.19$, $P = 0.12$) and overall connectivity (0.30 $\pm$ 0.05 versus 0.31 $\pm$ 0.07; $t = 0.63$, $P = 0.26$).

Following previous studies that found a correlation between the mPFC-hippocampal connection and disease severity variables,[3,8] we conducted a *post hoc* correlation analysis (using Pearson's correlation coefficient) between these regions and disease severity at the time of scan (mRS). Higher mRS scores were associated with a reduced connectivity between the parahippocampal gyrus (PHG) and the mPFC ($r = -0.28$, $P = 0.040$), as well as with lower connectivity between the hippocampus and the mPFC ($r = -0.27$, $P = 0.05$).

Dynamic functional network connectivity analysis

K-means clustering identified four connectivity states for HC and anti-NMDA receptor encephalitis patients (Fig. 2). Group-wise mean connectivity and modularity for each state are shown in Fig. 3. Multiple regression models for modularity and overall connectivity yielded a significant effect for the state (modularity, $P < 0.001$; overall connectivity, $P < 0.001$), but not for group or interaction. The dominant State 1 closely resembled the static FC pattern ($r = 0.94$, Supplementary Table 14) with low overall connectivity and moderate modularity. States 2 and 3 were both characterized by high overall connectivity, while only State 2 had a highly segregated structure (i.e. high modularity). In contrast to State 3, State 4 exhibited high modularity and low overall connectivity (Fig. 3, see Supplementary Tables 3–8 for detailed test statistics).

Anti-NMDA receptor encephalitis patients showed distinct FC alterations across the four connectivity states in comparison to controls (Fig. 2 and Table 2). As in the static FC group analysis, group differences comprised the DMN, VIS and FPN, but in a state-dependent fashion: in the static FC-resembling State 1, patients with anti-NMDA receptor encephalitis displayed decreased connectivity between the mPFC and the hippocampus, i.e. results very similar to the findings in the static FC analysis. The highly modular State 2 showed impaired connectivity between the mPFC and the angular gyrus (AG) as well as the parieto-occipital sulcus in patients. Furthermore, the inferior frontal gyrus (IFG) exhibited connectivity alterations with the putamen (bil.) and the visual cortex. Similarly, the densely connected/highly integrative State 3 was characterized by decreased connectivity from the IFG to the putamen. Additionally, connectivity between the TPOJ and the superior frontal gyrus was reduced in anti-NMDA receptor encephalitis patients compared to HC. For State 4, no significant alterations were observed after false discovery rate (FDR) correction.

Next, we obtained the correlation coefficient between all significant component pairs and disease severity (mRS at the time of scan) as well as disease duration (days in hospitalization): in the strongly segregated State 2, higher disease severity was significantly associated with a decrease in FC between mPFC and angular gyrus ($r = -0.37$, $P = 0.019$), while in the densely connected/highly integrative State 3, higher disease severity was significantly related to a decrease in connectivity between TPOJ and dorsolateral superior frontal gyrus ($r = -0.39$, $P = 0.046$). Due to the exploratory nature of the study, *post hoc* correlation analyses were not corrected for multiple comparisons.

State dynamics

In addition to state-wise connectivity patterns, we assessed state and group differences in dwell time, transition frequency, fraction time and occurrence rate using two-way ANOVAs. We found a significant state effect in *dwell times* ($P = 0.00021$): dwell times were higher for patients and controls in State 1 compared to States 2 ($T = -3.77$, $P = 0.0010$) and 3 ($T = -3.61$, $P = 0.0019$). Importantly, a significant group effect ($P = 0.010$) revealed a shift in dwell times between patients and controls: while patients showed lower dwell times in the dominant static FC-resembling State 1 ($P = 0.020$), they had higher dwell times in the strongly segregated State 2 compared to controls ($P = 0.032$; Fig. 4). Similarly, the model for *transition frequencies* yielded a significant effect for the group ($P = 0.044$) and state ($P < 0.001$). *Post hoc* group comparisons exhibited higher transition frequencies in patients between states with high and low overall connectivity, i.e. States 1 and 2 ($P = 0.043$), and between states with high and low across-

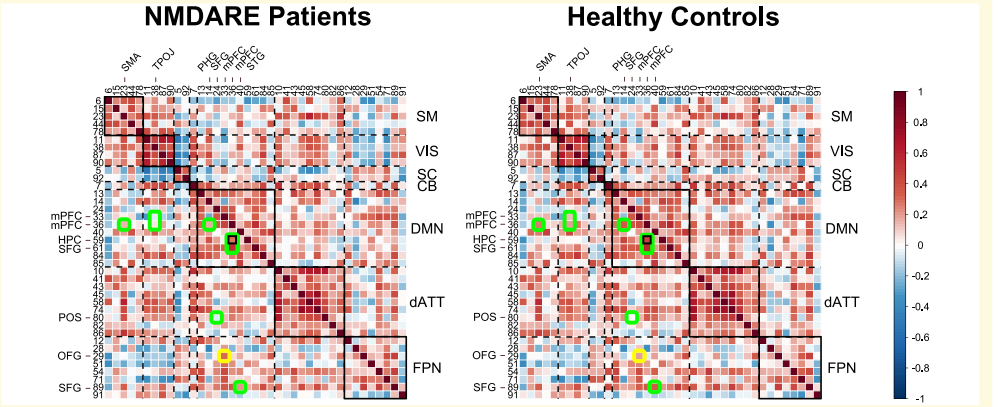

Figure 1 Mean static functional connectivity matrix across brain regions of anti-NMDA receptor encephalitis patients and HC. Darker red/blue colours indicate higher positive/negative correlation values between component pairs. Green circles mark lower correlation values in anti-NMDA receptor encephalitis compared to controls, and yellow circles indicate higher correlation values in anti-NMDA receptor encephalitis compared to controls. Small black rectangle indicates significant difference of FC between the hippocampus (Region 59) and the mPFC (Region 36) between patients and controls after FDR-correction ($P_{FDR} < 0.05$), while no rectangle indicates differences between groups for $P_{uncorr} < 0.001$. Highlighted regions are displayed with anatomical labels. A key for the region numbers is provided in Supplementary Table 2. Big diagonal rectangles indicate functional networks, e.g. the sensorimotor network that comprises regions 6, 15, 23, 44 and 78. NMDARE, anti-NMDA receptor encephalitis.

network connectivity, i.e. States 3 and 4 ($P = 0.0063$; Fig. 4), in comparison to controls. Furthermore, transitions from/to State 1 were significantly more frequent than transitions from States 2/3 to State 4 or vice versa. *Fraction time* differed across states ($P = 0.0023$), but not between groups ($P = 0.56$). A *post hoc* test revealed higher percentages of windows in State 1 compared to State 2 ($T = -3.23$, $P = 0.0077$) and 3 ($T = -3.02$, $P = 0.014$). *Occurrence rates* of dynamic FC states were similar in anti-NMDA receptor encephalitis patients and HC: the static FC-resembling State 1 showed the highest occurrence, followed by States 2 and 4; the lowest occurrence rates were observed for the densely connected/highly integrative State 3. Despite similar general occurrences, state-wise between-group proportion tests revealed that a higher number of patients visited the highly segregated State 2 compared to controls ($P = 0.019$), while the proportions were equal for both groups in States 1, 3 and 4. Detailed test statistics can be found in Table 3 and Supplementary Tables 9–13.

To identify a relationship between disease severity variables (i.e. acute days in hospitalization and mRS score at the time of scan) and dynamic metrics (i.e. dwell time and transition frequency), we conducted Pearson's correlation analyses between these variables. We found that increased transition frequency between States 1 and 2 was associated with disease severity at the time of scan ($r = 0.34$, $P = 0.012$). We further compared dwell time and transition frequency from patients with positive and negative schizophrenia-like psychiatric symptoms to those without respective psychiatric symptoms. Here, patients with positive symptoms exhibited higher dwell times ($z = 2.07$, $P = 0.038$) in the highly segregated State 4 compared to those without positive symptoms. In contrast, patients with negative symptoms showed higher dwell times ($z = 2.02$, $P = 0.043$) in the densely connected/highly integrative State 3 compared to those without negative symptoms.

Classification analyses

Binary classification (anti-NMDA receptor encephalitis patients versus HC) based on static connectivity features yielded an overall prediction accuracy of 72%, with balanced feature distribution across the networks (see Supplementary Fig. 3). When dynamic connectivity features were considered, discriminatory power differed in a state-wise fashion. Prediction performance was lowest for the dominant, static FC-resembling State 1 (overall accuracy of 61.5%), intermediate and similar to model performance with static feature input for the modular-structured States 2 (72.6%) and 4 (70.8%), and highest for the least frequent and densely connected/highly integrative State 3 (78.6%; see Supplementary Fig. 4 for the state-wise confusion matrices). Besides model evaluation outcomes, the feature selection frequencies over individual predictions in the LOOCV scheme also varied across states (Fig. 5). While States 1 and 3 yielded balanced selection rates over both across- and within-network connectivity features, States 2 and 4 showed fewer discriminatory features, and these were primarily across-network connections (FPN to VIS and DMN for State 2

Table 1. Test results of static functional network connectivity analysis

Regions	Network	Component #	P_{uncorr}	P_{FDR}	*T*	*d*
mPFC—hippocampus	DMN—DMN	36–59	<0.0001*	0.00024*	4.36	0.62
mPFC—SMA	DMN—SM	36–23	0.00092	0.15	3.30	0.44
mPFC—TPOJ	DMN—VIS	33–38	0.00084	0.15	3.26	0.54
mPFC—TPOJ	DMN—VIS	36–38	0.00061	0.15	3.40	0.45
mPFC—PHG	DMN—DMN	36–14	0.00016	0.12	3.85	0.55
SFG—POS	DMN—dATT	24–80	0.00072	0.15	3.29	0.52
mPFC—OFG	DMN—FPN	33–29	0.00043	0.15	−3.48	−0.37
mPFC—SFG	DMN—DMN	36–61	0.00087	0.15	3.27	0.40
STG—SFG	DMN—FPN	40–89	0.00057	0.15	3.24	0.49

Table includes component name, network assignment, number (#), *t*-value, *P*-value and effect size (*d*) of component pairs that are highlighted in Fig. 1.
*Significant after FDR-correction.

and DMN to VIS for State 4). Importantly, although some connectivity features were discriminatory across several states (e.g. component pairs 12–90 showed high selection frequency for States 1–3), the constellation of predictive features changed dynamically over connectivity states, emphasizing the uniqueness of each state.

Discussion

In this study, we applied dynamic FC analyses to characterize distinct connectivity patterns and temporal dynamics of network interactions in anti-NMDA receptor encephalitis. Investigating state-specific FC alterations, we found a marked impairment of FC between the hippocampus and the mPFC in the most visited, i.e. dominant state. This connectivity pattern closely mirrored observations in the static FC analysis and corroborated previous findings.[3,8] Three additionally identified states showed connectivity alterations within the DMN and between frontal, visual and SB areas—findings that remained undetected in the static FC analysis. Investigation of state dynamics showed a systematic shift in dwell time from the dominant state to a strongly segregated state in patients. Likewise, negative and positive schizophrenia-like symptoms were associated with distinct patterns of state preference. In addition, an increased volatility of transitions between states with high and low overall connectivity and states with high and low segregation was observed in patients. These state dynamics were associated with disease severity. Finally, classification analyses revealed that discriminatory network features and predictive power varied dynamically across states, exceeding the discriminatory power of static FC analyses and yielding the highest prediction in a highly connected/highly integrated state. Our observations demonstrate the potential of time-resolved FC analysis for a better characterization of disease mechanisms involved in anti-NMDA receptor encephalitis.

Static functional network connectivity analysis

In line with previous studies, conventional static FC analyses showed impaired connectivity between the mPFC and the hippocampus as well as altered connectivity patterns in frontal parts of the DMN.[3,8] Indeed, the CA1 subregion of the hippocampus and the prefrontal cortex contains the highest density of NMDA receptors.[24] Converging observations of disrupted hippocampal–prefrontal connectivity are thus biologically plausible and point to a robust disease biomarker and potential treatment target in anti-NMDA receptor encephalitis. Furthermore, both brain regions are main components of the DMN and are involved in memory and executive functions[25,26]—the two cognitive domains most frequently impaired in patients with anti-NMDA receptor encephalitis.[4,6,27,28]

Dynamic functional network connectivity analysis

However, these findings are inherently limited to a static account of connectivity changes. Time-varying FC, in contrast, captures moment-to-moment changes in connectivity, reflecting a more physiologically plausible model of brain activity. One line of thought hypothesizes that the temporal variability of FC networks enables a systematic exploration of network configurations, which allows brain regions to dynamically (dis-)engage, and modulate changes in cognition and behaviour.[29] Dynamic state analysis as employed in this study represents a powerful tool to describe these dynamics and potential instabilities of this process.[16]

Indeed, state-wise group comparisons revealed connectivity differences between patients and controls in three out of four states. These differences were most pronounced in within- and across-network connectivity of the DMN and almost exclusively manifested as reduced connectivity strength in anti-NMDA receptor encephalitis.

State 1 represented the dominant state, i.e. the most visited state, the state in which participants remained longest and that was involved in most transitions. The connectivity pattern of State 1 was characterized by low overall connectivity and low segregation. Anti-NMDA receptor encephalitis patients showed a significantly impaired hippocampal–prefrontal connectivity in comparison to controls that closely resembled the pattern observed in current and previous static FC analyses.[3,8] Thus, the connectivity pattern

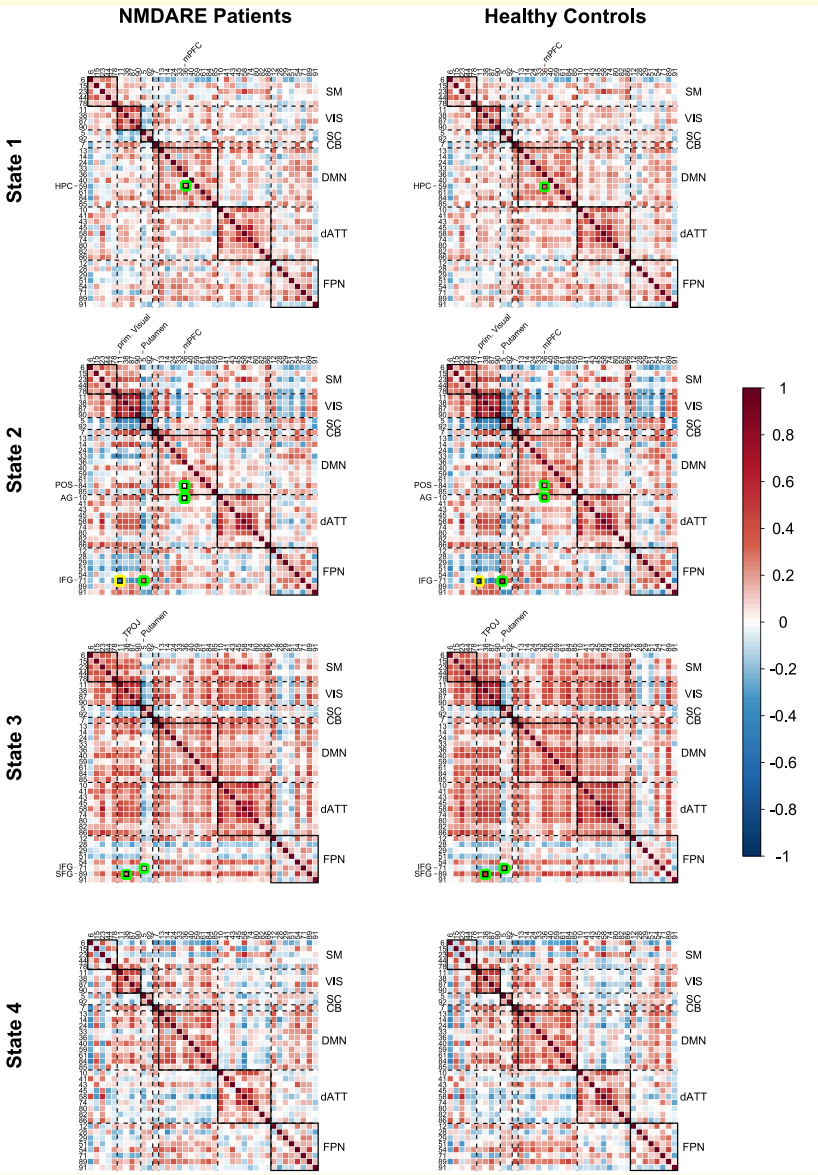

Figure 2 Dynamic functional network connectivity states for anti-NMDA receptor encephalitis patients and healthy controls. Darker red/blue colours indicate higher positive/negative correlation values between component pairs. Green circles mark lower correlation values in anti-NMDA receptor encephalitis compared to controls and yellow circles indicate higher correlation values in anti-NMDA receptor encephalitis compared to controls. Small black rectangles indicate significant differences of FC between patients and controls after FDR-correction ($P_{FDR} < 0.05$). Highlighted regions are displayed with anatomical labels. A key for the region numbers is provided in Supplementary Table 2. Big diagonal black rectangles indicate functional networks, e.g. the sensorimotor network that comprises regions 6, 15, 23, 44 and 78. NMDARE, anti-NMDA receptor encephalitis.

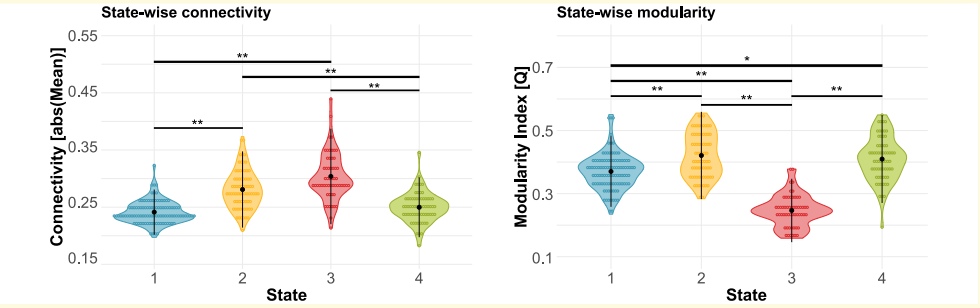

Figure 3 State-wise comparison of overall connectivity and modularity. In general, States 1 and 4 exhibited weak overall state connectivity compared to States 2 and 3. Segregation of functional networks, as measured with modularity, was highest in States 2 and 4, followed by State 1 and weakest in State 3. Black dots and vertical lines represent mean and standard deviation $^{**}P < 0.001$ (Bonferroni-corrected). $^{*}P < 0.01$ (Bonferroni-corrected). Detailed test statistics can be found in Supplementary Tables 3–8.

in the dominant State 1 seems to drive findings of altered connectivity in conventional static FC analyses. In contrast, States 2–4 showed strikingly different features. FC alterations in States 2 and 3 went beyond the aggregated findings of the static analysis and revealed impaired connectivity between the mPFC and parieto-occipital areas, and between the IFG and the putamen (State 2). The latter is also present in State 3 along with impaired frontal-parietal connectivity.

Importantly, correlation analyses revealed that these dynamic FC alterations were associated with disease severity and disease duration, primarily involving mPFC connectivity and highlighting the clinical relevance of these findings. Together, these results disentangle state-specific connectivity patterns observed in conventional FC analyses and indicate the potential differential contribution of state-wise FC alterations to clinical symptoms and disease stages.

State dynamics

In addition to these alterations in large-scale connectivity patterns in different states, anti-NMDA receptor encephalitis patients showed distinct temporal properties with respect to connectivity states, i.e. different transition frequencies and dwell times in comparison to controls. This involved a systematic shift in dwell time from the dominant State 1 to the segregated State 2, with patients nearly doubling their dwell time in State 2. Interestingly, recent evidence shows that successful working memory performance relies on increased network integration.[30] Prolonged dwelling in the segregated, less-integrated State 2 might thus be related to the frequently observed working memory deficits in anti-NMDA receptor encephalitis.[4] Remarkably, patients who experienced positive schizophrenia-like symptoms spent more time in the highly segregated State 4, while those with negative symptoms increased their dwell time in the highly integrative State 3. These observations are consistent with recent studies in schizophrenia showing an increased modular network structure in patients.[31]

Additionally, patients showed an increase in transition frequencies between States 1 and 2 as well as between States 3 and 4. These transition frequency alterations were significantly correlated with disease severity, indicating that severe anti-NMDA receptor encephalitis disease courses are associated with more volatile transition dynamics, while state preference (i.e. dwell time) is not affected. The dynamic interplay between brain regions—in the sense of the flexible (dis-)engagement of functional links and state transitions—is critical to efficiently process internal and external stimuli and flexibly adapt behaviour. While state transitions are

Table 2. Test results of dynamic functional network connectivity analysis

	Regions	Network	Component #	P_{FDR}	T	d
State 1	mPFC—hippocampus	DMN—DMN	36–59	0.0016	4.01	0.60
State 2	prim. Visual—IFG	VIS—FPN	11–71	0.016	−3.80	−0.57
	Putamen—IFG	SC—FPN	5–71	0.016	4.09	0.56
	mPFC—angular gyrus	DMN—DMN	36–84	0.016	3.83	0.54
	mPFC—POS	DMN—dATT	36–10	0.016	4.06	0.79
State 3	TPOJ—SFG	VIS—FPN	38–89	0.00021	4.33	0.78
	Putamen—IFG	SC—FPN	5–71	0.041	3.99	0.69

Table includes component name, network assignment, number (#), *t*-value, *P*-value and effect size (*d*) of component pairs that are highlighted in Fig. 2.

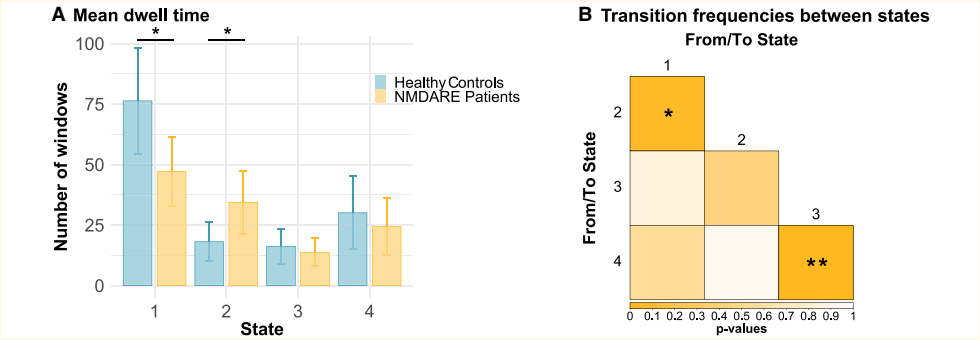

Figure 4 Group differences in state dynamics. (**A**) Group differences in average dwell time (in windows). Solid lines point to significant differences in *post hoc* testing between groups (non-parametric *t*-test, uncorrected). (**B**) Group differences in transition frequencies between states (*P*-values). For transition frequencies, the direction of transition was ignored. *Post hoc* group comparisons were calculated using a non-parametric *t*-test (uncorrected). *$P < 0.05$; **$P < 0.01$. NMDARE, anti-NMDA receptor encephalitis.

thought to be generally important to explore different brain states in order to facilitate and enhance cognitive flexibility, overly unstable transition dynamics may be linked to deficiencies in the integration and stable representation of information.[29,32] The imbalance of stability and volatility may, therefore, lead to impaired memory, perception or executive functions.[33,34] These suggestive links between state dynamics and impaired cognitive performance in anti-NMDA receptor encephalitis require further detailed investigations in combined task-based and resting-state fMRI studies.[35]

Relation to other brain disorders

Previous studies have applied dynamic FC analyses to brain disorders such as major depression, Alzheimer's disease or schizophrenia.[12,13,15,36,37] In these studies—and those with HC only[16]—the most visited state resembled the weakly connected dominant State 1 in the present study suggesting the brain's preference for a cost-efficient, energy-saving 'default' state.[38,39] Moreover, patient groups showed characteristic changes in state dynamics, such as altered state occurrences, transition frequency or dwell times.[12,13,36,37]

In patients with major depression, decreased variability in FC is the most prominent finding along with prolonged dwell times in the weakly connected dominant state.[13,40–42] Changes in dynamic metrics were associated with sadness and disease severity and may mirror main symptoms including negative, slow and ruminative thinking.[13,40]

A different pattern was found for patients with Alzheimer's disease. Similar to patients with anti-NMDA receptor encephalitis, state transitions are more volatile and patients tend to spent more time in less frequent,

Table 3. Group differences in dwell time (average number of windows), transition frequencies between states (absolute numbers) and fraction time (percentage).

	State	NMDARE patients (mean ± SD)	Healthy controls (mean ± SD)	P_{uncorr}	*d*
Dwell time	1	46.6 ± 53.8	75.7 ± 85.6	0.020*	0.43
	2	34.9 ± 49.9	17.6 ± 30.6	0.032*	−0.42
	3	14.2 ± 22.8	16.2 ± 28.0	0.21	0.22
	4	24.3 ± 45.0	30.3 ± 58.8	0.12	0.31
Transition frequency	1–2	1.3 ± 1.5	0.8 ± 1.37	0.043*	−0.34
	1–3	0.8 ± 1.4	0.8 ± 1.42	0.85	0.03
	1–4	1.3 ± 1.9	1.1 ± 1.95	0.55	−0.11
	2–3	0.5 ± 1.3	0.7 ± 1.31	0.44	0.14
	2–4	0.3 ± 0.8	0.3 ± 0.95	0.92	0.01
	3–4	0.3 ± 0.9	0.0 ± 0.13	0.0063*	−0.50
Fraction time	1	51.0 ± 33.1	54.7 ± 38.0	0.30	0.11
	2	31.5 ± 29.0	31.5 ± 25.8	0.48	0.01
	3	27.4 ± 27.7	32.3 ± 29.2	0.27	0.17
	4	32.8 ± 31.7	39.1 ± 33.9	0.22	0.20

Group differences were calculated using a two-sided non-parametric *t*-test. *P*-values and effect sizes (*d*) are shown. NMDARE, anti-NMDA receptor encephalitis.
*$P < 0.05$ (uncorrected).

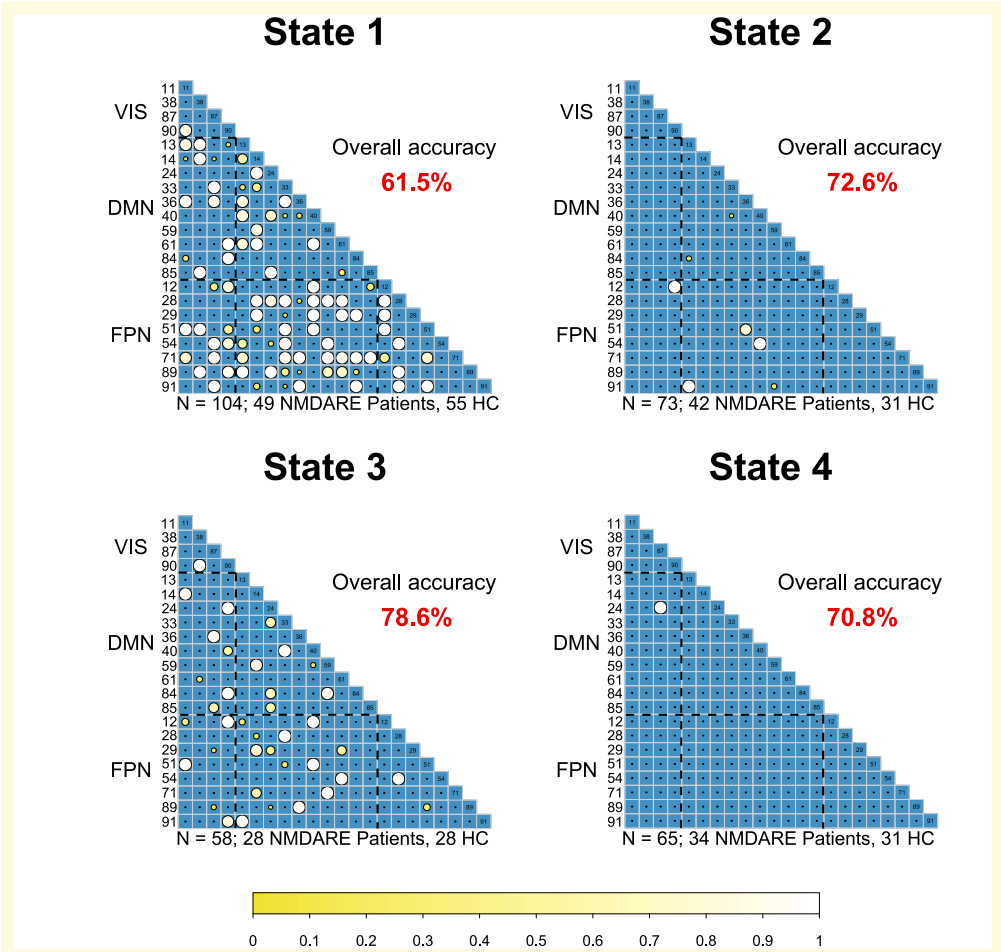

Figure 5 Feature selection matrices for state-wise predictions of group status (anti-NMDA receptor encephalitis patients versus healthy controls). The feature selection exceeding a minimum threshold at 10% of individuals within state predictions are displayed. Bigger and brighter circles indicate a higher selection rate. A key for the region numbers is provided in Supplementary Table 2. NMDARE, anti-NMDA receptor encephalitis.

functionally segregated states as compared to HC.[36,37] Interestingly, however, opposite results have also been reported,[43] potentially because dynamic connectivity pattern alterations change progressively across disease stages.

Furthermore, our results show a notable convergence with recent studies in patients with schizophrenia reporting a similarly marked shift in state preference[12] as well as increased overall transition frequencies,[44] and altered modular network structure.[31] Given the considerable overlap in psychiatric symptoms in patients with schizophrenia and anti-NMDA receptor encephalitis[45,46] and the glutamate hypothesis positing NMDA receptor dysfunction as the pathophysiological basis for cognitive and psychiatric symptoms in schizophrenia,[47,48] our findings raise the interesting possibility that the transdiagnostic psychopathological profile of both diseases[49] could be paralleled by a common set of dynamic network alterations.

Classification analyses

While our findings support the role of the hippocampus, the anterior DMN and frontal areas as potential connectivity

biomarkers in anti-NMDA receptor encephalitis, group-level analyses are not suited to estimate the discriminatory power of connectivity alterations or their value to predict disease severity.[50] To this end, we applied classification analyses based on logistic regression models to these data. Prediction performance and the set of selected network features were variable across the different connectivity states, indicating that discriminatory network constellations differ between states. Interestingly, the best performance (78.6% accuracy) was achieved in State 3, which showed the lowest overall occurrences but a highly integrative connectivity pattern. In contrast, static FC distinguished patients from controls with 72% accuracy. These results show that dynamic FC models can outperform static models and indicate the potential of spatiotemporal FC dynamics as prognostic biomarkers in anti-NMDA receptor encephalitis. However, further prospective studies are needed to identify biomarkers that can be used on the individual participant level and in clinical settings.

Limitations

Some limitations of the present study deserve mentioning. First, window-based approaches require the specification of windowing parameters and the optimal choices in this regard are an active area of research and debate.[51] Second, a given window size may only capture a part of the dynamic nature of the human brain, as networks may reconfigure over different time scales even within the possible temporal spectrum of MRI signals.[51] Lastly, for classification analyses, it is generally sensible to include large amounts of data.[50] While our study is based on a large study population in the light of the incidence of the disease, the sample sizes per state varied as not all participants visited all states.

Conclusions

Our analyses identified distinct brain states with characteristic patterns of FC alterations and shifted temporal dynamics in patients with anti-NMDA receptor encephalitis that remained undetected in conventional static analyses. Critically, dynamic FC measures correlated with disease severity and psychiatric symptoms, suggesting that altered resting-state dynamics carry meaningful clinical information about anti-NMDA receptor encephalitis. Given converging findings in other neuropsychiatric diseases, time-resolved FC analysis holds promise for an improved characterization and understanding of brain functioning in these disorders.

Acknowledgements

N.v.S. designed the study, conducted the static and dynamic functional network connectivity analysis, led the writing of the manuscript and produced the figures. S.K. implemented the classification analysis. S.K. and C.F. (principal investigator) significantly contributed to the design and interpretation of the analysis and writing. N.v.S., J.H. and C.F. rated the components from the group ICA. J.H., F.P., H.P. and C.F. were involved in conceiving/conducting the cohort study and data collection. All authors edited and revised the manuscript. The graphical abstract was created with BioRender.com.

Funding

C.F. was funded by the Deutsche Forschungsgemeinschaft [DFG, German Research Foundation, grant numbers 327654276 (SFB 1315), FI 2309/1-1 and FI 2309/2-1], the Bundesministerium für Bildung und Forschung [BMBF, German Ministry of Education and Research, grant number 01GM1908D (CONNECT-GENERATE)]. N.v.S. is a doctoral scholar at Cusanuswerk—Bischöfliche Studienförderung. S.K. was funded by the Bundesministerium für Bildung und Forschung [BMBF, German Ministry of Education and Research, grant number 13GW0206D]. The funders had no influence on study design, data collection, data analyses, data interpretation or writing.

Competing interests

N.v.S., S.K., J.H., H.P. and C.F. have nothing to disclose. F.P. reports grants and personal fees from Bayer, Biogen Idec, Merck Serono, Alexion, Guthy Jackson Foundation, Viela Bio, Novartis, Roche and Sanofi Genzyme. F.P. is the Academic Editor of *Plos One* and Associate Editor of *Neurology, Neuroimmunology & Neuroinflammation*. F.P. receives personal fees from Mitsubishi Tanabe PC (MTPC), and from UCB, outside the submitted work.

Supplementary material

Supplementary material is available at *Brain Communications* online.

References

1. Dalmau J, Lancaster E, Martinez-Hernandez E, Rosenfeld MR, Balice-Gordon R. Clinical experience and laboratory investigations in patients with anti-NMDAR encephalitis. *Lancet Neurol*. 2011; 10(1):63–74.
2. Kayser MS, Dalmau J. Anti-NMDA receptor encephalitis, autoimmunity, and psychosis. *Schizophr Res*. 2016;176(1):36–40.
3. Finke C, Kopp UA, Scheel M, *et al*. Functional and structural brain changes in anti-N-methyl-D-aspartate receptor encephalitis. *Ann Neurol*. 2013;24(2):284–296.
4. Finke C, Kopp UA, Prüss H, Dalmau J, Wandinger KP, Ploner CJ. Cognitive deficits following anti-NMDA receptor encephalitis. *J Neurol Neurosurg Psychiatry*. 2012;83(2):195–198.
5. Graus F, Titulaer MJ, Balu R, *et al*. A clinical approach to diagnosis of autoimmune encephalitis. *Lancet Neurol*. 2016;15(4):391–404.
6. Heine J, Kopp UA, Klag J, Ploner CJ, Prüss H, Finke C. Long-term cognitive outcome in anti-NMDA receptor encephalitis. *Ann Neurol*. 2021;90:949–961.

7. Heine J, Prüss H, Bartsch T, Ploner CJ, Paul F, Finke C. Imaging of autoimmune encephalitis – relevance for clinical practice and hippocampal function. *Neuroscience*. 2015;309:68–83.
8. Peer M, Prüss H, Ben-Dayan I, Paul F, Arzy S, Finke C. Functional connectivity of large-scale brain networks in patients with anti-NMDA receptor encephalitis: An observational study. *Lancet Psychiatry*. 2017;4(10):768–774.
9. Calhoun VD, Miller R, Pearlson G, Adalı T. The chronnectome: time-varying connectivity networks as the next frontier in fMRI data discovery. *Neuron*. 2014;84(2):262–274.
10. Hutchison RM, Womelsdorf T, Allen EA, *et al*. Dynamic functional connectivity: Promise, issues, and interpretations. *NeuroImage*. 2013;80:360–378.
11. Chang C, Glover GH. Time–frequency dynamics of resting-state brain connectivity measured with fMRI. *NeuroImage*. 2010; 50(1):81–98.
12. Damaraju E, Allen EA, Belger A, *et al*. Dynamic functional connectivity analysis reveals transient states of dysconnectivity in schizophrenia. *NeuroImage Clin*. 2014;5:298–308.
13. Demirtaş M, Tornador C, Falcón C, *et al*. Dynamic functional connectivity reveals altered variability in functional connectivity among patients with major depressive disorder. *Hum Brain Mapp*. 2016;37(8):2918–2930.
14. Jones DT, Vemuri P, Murphy MC, *et al*. Non-stationarity in the "resting brain's" modular architecture. *PLoS One*. 2012;7(6):e39731.
15. Bonkhoff AK, Espinoza FA, Gazula H, *et al*. Acute ischaemic stroke alters the brain's preference for distinct dynamic connectivity states. *Brain*. 2020;143(5):1525–1540.
16. Allen EA, Damaraju E, Plis SM, Erhardt EB, Eichele T, Calhoun VD. Tracking whole-brain connectivity dynamics in the resting state. *Cereb Cortex*. 2014;24(3):663–676.
17. Calhoun VD, Adali T, Pearlson GD, Pekar JJ. A method for making group inferences from functional MRI data using independent component analysis. *Hum Brain Mapp*. 2001;14(3):140–151.
18. Himberg J, Hyvarinen A. Icasso: Software for investigating the reliability of ICA estimates by clustering and visualization. In: IEEE XIII Workshop on Neural Networks for Signal Processing. IEEE. 2003.
19. Du Y, Fan Y. Group information guided ICA for fMRI data analysis. NeuroImage. 2013;69:157–197.
20. Thomas Yeo BT, Krienen FM, Sepulcre J, *et al*. The organization of the human cerebral cortex estimated by intrinsic functional connectivity. *J Neurophysiol*. 2011;106(3):1125–1165.
21. Blondel VD, Guillaume JL, Lambiotte R, Lefebvre E. Fast unfolding of communities in large networks. *J Stat Mech Theory Exp*. 2008(10):P10008.
22. Rubinov M, Sporns O. Complex network measures of brain connectivity: Uses and interpretations. *NeuroImage*. 2010;52(3): 1059–1069.
23. Glerean E, Pan RK, Salmi J, *et al*. Reorganization of functionally connected brain subnetworks in high-functioning autism. *Hum Brain Mapp*. 2016;37(3):1066–1079.
24. Monaghan DT, Cotman CW. Distribution of N-methyl-D-aspartate-sensitive L-[3H]glutamate-binding sites in rat brain. *J Neurosci*. 1985;5(11):2909–2919.
25. Miller EK, Cohen JD. An integrative theory of prefrontal cortex function. *Annu Rev Neurosci*. 2001;24(1):167–202.
26. Barbosa J, Stein H, Martinez RL, *et al*. Interplay between persistent activity and activity-silent dynamics in the prefrontal cortex underlies serial biases in working memory. *Nat Neurosci*. 2020;23(8):1016–1024.
27. McKeon GL, Robinson GA, Ryan AE, *et al*. Cognitive outcomes following anti-N-methyl-D-aspartate receptor encephalitis: A systematic review. *J Clin Exp Neuropsychol*. 2018;40(3):234–252.
28. Gibson LL, McKeever A, Coutinho E, Finke C, Pollak TA. Cognitive impact of neuronal antibodies: Encephalitis and beyond. *Transl Psychiatry*. 2020;10(1):304.
29. Deco G, Jirsa VK, McIntosh AR. Emerging concepts for the dynamical organization of resting-state activity in the brain. *Nat Rev Neurosci*. 2011;12(1):43–56.
30. Cohen JR, D'Esposito M. The segregation and integration of distinct brain networks and their relationship to cognition. *J Neurosci*. 2016;36(48):12083–12094.
31. Alexander-Bloch AF, Gogtay N, Meunier D, *et al*. Disrupted modularity and local connectivity of brain functional networks in childhood-onset schizophrenia. *Front Syst Neurosci*. 2010;4:147.
32. Li L, Lu B, Yan CG. Stability of dynamic functional architecture differs between brain networks and states. *NeuroImage*. 2020;216:116230.
33. Braun U, Schäfer A, Walter H, *et al*. Dynamic reconfiguration of frontal brain networks during executive cognition in humans. *Proc Natl Acad Sci USA*. 2015;112(37):11678–11683.
34. Sadaghiani S, Poline JB, Kleinschmidt A, D'Esposito M. Ongoing dynamics in large-scale functional connectivity predict perception. *Proc Natl Acad Sci USA*. 2015;112(27):8463–8468.
35. Lorenz R, Johal M, Dick F, Hampshire A, Leech R, Geranmayeh F. A Bayesian optimization approach for rapidly mapping residual network function in stroke. *Brain*. 2021;144(7):2120–2134.
36. Fu Z, Caprihan A, Chen J, *et al*. Altered static and dynamic functional network connectivity in Alzheimer's disease and subcortical ischemic vascular disease: shared and specific brain connectivity abnormalities. *Hum Brain Mapp*. 2019;40(11):3203–3221.
37. Gu Y, Lin Y, Huang L, *et al*. Abnormal dynamic functional connectivity in Alzheimer's disease. *CNS Neurosci Ther*. 2020;26(9): 962–971.
38. Fornito A, Zalesky A, Bassett DS, *et al*. Genetic influences on cost-efficient organization of human cortical functional networks. *J Neurosci*. 2011;31(9):3261–3270.
39. Krohn S, von Schwanenflug N, Waschke L, *et al*. A spatiotemporal complexity architecture of human brain activity. *Biorxiv*. 2021. doi:10.1101/2021.06.04.446948.
40. Marchitelli R, Paillère-Martinot M-L, Bourvis N, *et al*. Dynamic functional connectivity in adolescence-onset major depression: Relationships with severity and symptom dimensions. *Biol Psychiatry Cogn Neurosci Neuroimaging*. 2021:S2451902221001439.
41. Kaiser RH, Whitfield-Gabrieli S, Dillon DG, *et al*. Dynamic resting-state functional connectivity in major depression. *Neuropsychopharmacology*. 2016;41(7):1822–1830.
42. Yao Z, Shi J, Zhang Z, *et al*. Altered dynamic functional connectivity in weakly-connected state in major depressive disorder. *Clin Neurophysiol*. 2019;130(11):2096–2104.
43. Schumacher J, Peraza LR, Firbank M, *et al*. Dynamic functional connectivity changes in dementia with Lewy bodies and Alzheimer's disease. *NeuroImage Clin*. 2019;22:101812.
44. Rashid B, Damaraju E, Pearlson GD, Calhoun VD. Dynamic connectivity states estimated from resting fMRI Identify differences among Schizophrenia, bipolar disorder, and healthy control subjects. *Front Hum Neurosci*. 2014;8:897.
45. Al-Diwani A, Handel A, Townsend L, *et al*. The psychopathology of NMDAR-antibody encephalitis in adults: A systematic review and phenotypic analysis of individual patient data. *Lancet Psychiatry*. 2019;6(3):235–246.
46. Gibson LL, Pollak TA, Blackman G, Thornton M, Moran N, David AS. The psychiatric phenotype of anti-NMDA receptor encephalitis. *J Neuropsychiatry Clin Neurosci*. 2019;31(1):70–79.
47. Moghaddam B, Javitt D. From revolution to evolution: The glutamate hypothesis of schizophrenia and its implication for treatment. *Neuropsychopharmacology*. 2012;37(1):4–15.
48. Stein H, Barbosa J, Rosa-Justicia M, *et al*. Reduced serial dependence suggests deficits in synaptic potentiation in anti-NMDAR encephalitis and schizophrenia. *Nat Commun*. 2020;11(1):4250.
49. Finke C. A transdiagnostic pattern of psychiatric symptoms in autoimmune encephalitis. *Lancet Psychiatry*. 2019;6(3):191–193.
50. Arbabshirani MR, Plis S, Sui J, Calhoun VD. Single subject prediction of brain disorders in neuroimaging: Promises and pitfalls. *NeuroImage*. 2017;145:137–165.
51. Lurie DJ, Kessler D, Bassett DS, *et al*. Questions and controversies in the study of time-varying functional connectivity in resting fMRI. *Netw Neurosci*. 2020;4(1):30–69.

Excerpt from Journal Summary List: *Publication II*

Journal Data Filtered By: **Selected JCR Year: 2021** Selected Editions: SCIE,SSCI
Selected Categories: **"NEUROSCIENCES"** Selected Category Scheme: WoS
Gesamtanzahl: 274 Journale

Rank	Full Journal Title	Total Cites	Journal Impact Factor	Eigenfaktor
1	NATURE REVIEWS NEUROSCIENCE	54,312	38.755	0.04313
2	NATURE NEUROSCIENCE	82,161	28.771	0.11604
3	TRENDS IN COGNITIVE SCIENCES	36,688	24.482	0.03441
4	Nature Human Behaviour	11,204	24.252	0.04187
5	BEHAVIORAL AND BRAIN SCIENCES	12,872	21.357	0.00816
6	BRAIN BEHAVIOR AND IMMUNITY	31,770	19.227	0.03902
7	Molecular Neurodegeneration	8,377	18.879	0.01206
8	NEURON	121,714	18.688	0.15024
9	TRENDS IN NEUROSCIENCES	24,595	16.978	0.01777
10	ACTA NEUROPATHOLOGICA	30,046	15.887	0.03384
11	Annual Review of Neuroscience	15,839	15.553	0.00985
12	BRAIN	69,241	15.255	0.05988
13	MOLECULAR PSYCHIATRY	33,324	13.437	0.04914
14	BIOLOGICAL PSYCHIATRY	51,087	12.810	0.03831
15	NEUROPSYCHOBIOLOGY	3,757	12.329	0.00343
16	PSYCHIATRY AND CLINICAL NEUROSCIENCES	6,445	12.145	0.00577
17	JOURNAL OF PINEAL RESEARCH	13,422	12.081	0.00692
18	SLEEP MEDICINE REVIEWS	12,620	11.401	0.01356
19	Neurology-Neuroimmunology & Neuroinflammation	5,161	11.360	0.01049
20	ANNALS OF NEUROLOGY	45,647	11.274	0.03862
21	PROGRESS IN NEUROBIOLOGY	15,980	10.885	0.00886

Rank	Full Journal Title	Total Cites	Journal Impact Factor	Eigenfaktor
22	Translational Neurodegeneration	2,152	9.883	0.00300
23	NEURAL NETWORKS	23,717	9.657	0.02002
24	Journal of Neuroinflammation	23,947	9.587	0.02698
25	npj Parkinsons Disease	1,792	9.304	0.00340
26	Brain Stimulation	10,760	9.184	0.01497
27	NEUROSCIENCE AND BIOBEHAVIORAL REVIEWS	40,813	9.052	0.04464
28	Alzheimers Research & Therapy	7,513	8.823	0.01287
29	JOURNAL OF HEADACHE AND PAIN	6,592	8.588	0.01107
30	FRONTIERS IN NEUROENDOCRINOLOGY	5,624	8.333	0.00458
31	NEUROPSYCHOPHARMACOLOGY	34,562	8.294	0.03279
32	GLIA	19,109	8.073	0.01568
33	PAIN	46,662	7.926	0.02957
34	Annual Review of Vision Science	1,345	7.745	0.00387
35	Current Neuropharmacology	7,580	7.708	0.00713
36	BRAIN PATHOLOGY	7,083	7.611	0.00689
37	Acta Neuropathologica Communications	8,201	7.578	0.01628
38	NEUROIMAGE	131,266	7.400	0.10055
39	Journal of Neuroimmune Pharmacology	4,036	7.285	0.00302
40	NEUROSCIENTIST	6,603	7.235	0.00538
41	Neurobiology of Stress	2,462	7.142	0.00448
42	CURRENT OPINION IN NEUROBIOLOGY	18,337	7.070	0.02145
43	NEUROBIOLOGY OF DISEASE	23,538	7.046	0.01982
44	CNS Neuroscience & Therapeutics	6,186	7.035	0.00600

2

Selected JCR Year: 2021; Selected Categories: "NEUROSCIENCES"

Rank	Full Journal Title	Total Cites	Journal Impact Factor	Eigenfaktor
45	Fluids and Barriers of the CNS	2,427	6.961	0.00258
46	JOURNAL OF CEREBRAL BLOOD FLOW AND METABOLISM	24,048	6.960	0.01940
47	NEUROPSYCHOLOGY REVIEW	4,428	6.940	0.00335
48	Translational Stroke Research	4,125	6.800	0.00500
49	JOURNAL OF NEUROSCIENCE	192,643	6.709	0.10056
50	Molecular Autism	4,293	6.476	0.00611
51	SLEEP	31,283	6.313	0.01904
52	EUROPEAN JOURNAL OF NEUROLOGY	17,087	6.288	0.01965
53	CURRENT OPINION IN NEUROLOGY	7,258	6.283	0.00814
54	Frontiers in Molecular Neuroscience	12,806	6.261	0.02209
55	NEUROPATHOLOGY AND APPLIED NEUROBIOLOGY	5,197	6.250	0.00447
56	JOURNAL OF PHYSIOLOGY-LONDON	59,625	6.228	0.03113
57	Frontiers in Cellular Neuroscience	21,318	6.147	0.02851
58	Neurotherapeutics	7,998	6.088	0.00899
59	CEPHALALGIA	13,467	6.075	0.01470
60	Neural Regeneration Research	9,531	6.058	0.00956
61	Biological Psychiatry-Cognitive Neuroscience and Neuroimaging	3,343	6.050	0.00941
62	Current Neurology and Neuroscience Reports	5,335	6.030	0.00686
63	Multiple Sclerosis Journal	15,617	5.855	0.01778
64	Developmental Cognitive Neuroscience	6,003	5.811	0.01206
65	ACS Chemical Neuroscience	12,168	5.780	0.01655
66	Frontiers in Aging Neuroscience	17,276	5.702	0.02432
67	JOURNAL OF PSYCHIATRY & NEUROSCIENCE	4,487	5.699	0.00330

Selected JCR Year: 2021; Selected Categories: "NEUROSCIENCES"

Rank	Full Journal Title	Total Cites	Journal Impact Factor	Eigenfaktor
68	MOLECULAR NEUROBIOLOGY	22,883	5.682	0.02909
69	INTERNATIONAL JOURNAL OF NEUROPSYCHOPHARMACOLOGY	8,630	5.678	0.00655
70	CLINICAL AUTONOMIC RESEARCH	2,484	5.625	0.00248
71	EXPERIMENTAL NEUROLOGY	24,373	5.620	0.01396
72	JOURNAL OF NEUROCHEMISTRY	40,901	5.546	0.01646
73	Journal of Parkinsons Disease	4,493	5.520	0.00713
74	npj Science of Learning	536	5.513	0.00151
75	Annals of Clinical and Translational Neurology	5,916	5.430	0.01380
76	EUROPEAN NEUROPSYCHOPHARMACOLOGY	9,792	5.415	0.00876
77	HUMAN BRAIN MAPPING	29,646	5.399	0.03211
78	JOURNAL OF PAIN	13,915	5.383	0.01264
79	BIPOLAR DISORDERS	6,472	5.345	0.00541
80	JOURNAL OF SLEEP RESEARCH	9,708	5.296	0.00912
81	NEUROPHARMACOLOGY	28,216	5.273	0.02363
82	Neuroscience Bulletin	3,841	5.271	0.00476
83	Journal of NeuroEngineering and Rehabilitation	8,225	5.208	0.00756
84	PROGRESS IN NEURO-PSYCHOPHARMACOLOGY & BIOLOGICAL PSYCHIATRY	15,970	5.201	0.01295
85	ASN Neuro	1,324	5.200	0.00097
86	JOURNAL OF THE PERIPHERAL NERVOUS SYSTEM	2,488	5.188	0.00249
87	Frontiers in Neuroscience	38,212	5.152	0.05986
88	NEUROENDOCRINOLOGY	6,460	5.135	0.00584
89	NEUROBIOLOGY OF AGING	29,380	5.133	0.02039

4

Selected JCR Year: 2021; Selected Categories: “NEUROSCIENCES”

Rank	Full Journal Title	Total Cites	Journal Impact Factor	Eigenfaktor
90	Journal of Neural Engineering	11,475	5.043	0.01351
91	CHEMICAL SENSES	6,598	4.985	0.00342
92	Network Neuroscience	965	4.980	0.00323
93	Cognitive Computation	2,904	4.890	0.00290
94	JOURNAL OF NEUROTRAUMA	19,581	4.869	0.01717
95	CEREBRAL CORTEX	37,701	4.861	0.04009
96	CLINICAL NEUROPHYSIOLOGY	25,162	4.861	0.01585
97	REVIEWS IN THE NEUROSCIENCES	3,309	4.703	0.00279
98	PSYCHONEUROENDOCRINOLOGY	23,132	4.693	0.01932
99	Journal of Neuromuscular Diseases	1,350	4.693	0.00275
100	CORTEX	15,191	4.644	0.01887
101	MOLECULAR AND CELLULAR NEUROSCIENCE	7,464	4.626	0.00397
102	JOURNAL OF PSYCHOPHARMACOLOGY	9,324	4.562	0.00949
103	JOURNAL OF THE NEUROLOGICAL SCIENCES	23,403	4.553	0.01804
104	IEEE Transactions on Cognitive and Developmental Systems	1,276	4.546	0.00211
105	Cognitive Systems Research	2,101	4.541	0.00240
106	ACTA NEUROPSYCHIATRICA	1,481	4.513	0.00157
107	JOURNAL OF NEUROSCIENCE RESEARCH	15,750	4.433	0.00949
108	PSYCHOPHARMACOLOGY	27,078	4.415	0.01475
109	NEUROCHEMICAL RESEARCH	13,719	4.414	0.00881
110	Molecular Brain	4,714	4.399	0.00602
110	NEUROTOXICOLOGY	9,029	4.398	0.00551
112	eNeuro	6,426	4.363	0.01822

5

Selected JCR Year: 2021; Selected Categories: “NEUROSCIENCES”

Rank	Full Journal Title	Total Cites	Journal Impact Factor	Eigenfaktor
113	PSYCHOPHYSIOLOGY	18,298	4.348	0.01135
114	NEUROCHEMISTRY INTERNATIONAL	11,906	4.297	0.00714
115	International Review of Neurobiology	4,148	4.280	0.00345
116	BRAIN TOPOGRAPHY	3,529	4.275	0.00351
117	Current Opinion in Behavioral Sciences	4,875	4.261	0.01313
118	Social Cognitive and Affective Neuroscience	9,730	4.235	0.01210
119	CELLULAR AND MOLECULAR NEUROBIOLOGY	6,981	4.231	0.00587
120	Neurophotonics	1,761	4.212	0.00318
121	JOURNAL OF ALZHEIMERS DISEASE	36,110	4.160	0.04078
122	NEUROMOLECULAR MEDICINE	2,664	4.103	0.00164
123	Frontiers in Neurology	27,128	4.086	0.04871
124	Journal of Neurodevelopmental Disorders	2,054	4.074	0.00278
125	NEUROTOXICOLOGY AND TERATOLOGY	4,185	4.071	0.00182
126	NUTRITIONAL NEUROSCIENCE	3,695	4.062	0.00306
127	Epilepsia Open	1,125	4.026	0.00263
128	NEUROTOXICITY RESEARCH	5,010	3.978	0.00408
129	NEUROGASTROENTEROLOGY AND MOTILITY	11,600	3.960	0.01224
130	Purinergic Signalling	2,714	3.950	0.00159
131	Behavioral and Brain Functions	1,832	3.950	0.00070
132	JOURNAL OF NEUROENDOCRINOLOGY	6,699	3.870	0.00413
133	MUSCLE & NERVE	16,166	3.852	0.01052
134	JOURNAL OF NEURAL TRANSMISSION	9,768	3.850	0.00683
135	NEUROLOGICAL SCIENCES	10,952	3.830	0.01262

Selected JCR Year: 2021; Selected Categories: "NEUROSCIENCES"

Rank	Full Journal Title	Total Cites	Journal Impact Factor	Eigenfaktor
136	Experimental Neurobiology	1,654	3.800	0.00187
137	Neural Development	1,193	3.800	0.00116
138	NEUROLOGIC CLINICS	3,546	3.787	0.00283
139	Frontiers in Systems Neuroscience	6,508	3.785	0.00622
140	HIPPOCAMPUS	9,803	3.753	0.00676
141	Brain Structure & Function	9,468	3.748	0.01458
142	Frontiers in Neuroinformatics	4,037	3.739	0.00442
143	JOURNAL OF NEUROVIROLOGY	3,915	3.739	0.00362
144	Clinical Psychopharmacology and Neuroscience	1,412	3.731	0.00196
145	BRAIN RESEARCH BULLETIN	13,000	3.715	0.00792
146	NEUROSCIENCE	52,150	3.708	0.02776
147	GENES BRAIN AND BEHAVIOR	4,571	3.708	0.00380
148	EUROPEAN JOURNAL OF NEUROSCIENCE	29,305	3.698	0.01492
149	PHARMACOLOGY BIOCHEMISTRY AND BEHAVIOR	13,544	3.697	0.00425
150	HEARING RESEARCH	12,747	3.672	0.00867
151	METABOLIC BRAIN DISEASE	5,309	3.655	0.00502
152	EUROPEAN JOURNAL OF PAIN	9,804	3.651	0.00876
153	CEREBELLUM	4,040	3.648	0.00454
154	Frontiers in Behavioral Neuroscience	10,765	3.617	0.01286
155	BRAIN RESEARCH	57,779	3.610	0.01788
156	Frontiers in Synaptic Neuroscience	1,321	3.567	0.00211
157	Frontiers in Neuroanatomy	5,058	3.543	0.00720
158	NEUROMUSCULAR DISORDERS	7,104	3.538	0.00684

Selected JCR Year: 2021; Selected Categories: “NEUROSCIENCES”

Publication II: Reduced resilience of brain state transitions in anti-N-methyl D-aspartate receptor encephalitis

Received: 5 August 2022 | Revised: 28 November 2022 | Accepted: 29 November 2022

DOI: 10.1111/ejn.15901

RESEARCH REPORT

EJN European Journal of Neuroscience FENS WILEY

Reduced resilience of brain state transitions in anti-*N*-methyl-D-aspartate receptor encephalitis

Nina von Schwanenflug[1,2] | **Juan P. Ramirez-Mahaluf**[3] | **Stephan Krohn**[1,2] | **Amy Romanello**[1,2] | **Josephine Heine**[1] | **Harald Prüss**[1,4] | **Nicolas A. Crossley**[3,5,6,7] | **Carsten Finke**[1,2]

[1]Department of Neurology and Experimental Neurology, Charité - Universitätsmedizin Berlin, Berlin, Germany

[2]Berlin School of Mind and Brain, Humboldt-Universität zu Berlin, Berlin, Germany

[3]Department of Psychiatry, School of Medicine, Pontificia Universidad Católica de Chile, Santiago, Chile

[4]German Centre for Neurodegenerative Diseases (DZNE) Berlin, Berlin, Germany

[5]Biomedical Imaging Center, Pontificia Universidad Católica de Chile, Santiago, Chile

[6]Millennium Nucleus for Cardiovascular Magnetic Resonance, Santiago, Chile

[7]Institute of Psychiatry, Psychology and Neuroscience, King's College London, London, UK

Correspondence
Carsten Finke, Department of Neurology and Experimental Neurology, Charité - Universitätsmedizin Berlin, Freie Universität Berlin, Humboldt-Universität zu Berlin, and Berlin Institute of Health, Charitéplatz 1, Berlin 10117, Germany.
Email: carsten.finke@charite.de

Funding information
Deutsche Forschungsgemeinschaft,

Abstract

Patients with anti-*N*-methyl-aspartate receptor (NMDA) receptor encephalitis suffer from a severe neuropsychiatric syndrome, yet most patients show no abnormalities in routine magnetic resonance imaging. In contrast, advanced neuroimaging studies have consistently identified disrupted functional connectivity in these patients, with recent work suggesting increased volatility of functional state dynamics. Here, we investigate these network dynamics through the spatiotemporal trajectory of meta-state transitions, yielding a time-resolved account of brain state exploration in anti-NMDA receptor encephalitis. To this end, resting-state functional magnetic resonance imaging data were acquired in 73 patients with anti-NMDA receptor encephalitis and 73 age- and sex-matched healthy controls. Time-resolved functional connectivity was clustered into brain meta-states, giving rise to a time-resolved transition network graph with states as nodes and transitions between brain meta-states as weighted, directed edges. Network topology, robustness and transition cost of these transition networks were compared between groups. Transition networks of patients showed significantly lower local efficiency ($t = -2.41$, $p_{FDR} = .029$), lower robustness ($t = -2.01$, $p_{FDR} = .048$) and higher leap size ($t = 2.18$, $p_{FDR} = .037$) compared with controls. Furthermore, the ratio of within-to-between module transitions and state similarity was significantly lower in patients. Importantly, alterations of brain state transitions correlated with disease severity. Together, these findings reveal systematic alterations of transition networks in patients, suggesting that anti-NMDA receptor encephalitis is characterized by reduced stability of brain state transitions and that this

List of abbreviations: BOLD signal, blood-oxygen-level-dependent signal; DAMS, distance across meta-states; dATT, dorsal attention network; DMN, default mode network; FC, functional connectivity; FD, framewise displacement; FDR, false discovery rate; FPN, fronto-parietal network; HC, healthy controls; LIM, limbic network; MRI, magnetic resonance imaging; mRS, modified Rankin Scale; NMDAR, anti-*N*-methyl-aspartate receptor; $ratio_{sim}$, ratio of within-to-between meta-state similarity; $ratio_{trans}$, ratio of within-to-between meta-state trasnitions; ROI, region of interest; rs-fMRI, resting-state fMRI; SC, subcortical network; SM, sensorimotor network; TE, echo time; TR, repitition time; vATT, ventral attention network; VIS, visual network.

Grant/Award Numbers: 1274/6-1, 327654276, FI 2309/1-1, FI 2309/2-1; Deutsches Ministerium für Bildung und Forschung, Grant/Award Numbers: 01GM1908D, CONNECT-GENERATE; Helmholtz Association, Grant/Award Number: HIL-A03; Agencia Nacional de Investigación y Desarrollo, Grant/Award Numbers: 1200601, 3190311, ACT192064

Edited by: Yoland Smith

reduced resilience of transition networks plays a clinically relevant role in the manifestation of the disease.

KEYWORDS
autoimmune encephalitis, functional brain states, functional connectivity dynamics, graph analysis, transition trajectories

1 | INTRODUCTION

Anti-*N*-methyl-aspartate receptor (NMDAR) encephalitis is an immune-mediated disorder of the central nervous system caused by autoantibodies targeting the NMDA receptor and leading to a dysregulation of the glutamatergic neurotransmitter system (Dalmau et al., 2019). The disease manifests in a complex neuropsychiatric syndrome with prominent psychiatric symptoms (e.g., delusions and psychosis) and seizures, dyskinesia, psychosis, decreased levels of consciousness and cognitive dysfunction (Finke et al., 2012; Graus et al., 2016; Heine et al., 2021). Despite the severe disease course, only 50–70% of patients show abnormalities in standard structural magnetic resonance imaging (MRI) (Graus et al., 2016; Heine et al., 2015), resulting in a clinico-radiological paradox. In contrast, several functional MRI studies have suggested disrupted functional connectivity (FC) in NMDAR encephalitis that is linked to disease severity, disease duration and cognitive symptoms (Finke et al., 2012, 2013; Gibson et al., 2019, 2020; Heine et al., 2021; Peer et al., 2017; von Schwanenflug et al., 2022). In contrast, several functional MRI studies have suggested disrupted FC in NMDAR encephalitis that is linked to disease severity, disease duration and cognitive symptoms (Finke et al., 2012, 2013; Gibson et al., 2019, 2020; Heine et al., 2021; Peer et al., 2017; von Schwanenflug et al., 2022). These functional alterations include large-scale functional networks, such as sensorimotor, frontoparietal, lateral-temporal and visual networks (Peer et al., 2017). In addition, the hippocampus and the medial prefrontal cortex—regions with the highest NMDAR density (Dalmau et al., 2011)—have been associated with deficits in memory performance and executive function, two core cognitive symptoms in NMDAR encephalitis (Finke et al., 2012; Heine et al., 2021).

FC as measured with resting-state functional MRI (rs-fMRI) is estimated from the pairwise correlation of blood-oxygen-level-dependent (BOLD) activity between brain regions without the presence of an explicit task (Biswal et al., 1995). However, traditional 'static' approaches obtain FC as an average across several minutes, therefore missing important information that may be derived from dynamic changes in functional connections (Allen et al., 2014; Calhoun et al., 2014). Hence, the analysis of FC has been recently refined from a time-*invariant* static account to a time-*varying* description. This methodological progress allows to unveil temporal properties of functional brain organization, such as the identification of functional states, that is, transient connectivity patterns, and their transition trajectories. These FC dynamics are thought to reflect brain state exploration that facilitates cognition and behaviour and may vary with disease (Bassett et al., 2011; Deco et al., 2011; Kringelbach & Deco, 2020). Accordingly, a recent case–control study investigating FC dynamics in NMDAR encephalitis showed that patients exhibited altered state preference as well as increased transition frequencies between major connectivity patterns (von Schwanenflug et al., 2022). However, a detailed investigation of the transition trajectory of brain states and its link to clinical symptoms is still missing. Brain state exploration—facilitated by transitions between functional states—is thought to ensure stable information representation while promoting functional integration across distant brain regions and subsystems and, if disturbed, potentially affects information integration and behaviour (Deco et al., 2011; Lord et al., 2019). Hence, identifying mechanisms and disruptions of these transition trajectories may contribute to the understanding of the pathophysiology of NMDAR encephalitis and further neuropsychiatric diseases that are associated with NMDAR dysfunction, for example, schizophrenia.

Graph theoretical approaches are well-suited to study the temporal architecture of state exploration. Ramirez-Mahaluf et al. (2020) recently introduced the concept of transition networks to investigate the trajectory of traversing functional states (from hereon also referred to as meta-states). In this concept, transition networks are represented as graphs with brain states as nodes and transitions between meta-states as directed and weighted edges. Similar to other biological systems (Latora & Marchiori, 2001), transition networks show properties of complex networks (i.e., heavy-tailed degree distribution, high local efficiency and modularity) indicating an

organized, cost-efficient, non-random temporal trajectory of brain states (Ramirez-Mahaluf et al., 2020). Furthermore, transition network characteristics have been related to motor function and cognitive performance in healthy controls indicating behavioural relevance (Ramirez-Mahaluf et al., 2020).

Here, we aimed to specify alterations of the spatio-temporal trajectory of state transitions and its relation to disease severity in NMDAR encephalitis. Therefore, we constructed transition networks for a large sample of patients and age- and sex-matched healthy controls. We hypothesized that the temporal structure of state exploration in NMDAR encephalitis would show altered dynamics (von Schwanenflug et al., 2022) and weakened stability of transition networks compared with a group of healthy controls.

2 | MATERIALS AND METHODS

2.1 | Participants

For this study, 73 patients with NMDAR encephalitis were recruited from the Department of Neurology at Charité - Universitätsmedizin Berlin. All patients fulfilled diagnostic criteria including characteristic clinical presentation and detection of IgG NMDA receptor antibodies in the cerebrospinal fluid (Graus et al., 2016). Patients were in the post-acute phase of their disease with a median of 2.97 years (interquartile range [IQR]: 2.48) after disease onset. Disease severity at the time of scan and peak of disease was assessed with the modified Rankin Scale (mRS). The control group consisted of 73 age- and sex-matched healthy participants without any history of neurological or psychiatric disease. Data from 49 patients and 25 controls were analysed in a recent study by von Schwanenflug et al. (2022) investigating functional dynamics in NMDAR encephalitis. For the current study, patient-control matching was optimized for age and sex through a computational matching algorithm (see Data S1). The two groups were perfectly balanced for sex and did not differ significantly in age as tested with a Wilcoxon rank sum test ($p = .61$). Clinical and demographic characteristics are summarized in (Table 1). The study was approved by the ethics committee of the Charité - Universitätsklinikum Berlin and conducted according to the ethical principles of the WMA Declaration of Helsinki.

2.2 | MRI data acquisition

MRI data were collected at the Berlin Center for Advanced Neuroimaging at Charité – Universitätsmedizin Berlin using a 3T Trim Trio scanner equipped with a 20-channel head coil (Siemens, Erlangen, Germany). RS functional images were acquired using an echoplanar imaging sequence (repetition time [TR] = 2.25 s, echo time [TE] = 30 ms, 260 volumes, voxel size = 3.4 × 3.4 × 3.4 mm^3). High-resolution T1-weighted structural scans were collected using a magnetization-prepared rapid gradient echo sequence (MPRAGE; voxel size = 1 × 1 × 1 mm^3).

TABLE 1 Demographic variables and clinical measures of the participants. Table lists median and interquartile range (IQR) of age, mRS at scan, mRS at peak of disease, disease duration and time between scan and diagnosis. Treatment and medication during disease course were evaluated using a binary scale (present: 'yes' vs. absent: 'no'). Disease duration = days in acute care; *N* = number of participants; mRS = modified Rankin Scale

		NMDAR encephalitis patients	Healthy controls
N		73	73
Sex	Female/male	62/11	62/11
Age (years)	Median ± IQR (*N*)	28.55 ± 8.7 (73)	28.50 ± 8.5 (73)
mRS at scan	Median ± IQR (*N*)	1.00 ± 1.5 (70)	..
mRS at peak of disease	Median ± IQR (*N*)	4 ± 2 (67)	..
Disease duration (hospitalization time)	Median ± IQR (*N*)	67.50 ± 72.00 (68)	..
Years between disease onset and study	Mean ± SD (*N*)	2.97 ± 2.48 (71)	..
First-line treatment		72/73	..
Second-line treatment		37/73	..
Anticonvulsant medication		51/73	..
Antipsychotic medication		48/73	..

Abbreviation: NMDAR, anti-*N*-methyl-aspartate receptor.

2.3 | MRI data analysis

Prior to preprocessing, framewise displacement (FD) was calculated for each participant and assessed against a mean FD cutoff of .50 mm (Eijlers et al., 2019; Power et al., 2014). No participant had a mean FD greater than or equal to .50 mm. For preprocessing, we applied the 'ICA-AROMA+2Phys'-Pipeline proposed by Parkes et al. (2018) to our data: The pipeline included removal of the first 4 volumes of each participant's rs-fMRI scan, volume realignment, slice-timing correction, detrending of BOLD time series, intensity normalization, spatial smoothing with 6 mm full width at half maximum, ICA-AROMA for head motion correction to robustly remove motion-induced signal artefacts from the functional MRI data (Pruim et al., 2015), regression of white matter and cerebrospinal fluid time series to control for physiological fluctuations of non-neuronal origin, demeaning and band-pass filtering to retain frequencies between .008 and .08 Hz.

2.4 | Participant-wise meta-state estimation and transition network construction

The following steps were performed with the same parameters as previously described and evaluated in Ramirez-Mahaluf et al. (2020). Time-series extraction was done using a whole-brain parcellation template with 638 similarly sized regions of interests (ROIs) (Crossley et al., 2013). Extracted functional time series were segmented into 127 consecutive time windows of 2TRs (≙4.5 s), which yielded reliable results in previous work (Ramirez-Mahaluf et al., 2020). The comparatively short window length was necessary to be able to meaningfully track state transitions across a large number of meta-states. For each window, FC was estimated between any two ROIs using Multiplication of Temporal Derivatives, a method that is suitable to estimate FC across a range of correlation strengths and (short) window lengths (Shine et al., 2015). The resulting ROI-by-ROI (638-by-638) matrices were then Pearson-correlated, resulting in a 127-by-127 similarity matrix of windows. To obtain discrete brain meta-states, MATLAB-inbuilt k-means clustering was applied to the similarity matrix using 10,000 maximum iterations and 2000 replicates with random initial positions. For each meta-state, all windows belonging to that state were averaged, yielding a mean ROI-by-ROI (638-by-638) connectivity matrix. To scrutinize our analyses across multiple numbers of meta-states, we extracted k meta-states ($k = 35$, 40, 45, 50 and 55) following the range of k in (Ramirez-Mahaluf et al., 2020) for each participant separately.

Finally, transition networks were constructed for each participant and k number of meta-states: A transition network is a graph network, where each meta-state corresponds to a node and transitions between meta-states represent the edges of that graph. The edges are directed and weighted according to the number of transitions from meta-state i to meta-state j (Ramirez-Mahaluf et al., 2020).

Importantly, this novel approach runs k-means clustering on each individual time series to describe individual temporal trajectories of meta-state transitions. Hence, this approach differs fundamentally from the definition of dynamic FC states across individuals (von Schwanenflug et al., 2022), which searches for common patterns of recurring connectivity on a group level.

2.5 | Group comparisons of transition network properties

From each of the transition networks, we derived three widely used graph theoretical measures (*modularity*, *local efficiency* and *global efficiency*), two custom measures that are thought to capture the biological costs of meta-state transitions (*leap size* and *immobility*) (Ramirez-Mahaluf et al., 2020), as well as one measure that assesses the *robustness* of the network against perturbations. Note that modularity, local and global efficiency and immobility were calculated on the transition matrix (matrix containing the number of transitions between each pair of meta-states) for each participant, whereas leap size was based on the distance matrix (i.e., 1-correlation for each meta-state pair). To assess robustness, we employed the *NetSwan* package available for *R* to randomly remove one node after another from the network and recalculate the size of the largest connected component (Achard, 2006; Lynall et al., 2010). A more detailed description of the graph theoretical metrics is provided in (Table S1).

In addition, *transition frequency*, *ratio of within-to-between module meta-state similarity* and *ratio of within-to-between module transitions* were compared between patients and controls. Here, a 'module' refers to a group of meta-states assigned to the same community as defined by the modularity algorithm (*community_louvain.m*). Whereas transition frequency is calculated as the absolute number of transitions between different meta-states, the ratio of within-to-between meta-state similarity ($ratio_{sim}$) is defined as the average correlation of meta-states within a module

divided by the average correlation of meta-states between modules. Similarly, the ratio of within-to-between module transitions ($ratio_{trans}$) is the absolute number of transitions within the same module divided by the absolute number of transitions between modules.

Between-group comparisons of graph theoretical measures, transition frequencies, $ratio_{sim}$, and $ratio_{trans}$ were assessed by comparing the area under the curve (AUC; MATLAB's *trapz*) between patients and controls. The AUC was calculated from $k = 35$ to $k = 55$ for each metric and participant, which allowed us to derive one inference measure across all number of meta-states. For each metric separately, the AUC was entered into a regression model controlling for head motion (FD), age, and sex as nuisance variables. Group comparisons were performed on the residuals using a permutation-based t-test and FDR-corrected using Benjamini-Hochberg (Benjamini & Hochberg, 1995).

2.6 | Correlation of network properties with disease severity

Next, we investigated the relationship of transition network properties with disease severity of patients. To this end, mRS scores at the time of scanning and disease duration (days in acute care) were *z*-transformed across patients and subsequently averaged, resulting in a composite *z* score for each patient that reflects disease severity clinical disability. The Pearson's correlation coefficient between dynamic network properties and disease severity was obtained and corrected for multiple comparisons.

2.7 | Functional network topology of meta-states

Lastly, each meta-state can be represented by a whole-brain FC matrix (638-by-638), in which each edge corresponds to the coupling strength between two given brain regions. Consequently, we sought to evaluate the spatial differences in functional topology of these edges across all meta-states. To this end, we quantified how much each edge differed across meta-states by computing the distance across meta-states (DAMS), a previously defined summary measure by Krohn and colleagues (Krohn et al., 2021), which is defined as the cumulative difference across a specified state space. Here, this distance was computed for each edge across all possible meta-state comparisons given a particular value of *k*, then normalized over *k*, and finally averaged over the applied range of *k* values. In consequence, we obtain a single distance measure for each edge and participant, where a high value of DAMS between any two ROIs indicates that the connectivity between these regions differs strongly between meta-states. In contrast, a low DAMS indicates that the connectivity between these regions is similar across all meta-states of a transition network. Subsequently, group differences for each edge in the distance matrix were assessed with a two-sample *t* test and FDR-corrected for multiple comparisons using Benjamini–Hochberg (Benjamini & Hochberg, 1995). Finally, the participant-specific DAMS values were averaged across participants to obtain the distance matrix shown in (Figure 4).

3 | RESULTS

3.1 | Group differences in network properties

Group comparisons of graph theoretical measures yielded significantly lower local efficiency ($t = -2.41$, $p_{FDR} = .029$, $d = .40$), higher leap size ($t = 2.18$, $p_{FDR} = .037$, $d = .36$) and lower robustness ($t = -2.01$, $p_{FDR} = .048$, $d = .33$) of transition networks in patients compared with controls. In contrast, modularity ($t = -1.43$, $p_{FDR} = .12$, $d = .27$), global efficiency ($t = 1.00$, $p_{FDR} = .20$, $d = .17$) and immobility ($t = -.32$, $p_{FDR} = .38$, $d = .05$) of transitions networks did not differ between groups (Figure 1). The transition networks of six exemplary participants with high and low leap size are shown in Figure S1.

Correlation of similarity and the number of transitions between two meta-states revealed that transition frequency was higher between similar meta-states for both groups and all numbers of meta-states (rho = [.48, .53, .54, .54, .52] for the different *k* meta-states; all $p < .001$, Figure 2). Accordingly, transitions within modules were on average 3.4 times more likely than between modules with a $ratio_{trans}$ (ratio of within-to-between module transitions) = [2.40, 2.94, 3.44, 3.89, 4.44] depending on the number of meta-states. This result was expected as modularity is calculated on the transition matrix. Interestingly, however, the $ratio_{trans}$ was significantly lower in patients with NMDAR encephalitis compared to controls ($t = -2.48$, $p_{FDR} = .026$, $d = .40$), whereas the overall number of transitions between different meta-states did not differ between groups ($t = .32$, $p_{FDR} = .377$, $d = .05$). Similar to $ratio_{trans}$, $ratio_{sim}$ (ratio of within-to-between meta-state similarity) was on average 3.2 ($ratio_{sim}$ = [2.9, 3.1, 3.2, 3.3, 3.4], for *the different k* meta-states). Again, the $ratio_{sim}$ was significantly lower in patients compared with controls ($t = -2.48$,

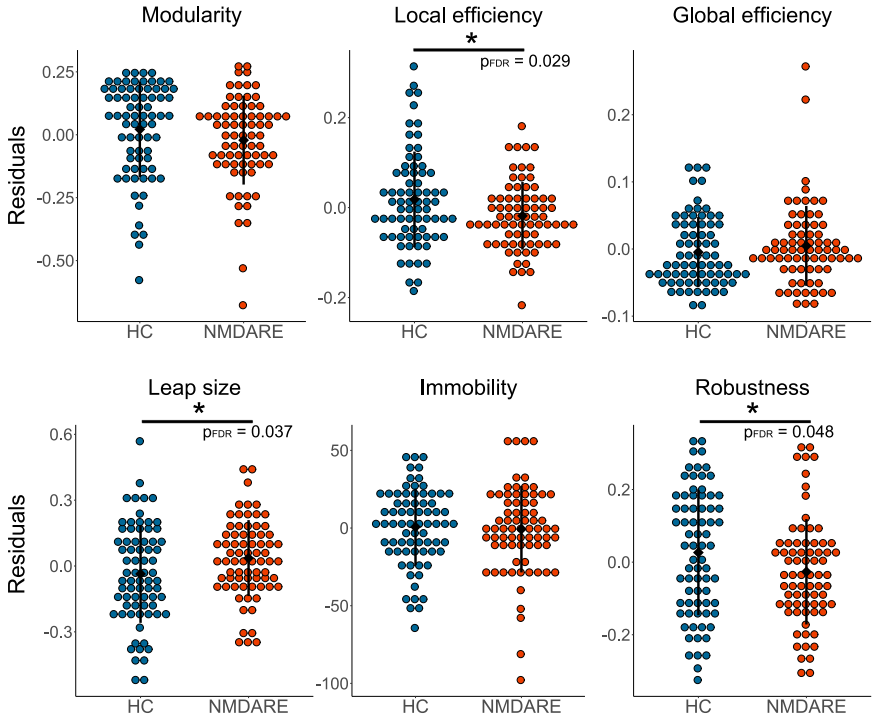

FIGURE 1 Between-group comparisons of graph theoretical measures. Coloured dots represent the residuals after nuisance regression. Black dots and whiskers represent the mean and standard deviation, respectively. HC = healthy controls, NMDAR encephalitis = patients with anti-NMDA receptor encephalitis. * indicates significant difference $p_{FDR} < .05$.

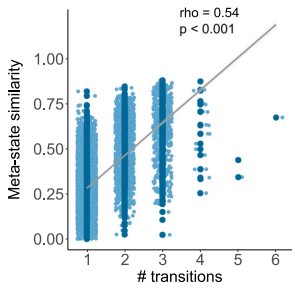

FIGURE 2 Correlation between meta-state similarity and number of transitions between them (here shown for $k = 45$; see Figure S2 for k's = [35, 40, 50, 55]). Meta-state similarity (y-axis) was estimated calculating Spearman's ϱ. The regression line is included for visualization purposes. Number of transitions (x-axis) are the sum of transitions between any two meta-states, independent of the direction of transitions.

$p_{FDR} = .026$, $d = .41$). This suggests that patients transition between topologically more different meta-states (from different modules) compared with controls, whereas the overall transition frequency remains unaltered.

3.2 | Correlation of network properties with disease severity

Next, we investigated the relationship of significant graph metrics, that is, local efficiency, leap size and robustness, ratio_{trans} and ratio_{sim}, with a composite z score for disease severity. Higher disease severity was significantly associated with higher leap size (Pearson's $r = .37$, $p_{FDR} = .0030$, Figure 3), decreased robustness (Pearson's $r = -.37$, $p_{FDR} = .0030$, Figure 3), lower ratio_{sim} (Pearson's $r = -.40$, $p_{FDR} = .0030$, Figure S3) and lower

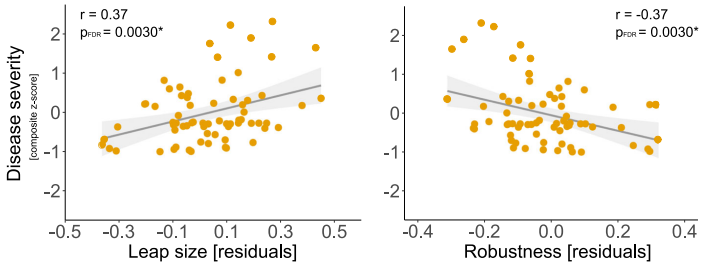

FIGURE 3 Correlation between disease severity (composite z-score) and altered network properties (residuals after nuisance regression). Correlation plots for local efficiency, ratio$_{sim}$ and ratio$_{trans}$ are shown in Figure S3. * indicates significant difference $p_{FDR} < .05$.

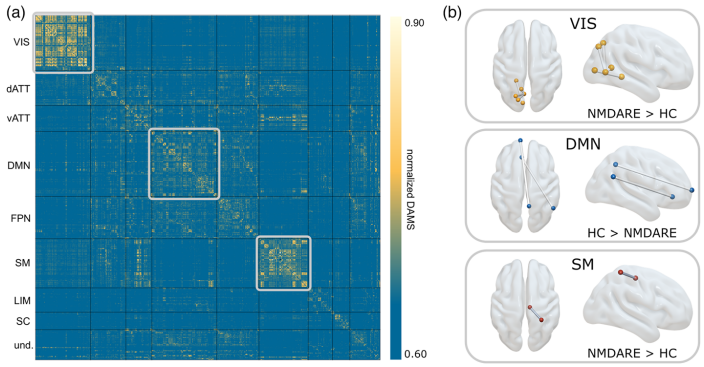

FIGURE 4 Interregional distance across meta-states (DAMS). (a) The DAMS matrix visualizes interregional differences in coupling strength across meta-states averaged across all participants. High DAMS values (yellow) indicate strong differences in connectivity strength across meta-states, whereas low DAMS values (blue) indicate that the connectivity strength between regions is more similar across meta-states. (b) Brain plots show results from group-comparison within each functional network. Differences in DAMS between patients and healthy controls were found for edges within the visual, default-mode and sensorimotor network (false discovery rate [FDR]-corrected). Network assignment of regions is based on the labels proposed by Yeo et al. (2011). Subcortical regions were subsumed as a subcortical network. VIS = visual network, dATT = dorsal attention network, vATT = ventral attention network, DMN = default mode network, FPN = fronto-parietal network, SM = sensorimotor network, LIM = limbic network, SC = subcortical network, und. = undefined, HC = healthy controls, NMDAR encephalitis = patients with anti-NMDA receptor encephalitis.

ratio$_{trans}$ (Pearson's $r = -.33$, $p_{FDR} = .0064$, Figure S3) but not with local efficiency (Pearson's $r = -.11$, $p_{FDR} = .35$, Figure S3).

3.3 | Functional network topology of meta-states

The edges with the highest DAMS, that is, edges that exhibited most pronounced differences in coupling strength across meta-states, clustered predominantly in unimodal networks, namely, the sensorimotor and visual network (Figure 4a). This topological pattern is highly convergent with recent findings from Krohn and colleagues (Krohn et al., 2021) and is akin across groups (Figure S4).

Whole-brain group comparison yielded no significant difference in DAMS between groups after correction for multiple comparison. Therefore, we explored group differences in DAMS within each functional RS network separately. This network-wise group comparison revealed significant differences between edges within the visual, default mode and sensorimotor networks (FDR-corrected, Figure 4b). Remarkably, significant edges showed higher DAMS in patients within the visual and sensorimotor network but lower DAMS within the default-mode network (Table S3).

4 | DISCUSSION

Ongoing brain activity can be described as transient FC patterns (so-called brain states) that are visited in a structured, non-random trajectory (Ramirez-Mahaluf et al., 2020). These brain state dynamics are thought to

facilitate cognition and behaviour and may vary in disease (Kringelbach & Deco, 2020). In this study, we employed a time-resolved analysis of brain activity to capture the spatiotemporal dynamics of brain state transitions in a large sample of patients with NMDAR encephalitis. Our results indicate reduced resilience of state transition networks in patients compared with controls. This manifests in lower local efficiency of the network (fewer transitions from or to neighbouring, i.e., similar and meta-states), higher leap size (transitions between more distinct meta-states) and reduced robustness of the patients' transition networks against random attacks. Furthermore, the ratio of within-to-between module transitions and meta-state similarity was significantly reduced in patients. Importantly, these state dynamic metrics were correlated with disease severity, highlighting the clinical relevance of our findings.

In patients with NMDAR encephalitis, autoantibodies target the NR1 subunit of the NMDA receptor causing an internalization of the receptor (Dalmau et al., 2011). Although this results in a broad range of psychiatric and neurological symptoms, standard clinical MRI shows no or only minor abnormalities in most patients (Graus et al., 2016; Heine et al., 2015). In contrast, FC analyses were able to identify characteristic connectivity alterations: *Static* RS FC analyses that average connectivity across an entire scanning session showed widespread disrupted connectivity in visual, temporal, hippocampal and mid-frontal areas associated with the severity of cognitive and psychiatric symptoms (Cai et al., 2020; Finke et al., 2013; Peer et al., 2017). However, given that brain activity is inherently dynamic (Chang & Glover, 2010), models that incorporate spatiotemporal features of connectivity may complement our knowledge about functional disruptions in neuropsychiatric disorders. Indeed, we recently found that *dynamic* FC showed a shift in state preference and transition probabilities in patients with NMDAR encephalitis that was associated with disease severity and disease duration (von Schwanenflug et al., 2022). In the present study, we further expand on these dynamic FC findings and investigated alterations in the *spatiotemporal trajectory* of functional state exploration through the underlying state space. State exploration is thought to reflect the dynamic repertoire of intrinsic brain activity that is important for information integration and mental processes (Deco et al., 2011; Gu et al., 2017; Lord et al., 2019). Therefore, disruptions in the temporal organization of state transitions may account for clinical symptoms in disease (Deco et al., 2017; Kringelbach & Deco, 2020). In fact, we found a characteristic spatiotemporal reorganization of the transition trajectory in patients compared with controls that was related to disease severity. This spatiotemporal reorganization—as reflected by lower local efficiency, lower robustness and higher leap size of the transition network—may represent overly unstable transition dynamics in NMDAR encephalitis (von Schwanenflug et al., 2022) that could be linked to deficiencies in information integration (Deco et al., 2017; Lord et al., 2019).

At a scale of seconds to minutes, the human brain operates through continuously evolving activity that can be characterized as transient quasi-stable brain states (Allen et al., 2014; Calhoun et al., 2014). This evolution of brain activity is non-random, allowing for a systematic exploration of brain states (Ramirez-Mahaluf et al., 2020). Analogous to the modular spatial organization of the cortex, the temporal trajectory of brain state transitions shows similar topological properties; that is, brain states are grouped into modules of similar meta-states, with higher transition frequencies within a module than between modules (see methods and results section: $ratio_{trans}/ratio_{sim}$). This modular organization is thought to promote segmented and cost-efficient information processing, while enabling the exploration of the functional repertoire via transitions to meta-states of a different module (Bassett et al., 2011; Bertolero et al., 2015; Deco et al., 2017; Sporns & Betzel, 2016; Tognoli & Kelso, 2014). In line with the modular structure, transition networks in healthy controls show high local efficiency and low global efficiency (as compared with a null model) (Ramirez-Mahaluf et al., 2020). Although a high local efficiency allows for locally specialized functioning, a comparatively smaller number of connections between subsystems of a network, that is, low global efficiency, still allow for distributed information processing across different subsystems (Sporns & Betzel, 2016). Moreover, a high local efficiency enhances the robustness of a system. By providing alternative pathways between two nodes (i.e., meta-states), the system compensates for potential disturbances and provides stable representation of information (De Vico Fallani et al., 2009). Interestingly, the spatiotemporal organization of state exploration may also be directly relevant to behaviour. A recent study on transition networks in a healthy population suggests that the efficiency of the network is associated with performance in cognition and motor function (Ramirez-Mahaluf et al., 2020). Thus, state exploration may vary across diseases potentially accounting for a multitude of symptoms (Kringelbach & Deco, 2020).

Indeed, the present study highlights significant differences in the temporal architecture of transition networks between patients with NMDAR encephalitis and healthy controls. We found that patients exhibited decreases in local efficiency and robustness and increases in leap size. Decreased local efficiency hints at unstable

representation of information due to lower redundancy of the transition network, which is described in more detail in the previous paragraph. Leap size is thought to reflect metabolic cost and is measured as the magnitude of 'jumps' between topologically different meta-states. Eliciting state transitions is energetically costly (Gu et al., 2017; Lord et al., 2013) and possibly increases when traversing states that show highly disparate activation profiles. This intuition is supported by our finding that (low-cost) transitions between two similar meta-states are more likely than (cost-intensive) transitions between distant meta-states. Accordingly, higher leap size in patients may indicate higher metabolic demand along with higher volatility of state transitions. Lastly, we evaluated the robustness of the transition network, which is the ability of maintaining information processing within the network before collapsing (Aerts et al., 2016). We found that transition networks of patients with NMDAR encephalitis are less robust compared to those of controls when removing the nodes (i.e., meta-states) one by one. Together with a decreased local efficiency and higher leap size, this points to a destabilization and reduced resilience of transition networks in patients with NMDAR encephalitis, corroborating earlier findings in this patient population (von Schwanenflug et al., 2022). This notion is furthermore supported by decreased ratios of within-to-between module transitions and within-to-between module meta-state similarity in patients. In addition, four out of five network measures—leap size, robustness, $ratio_{trans}$ and $ratio_{sim}$—were correlated with a composite score of disease severity, supporting clinical relevance of our findings.

The neural basis for functional brain state transitions is a matter of ongoing investigation. Neural dynamics may coordinate whole-brain FC patterns, thereby enabling the exploration of the brain's functional repertoire (Gu et al., 2017; Kringelbach & Deco, 2020; Lord et al., 2019). In NMDAR encephalitis, internalization of the NMDAR alters glutamatergic synaptic transmission, impacting the coordination between large-scale functional networks. Interestingly, reduced resilience of transition networks in patients with NMDAR encephalitis is supported by findings from attractor-based computational models that postulate that NMDAR dysfunction may lead to overly unstable attractors in brain activity (Rolls, 2012, 2021). NMDAR hypofunction, as in NMDAR encephalitis and schizophrenia, may lead to a flattening of the attractors (destabilizing effect), facilitating perturbations to provoke transitions between attractors (Loh et al., 2007; Rolls, 2012).

Finally, our study provides evidence that a subset of regions preferentially promotes brain state transitions (Kringelbach & Deco, 2020; Krohn et al., 2021). Convergent with recent work on brain dynamics, we found that changes in connectivity across states are most pronounced in regions of the visual and sensorimotor areas, potentially following a hierarchy from unimodal to transmodal networks (Krohn et al., 2021). Interestingly, in patients with NMDAR encephalitis, connectivity changes across meta-states within unimodal networks were even more pronounced, providing a spatial correlate of the increased temporal volatility in state transitions. Both the visual and the sensorimotor network have been reported to show reduced static FC in patients with NMDAR encephalitis; these effects correlated with disease severity; that is, they were more pronounced in more severely affected patients (Peer et al., 2017). Along with altered FC found in other large-scale functional networks (Chen et al., 2022; Finke et al., 2013; Heine et al., 2015; Peer et al., 2017), these findings reflect the prominent expression of NMDARs throughout the cortex, their pathophysiological role in NMDAR encephalitis and potentially their contribution to the orchestration of brain dynamics. Limiting state transitions to a defined number of regions initiating those transitions raise the intriguing possibility that controlled external stimulation of these particular regions could be applied to achieve a rebalancing of state dynamics (Gu et al., 2017; Kringelbach & Deco, 2020).

Some limitations of our study deserve mentioning: First, statistical comparison of dynamic metrics revealed several significant group differences, albeit with moderate effect sizes. Thus, future work should consider acquiring larger samples and potentially examine subgroup differences in this disease to better characterize the potential clinical significance of these alterations, with the ultimate goal of moving beyond group-level effects and towards individual patients. Second, the window length of 2 TR (≙4.5 s) is comparatively short and may decrease the signal-to-noise ratio. However, the size of this time window has been recognized as a good trade-off between sensitivity and specificity (Shine et al., 2015). Furthermore, a high reliability of meta-state estimation was previously shown using a very similar window length (Ramirez-Mahaluf et al., 2020). Third, k-means clustering is applied to each participant separately. Although this approach poses inherent limitations to study between-group differences in meta-state topology, it is particularly suited to investigate individualized temporal dynamics and characteristics of the transition trajectory of functional states. Forth, the applied k enforces the extraction of a large number of (potentially similar) meta-states for each participant. While most studies focus on 3–5 distinct major connectivity states defined on a group level, this number of states may not be sufficient to represent the full repertoire of functional configurations

of the human brain. Furthermore, a small number of states limit a detailed investigation of individual transition trajectories between these states, which was the main purpose of the present study.

5 | CONCLUSION

In this study, we employed a time-resolved graph analytical framework to study the spatiotemporal trajectory of brain state transitions in patients with NMDAR encephalitis. Besides decreases in local efficiency, we observed reduced robustness of the patients' transition networks against random attacks compared with those of healthy controls. Together with higher leap size in patients, these findings show reduced resilience of functional state transitions in patients, that is, related to disease severity. Hence, our findings add to the evidence that disturbance of functional brain network dynamics plays a key role in the pathophysiology of NMDAR encephalitis.

ACKNOWLEDGEMENTS

This study was funded by the Deutsche Forschungsgemeinschaft (DFG, German Research Foundation, grant numbers 327654276 [SFB 1315], FI 2309/1-1, FI 2309/2-1 and PR 1274/6-1) and Deutsches Ministerium für Bildung und Forschung (BMBF, German Ministry of Education and Research, grant number 01GM1908D, CONNECT-GENERATE). HP received funding from the Helmholtz Association (HIL-A03). NS is a doctoral scholar at Cusanuswerk – Bischöfliche Studienförderung. AR is a doctoral scholar at the Berlin School of Mind and Brain, Humboldt-Universität zu Berlin. JRM and NAC were funded by the Agencia Nacional de Investigación y Desarrollo from Chile (ANID), through its programmes FONDECYT postdoctorado (Ref: 3190311 to JRM), FONDECYT regular (Ref: 1200601 to NAC) and Anillo ACT192064. The funders had no influence on study design, data collection, data analyses, data interpretation or writing. Open Access funding enabled and organized by Projekt DEAL.

CONFLICT OF INTEREST

NS, JRM, SK, AR, JH, HP and CF have no competing interests. NAC has received personal fees from Janssen (Johnson & Johnson), outside the submitted work.

AUTHOR CONTRIBUTIONS

Nina von Schwanenflug: Conceptualization; data curation; formal analysis; investigation; methodology; project administration; software; visualization; writing-original draft. **Juan P. Ramirez-Mahaluf:** Conceptualization; formal analysis; investigation; methodology; project administration; software; writing-review and editing. **Stephan Krohn:** Data curation; investigation; methodology; software; supervision; writing-original draft; writing-review and editing. **Amy Romanello:** Formal analysis; investigation; writing-review and editing. **Josephine Heine:** Data curation; writing-review and editing. **Harald Pruess:** Data curation; writing-review and editing. **Nicolas Crossley:** Conceptualization; methodology; writing-review and editing. **Carsten Finke:** Conceptualization; formal analysis; funding acquisition; investigation; methodology; project administration; supervision; writing-original draft; writing-review and editing.

PEER REVIEW

The peer review history for this article is available at https://publons.com/publon/10.1111/ejn.15901.

DATA AVAILABILITY STATEMENT

Sample data and analysis code supporting the presented results are available on github (https://github.com/nivons/transitionnetworksNMDARE). With respect to the sensitivity of the data, de-identified data of the full sample will be provided upon reasonable request, subject to a material transfer agreement.

ORCID

Nina von Schwanenflug https://orcid.org/0000-0001-5573-259X
Juan P. Ramirez-Mahaluf https://orcid.org/0000-0002-0821-1174
Stephan Krohn https://orcid.org/0000-0003-0683-5386
Amy Romanello https://orcid.org/0000-0003-1257-9593
Josephine Heine https://orcid.org/0000-0001-5226-6650
Harald Prüss https://orcid.org/0000-0002-8283-7976
Nicolas A. Crossley https://orcid.org/0000-0002-3060-656X
Carsten Finke https://orcid.org/0000-0002-7665-1171

REFERENCES

Achard, S. (2006). A resilient, low-frequency, small-world human brain functional network with highly connected association cortical hubs. *Journal of Neuroscience*, *26*(1), 63–72. https://doi.org/10.1523/JNEUROSCI.3874-05.2006

Aerts, H., Fias, W., Caeyenberghs, K., & Marinazzo, D. (2016). Brain networks under attack: Robustness properties and the impact of lesions. *Brain*, *139*(12), 3063–3083. https://doi.org/10.1093/brain/aww194

Allen, E. A., Damaraju, E., Plis, S. M., Erhardt, E. B., Eichele, T., & Calhoun, V. D. (2014). Tracking whole-brain connectivity dynamics in the resting state. *Cerebral Cortex (New York, N.Y.: 1991)*, *24*(3), 663–676. https://doi.org/10.1093/cercor/bhs352

Bassett, D. S., Wymbs, N. F., Porter, M. A., Mucha, P. J., Carlson, J. M., & Grafton, S. T. (2011). Dynamic reconfiguration of human brain networks during learning. *Proceedings of*

the National Academy of Sciences, *108*(18), 7641–7646. https://doi.org/10.1073/pnas.1018985108

Benjamini, Y., & Hochberg, Y. (1995). Controlling the false discovery rate: A practical and powerful approach to multiple testing. *Journal of the Royal Statistical Society: Series B (Methodological)*, *57*(1), 289–300. https://doi.org/10.1111/j.2517-6161.1995.tb02031.x

Bertolero, M. A., Yeo, B. T. T., & D'Esposito, M. (2015). The modular and integrative functional architecture of the human brain. *Proceedings of the National Academy of Sciences*, *112*(49), E6798–E6807. https://doi.org/10.1073/pnas.1510619112

Biswal, B., Zerrin Yetkin, F., Haughton, V. M., & Hyde, J. S. (1995). Functional connectivity in the motor cortex of resting human brain using echo-planar mri. *Magnetic Resonance in Medicine*, *34*(4), 537–541. https://doi.org/10.1002/mrm.1910340409

Cai, L., Liang, Y., Huang, H., Zhou, X., & Zheng, J. (2020). Cerebral functional activity and connectivity changes in anti-N-methyl-D-aspartate receptor encephalitis: A resting-state fMRI study. *NeuroImage: Clinical*, *25*, 102189. https://doi.org/10.1016/j.nicl.2020.102189

Calhoun, V. D., Miller, R., Pearlson, G., & Adalı, T. (2014). The Chronnectome: Time-varying connectivity networks as the next frontier in fMRI data discovery. *Neuron*, *84*(2), 262–274. https://doi.org/10.1016/j.neuron.2014.10.015

Chang, C., & Glover, G. H. (2010). Time–frequency dynamics of resting-state brain connectivity measured with fMRI. *NeuroImage*, *50*(1), 81–98. https://doi.org/10.1016/j.neuroimage.2009.12.011

Chen, Z., Zhou, J., Wu, D., Ji, C., Luo, B., & Wang, K. (2022). Altered executive control network connectivity in anti-NMDA receptor encephalitis. *Annals of Clinical and Translational Neurology*, *9*(1), 30–40. https://doi.org/10.1002/acn3.51487

Crossley, N. A., Mechelli, A., Vertes, P. E., Winton-Brown, T. T., Patel, A. X., Ginestet, C. E., McGuire, P., & Bullmore, E. T. (2013). Cognitive relevance of the community structure of the human brain functional coactivation network. *Proceedings of the National Academy of Sciences*, *110*(28), 11583–11588. https://doi.org/10.1073/pnas.1220826110

Dalmau, J., Armangué, T., Planagumà, J., Radosevic, M., Mannara, F., Leypoldt, F., Geis, C., Lancaster, E., Titulaer, M. J., Rosenfeld, M. R., & Graus, F. (2019). An update on anti-NMDA receptor encephalitis for neurologists and psychiatrists: Mechanisms and models. *The Lancet Neurology*, *18*(11), 1045–1057. https://doi.org/10.1016/S1474-4422(19)30244-3

Dalmau, J., Lancaster, E., Martinez-Hernandez, E., Rosenfeld, M. R., & Balice-Gordon, R. (2011). Clinical experience and laboratory investigations in patients with anti-NMDAR encephalitis. *The Lancet Neurology*, *10*(1), 63–74. https://doi.org/10.1016/S1474-4422(10)70253-2

de Vico Fallani, F., Aparecido, R. F., da Fontoura, C. L., Mattia, D., Cincotti, F., Astolfi, L., Vecchiato, G., Tabarrini, A., Salinari, S., & Babiloni, F. (2009). Analysis of the connection redundancy in functional networks from high-resolution EEG: A preliminary study. *Annual International Conference of the IEEE Engineering in Medicine and Biology Society*, *2009*, 2204–2207. https://doi.org/10.1109/IEMBS.2009.5334882

Deco, G., Jirsa, V. K., & McIntosh, A. R. (2011). Emerging concepts for the dynamical organization of resting-state activity in the brain. *Nature Reviews Neuroscience*, *12*(1), 43–56. https://doi.org/10.1038/nrn2961

Deco, G., Kringelbach, M. L., Jirsa, V. K., & Ritter, P. (2017). The dynamics of resting fluctuations in the brain: Metastability and its dynamical cortical core. *Scientific Reports*, *7*(1), 3095. https://doi.org/10.1038/s41598-017-03073-5

Eijlers, A. J. C., Wink, A. M., Meijer, K. A., Douw, L., Geurts, J. J. G., & Schoonheim, M. M. (2019). Reduced network dynamics on functional MRI signals cognitive impairment in multiple sclerosis. *Radiology*, *292*(2), 449–457. https://doi.org/10.1148/radiol.2019182623

Finke, C., Kopp, U. A., Prüss, H., Dalmau, J., Wandinger, K.-P., & Ploner, C. J. (2012). Cognitive deficits following anti-NMDA receptor encephalitis. *Journal of Neurology, Neurosurgery & Psychiatry*, *83*(2), 195–198. https://doi.org/10.1136/jnnp-2011-300411

Finke, C., Kopp, U. A., Scheel, M., Pech, L.-M., Soemmer, C., Schlichting, J., Leypoldt, F., Brandt, A. U., Wuerfel, J., Probst, C., Ploner, C. J., Prüss, H., & Paul, F. (2013). Functional and structural brain changes in anti-N-methyl-D-aspartate receptor encephalitis. *Annals of Neurology*, *74*(2), 284–296. https://doi.org/10.1002/ana.23932

Gibson, L. L., McKeever, A., Coutinho, E., Finke, C., & Pollak, T. A. (2020). Cognitive impact of neuronal antibodies: Encephalitis and beyond. *Translational Psychiatry*, *10*(1), 304. https://doi.org/10.1038/s41398-020-00989-x

Gibson, L. L., Pollak, T. A., Blackman, G., Thornton, M., Moran, N., & David, A. S. (2019). The psychiatric phenotype of anti-NMDA receptor encephalitis. *The Journal of Neuropsychiatry and Clinical Neurosciences*, *31*(1), 70–79. https://doi.org/10.1176/appi.neuropsych.17120343

Graus, F., Titulaer, M. J., Balu, R., Benseler, S., Bien, C. G., Cellucci, T., Cortese, I., Dale, R. C., Gelfand, J. M., Geschwind, M., Glaser, C. A., Honnorat, J., Höftberger, R., Iizuka, T., Irani, S. R., Lancaster, E., Leypoldt, F., Prüss, H., Rae-Grant, A., … Dalmau, J. (2016). A clinical approach to diagnosis of autoimmune encephalitis. *The Lancet. Neurology*, *15*(4), 391–404. https://doi.org/10.1016/S1474-4422(15)00401-9

Gu, S., Betzel, R. F., Mattar, M. G., Cieslak, M., Delio, P. R., Grafton, S. T., Pasqualetti, F., & Bassett, D. S. (2017). Optimal trajectories of brain state transitions. *NeuroImage*, *148*, 305–317. https://doi.org/10.1016/j.neuroimage.2017.01.003

Heine, J., Kopp, U. A., Klag, J., Ploner, C. J., Prüss, H., & Finke, C. (2021). Long-term cognitive outcome in anti–N-methyl-D-aspartate receptor encephalitis. *Annals of Neurology*, *90*(6), 949–961. https://doi.org/10.1002/ana.26241

Heine, J., Prüss, H., Bartsch, T., Ploner, C. J., Paul, F., & Finke, C. (2015). Imaging of autoimmune encephalitis—Relevance for clinical practice and hippocampal function. *Neuroscience*, *309*, 68–83. https://doi.org/10.1016/j.neuroscience.2015.05.037

Kringelbach, M. L., & Deco, G. (2020). Brain states and transitions: Insights from computational neuroscience. *Cell Reports*, *32*(10), 108128. https://doi.org/10.1016/j.celrep.2020.108128

Krohn, S., von Schwanenflug, N., Waschke, L., Romanello, A., Gell, M., Garrett, D. D., & Finke, C. (2021). A spatiotemporal complexity architecture of human brain activity [preprint]. *bioRxiv*. https://doi.org/10.1101/2021.06.04.446948

Latora, V., & Marchiori, M. (2001). Efficient behavior of small-world networks. *Physical Review Letters*, *87*(19), 198701. https://doi.org/10.1103/PhysRevLett.87.198701

Loh, M., Rolls, E. T., & Deco, G. (2007). A dynamical systems hypothesis of schizophrenia. *PLoS Computational Biology*, *3*(11), e228. https://doi.org/10.1371/journal.pcbi.0030228

Lord, L.-D., Expert, P., Atasoy, S., Roseman, L., Rapuano, K., Lambiotte, R., Nutt, D. J., Deco, G., Carhart-Harris, R. L., Kringelbach, M. L., & Cabral, J. (2019). Dynamical exploration of the repertoire of brain networks at rest is modulated by psilocybin. *NeuroImage*, *199*, 127–142. https://doi.org/10.1016/j.neuroimage.2019.05.060

Lord, L.-D., Expert, P., Huckins, J. F., & Turkheimer, F. E. (2013). Cerebral energy metabolism and the brain's functional network architecture: An integrative review. *Journal of Cerebral Blood Flow & Metabolism*, *33*(9), 1347–1354. https://doi.org/10.1038/jcbfm.2013.94

Lynall, M.-E., Bassett, D. S., Kerwin, R., McKenna, P. J., Kitzbichler, M., Muller, U., & Bullmore, E. (2010). Functional connectivity and brain networks in schizophrenia. *Journal of Neuroscience*, *30*(28), 9477–9487. https://doi.org/10.1523/JNEUROSCI.0333-10.2010

Parkes, L., Fulcher, B., Yücel, M., & Fornito, A. (2018). An evaluation of the efficacy, reliability, and sensitivity of motion correction strategies for resting-state functional MRI. *NeuroImage*, *171*, 415–436. https://doi.org/10.1016/j.neuroimage.2017.12.073

Peer, M., Prüss, H., Ben-Dayan, I., Paul, F., Arzy, S., & Finke, C. (2017). Functional connectivity of large-scale brain networks in patients with anti-NMDA receptor encephalitis: An observational study. *The Lancet. Psychiatry*, *4*(10), 768–774. https://doi.org/10.1016/S2215-0366(17)30330-9

Power, J. D., Mitra, A., Laumann, T. O., Snyder, A. Z., Schlaggar, B. L., & Petersen, S. E. (2014). Methods to detect, characterize, and remove motion artifact in resting state fMRI. *NeuroImage*, *84*, 320–341. https://doi.org/10.1016/j.neuroimage.2013.08.048

Pruim, R. H. R., Mennes, M., van Rooij, D., Llera, A., Buitelaar, J. K., & Beckmann, C. F. (2015). ICA-AROMA: A robust ICA-based strategy for removing motion artifacts from fMRI data. *NeuroImage*, *112*, 267–277. https://doi.org/10.1016/j.neuroimage.2015.02.064

Ramirez-Mahaluf, J. P., Medel, V., Tepper, Á., Alliende, L. M., Sato, J. R., Ossandon, T., & Crossley, N. A. (2020). Transitions between human functional brain networks reveal complex, cost-efficient and behaviorally-relevant temporal paths. *NeuroImage*, *219*, 117027. https://doi.org/10.1016/j.neuroimage.2020.117027

Rolls, E. T. (2012). Glutamate, obsessive–compulsive disorder, schizophrenia, and the stability of cortical attractor neuronal networks. *Pharmacology Biochemistry and Behavior*, *100*(4), 736–751. https://doi.org/10.1016/j.pbb.2011.06.017

Rolls, E. T. (2021). Attractor cortical neurodynamics, schizophrenia, and depression. *Translational Psychiatry*, *11*(1), 215. https://doi.org/10.1038/s41398-021-01333-7

Shine, J. M., Koyejo, O., Bell, P. T., Gorgolewski, K. J., Gilat, M., & Poldrack, R. A. (2015). Estimation of dynamic functional connectivity using multiplication of temporal derivatives. *NeuroImage*, *122*, 399–407. https://doi.org/10.1016/j.neuroimage.2015.07.064

Sporns, O., & Betzel, R. F. (2016). Modular brain networks. *Annual Review of Psychology*, *67*(1), 613–640. https://doi.org/10.1146/annurev-psych-122414-033634

Tognoli, E., & Kelso, J. A. S. (2014). The metastable brain. *Neuron*, *81*(1), 35–48. https://doi.org/10.1016/j.neuron.2013.12.022

von Schwanenflug, N., Krohn, S., Heine, J., Paul, F., Prüss, H., & Finke, C. (2022). State-dependent signatures of anti-*N*-methyl-D-aspartate receptor encephalitis. *Brain Communications*, *4*(1), fcab298. https://doi.org/10.1093/braincomms/fcab298

Yeo, B. T., Krienen, F. M., Sepulcre, J., Sabuncu, M. R., Lashkari, D., Hollinshead, M., Roffman, J. L., Smoller, J. W., Zöllei, L., Polimeni, J. R., Fischl, B., Liu, H., & Buckner, R. L. (2011). The organization of the human cerebral cortex estimated by intrinsic functional connectivity. *Journal of Neurophysiology*, *106*(3), 1125–1165. https://doi.org/10.1152/jn.00338.2011

SUPPORTING INFORMATION

Additional supporting information can be found online in the Supporting Information section at the end of this article.

How to cite this article: von Schwanenflug, N., Ramirez-Mahaluf, J. P., Krohn, S., Romanello, A., Heine, J., Prüss, H., Crossley, N. A., & Finke, C. (2023). Reduced resilience of brain state transitions in anti-*N*-methyl-D-aspartate receptor encephalitis. *European Journal of Neuroscience*, *57*(3), 568–579. https://doi.org/10.1111/ejn.15901

Curriculum vitae

Mein Lebenslauf wird aus datenschutzrechtlichen Gründen in der elektronischen Version meiner Arbeit nicht veröffentlicht.

List of publications

Scope of this thesis

von Schwanenflug, N., Krohn, S., Heine, J., Paul, F., Prüss, H., & Finke, C. (2022). *State-dependent signatures of anti-N-methyl-D-aspartate receptor encephalitis.* Brain Communications, 4(1), fcab298. https://doi.org/10.1093/braincomms/fcab298
IF: 4.8

von Schwanenflug, N., Ramirez-Mahaluf, J. P., Krohn, S., Romanello, A., Heine, J., Prüss, H., Crossley, N. A., & Finke, C. (2023). *Reduced resilience of brain state transitions in anti-N-methyl-D-aspartate receptor encephalitis.* European Journal of Neuroscience, 57(3), 568–579. https://doi.org/10.1111/ejn.15901
IF: 3.69

Von Schwanenflug, N., Koch, S. P., Krohn, S., Broeders, T. A. A., Lydon-Staley, D. M., Bassett, D. S., Schoonheim, M. M., Paul, F., & Finke, C. (2023). *Increased flexibility of brain dynamics in patients with multiple sclerosis.* Brain Communications, fcad143. https://doi.org/10.1093/braincomms/fcad143
IF: 4.8

Krohn, S., **von Schwanenflug, N.**, Waschke, L., Romanello, A., Gell, M., Garrett, D. D., & Finke, C. (2023). *A spatiotemporal complexity architecture of human brain activity.* Science Advances, 9(5), eabq3851. https://doi.org/10.1126/sciadv.abq3851
IF: 14.98

Romanello, A., Krohn, S., **Von Schwanenflug, N.**, Chien, C., Bellmann-Strobl, J., Ruprecht, K., Paul, F., & Finke, C. (2022). *Functional connectivity dynamics reflect disability and multi-domain clinical impairment in patients with relapsing-remitting multiple sclerosis.* NeuroImage: Clinical, 36, 103203. https://doi.org/10.1016/j.nicl.2022.103203
IF: 4.89

Krohn S., Von Schwanenflug N., Romanello A., Madan CR., Finke C. (2023) *The formation of brain shape in human newborns.* bioRxiv https://doi.org/10.1101/2023.01.01.521756 (Preprint)

Acknowledgements

Ich danke Dima, meiner Mutter, Stephan, Anna & Heike, Carsten, dem Cusanuswerk, der Berlin School of Mind and Brain und allen, die mich auf dem Weg begleitet haben.
Ciao.